

**MATERIAL CHARACTERIZATION OF NITINOL WIRES FOR THE DESIGN  
OF ACTUATION SYSTEMS**

A Thesis

presented to

the Faculty of California Polytechnic State University,

San Luis Obispo

In Partial Fulfillment

of the Requirements for the Degree

Master of Science in Mechanical Engineering

by

Sean P. Kennedy

August 2013

© 2013  
Sean P. Kennedy  
ALL RIGHTS RESERVED

## COMMITTEE MEMBERSHIP

TITLE: Material Characterization of Nitinol Wires for the Design  
of Actuator Systems

AUTHOR: Sean P. Kennedy

DATE SUBMITTED: August 2013

COMMITTEE CHAIR: Dr. Saeed B. Niku, Graduate Advisor,  
Mechanical Engineering Department

COMMITTEE MEMBER: Dr. William R. Murray, Mechanical Engineering Professor

COMMITTEE MEMBER: Dr. John R. Ridgely, Mechanical Engineering Professor

## **ABSTRACT**

### Material Characterization of Nitinol Wires for the Design of Actuator Systems

Sean P. Kennedy

A series of tests were performed on nickel-titanium alloy wire, also known as nitinol, to determine the plausibility of designing an actuator using this wire as the method of actuation. These tests have been designed to fully characterize how the wire behaves under steady state and transient conditions allowing for a specific wire selection to be made given known actuator specifications which will result in an efficient design. The wire transient data can be used to design a controller which reduces the actuation time. The research done for the overall project covers a wide scope including wire hysteresis, nitinol transition temperature, variable wire resistance, wire actuation as a function of current and pull force, cable fabrication, and wire actuation control to optimize performance. Using these test results, a prototype actuator has been designed using nitinol wire. It has been determined that an actuator can be efficiently designed using this material.

Keywords: nitinol, wire, shape memory, actuation, actuator, test, research, contract, extend, hysteresis, transition, temperature, resistance, current, force, work, cable, control, algorithm, design, biometal, flexinol, nickel, titanium, lever, logistic growth, exponential decay, Images Scientific Instruments.

## **ACKNOWLEDGMENTS**

I would like to thank my committee for their continued support of my research: Dr. Saeed Niku, my committee chair; Dr. William Murray; and Dr. John Ridgely. These individuals provided me with the tools to succeed, and for that I offer my appreciation.

This project could not have been successful if not for the financial support of the Mechanical Engineering Student Fee Allocation Committee (MESFAC), the organization that provided me with the large majority of the funds needed for this research project.

Finally, I would like to thank my family, friends, and fellow classmates who have supported me every step of the way. Though only some of this support was in the form of engineering insight, all was essential to give me the motivation to succeed.

To all of these individuals, I give my deepest gratitude.

## TABLE OF CONTENTS

	Page
List of Tables.....	viii
List of Figures.....	ix
Chapter 1. Introduction.....	1
1.1. Problem Statement.....	1
1.2. Background.....	2
1.3. Nitinol Testing Overview.....	5
1.4. General Test Setup.....	6
Chapter 2. Nitinol Wire Testing and Results.....	8
2.1. Wire Contraction Test.....	8
2.1.1. Purpose of Test.....	8
2.1.2. Setup and Procedure.....	8
2.1.3. Results.....	9
2.2. Current Hysteresis Test.....	13
2.2.1. Purpose of Test.....	13
2.2.2. Setup and Procedure.....	14
2.2.3. Results.....	14
2.3. Wire Hysteresis Test.....	17
2.3.1. Purpose of Test.....	17
2.3.2. Setup and Procedure.....	17
2.3.3. Results.....	18
2.4. Final Displacement Model.....	20
2.5. Maximum Pull Force.....	23
2.5.1. Purpose of Test.....	23
2.5.2. Setup and Procedure.....	23
2.5.3. Results.....	24
2.6. Variable Wire Resistance.....	29
2.6.1. Purpose of Test.....	29
2.6.2. Setup and Procedure.....	29
2.6.3. Results.....	29
2.7. Temperature Test.....	32
2.7.1. Purpose of Test.....	32
2.7.2. Setup and Procedure.....	32

2.7.3. Results.....	34
2.8. Transient Test .....	38
2.8.1. Purpose of Test.....	38
2.8.2. Setup and Procedure .....	38
2.8.3. Results.....	40
2.9. Control Algorithm.....	43
2.10. Cable Fabrication and Testing.....	46
2.10.1. Purpose of Cables .....	46
2.10.2. Cable Testing.....	47
2.10.3. Cable Transient Test.....	47
2.10.4. Cable Resistance .....	48
2.10.5. Cable Hysteresis.....	48
2.10.6. Cable Conslusions.....	49
2.11. Interpretation of Test Results .....	50
Chapter 3. Actuator Design and Tesing.....	51
3.1. Introduction.....	51
3.2. Concepts.....	51
3.3. Design .....	52
3.4. Actuator Testing and Results .....	54
3.5. Future Improvements to Design.....	56
3.6. Design of a Custom Actuator .....	56
3.6.1. Design Example .....	58
Conclusion .....	60
List of References .....	61
Appendix A. Test Setup and Equipment Photos.....	62
Appendix B. Results From Tests For All Wires.....	72
Appendix C. Solidwords Drawings and Photos of Actuator .....	99

## LIST OF TABLES

	Page
Table 1.1. Flexinol® wire properties [3].....	4
Table 2.1. Constants from wire contraction test. ....	11
Table 2.2. Constants for final displacement model.....	22
Table 2.3. Constants for force curves.....	25
Table 2.4. Maximum force and work values for all wires. ....	27
Table 2.5. Resistance values for varying wire diameter.....	31
Table 2.6. Temperature curve constants using the compensated regression curves.....	35
Table 2.7. Contraction and extension time constants.....	40
Table 2.8. Current values for control algorithm.....	44
Table 2.9. Contraction time constants for 6 mil wire diameter cables.....	47
Table 2.10. Resistances for 6 mil diameter cables with varying number of strands. ....	48
Table 2.11. Constants from wire hysteresis test for single strands and cables.....	49
Table 3.1. Results from actuator testing.....	54



## LIST OF FIGURES

	Page
Figure 1.1. Shape memory effect [1]. .....	2
Figure 1.2. General test setup for all tests.....	7
Figure 2.1. Wire contraction curve for 6 mil diameter wire. ....	9
Figure 2.2. Transition temperature hysteresis trend [6]. .....	13
Figure 2.3. Wire contraction and extension curves for 6 mil diameter wire.....	15
Figure 2.4. Current hysteresis as a function of pull force for 6 mil diameter wire. ....	16
Figure 2.5. Test setup for wire hysteresis test. ....	17
Figure 2.6. Wire hysteresis as a function of pull force for 6 mil diameter wire. ....	18
Figure 2.7. Final displacement model.....	20
Figure 2.8. Force curves for any wire diameter. ....	24
Figure 2.9. Work curve for 6 mil diameter wire. ....	26
Figure 2.10. Force curves for any wire diameter including $F_{\max\_w}$ .....	28
Figure 2.11. Resistance curve for 6 mil diameter wire for increasing current values. ....	30
Figure 2.12. Test setup for temperature test.....	33
Figure 2.13. Initial temperature data with double parabolic regression. ....	34
Figure 2.14. Temperature curves with transition temperature for 6 mil diameter wire. ...	36
Figure 2.15. Transition current as a function of Nickel to Titanium ratio [5].....	37
Figure 2.16. Test setup for transient test. ....	39
Figure 2.17. Time to contraction values at varying initial currents. ....	41
Figure 2.18. Time to extension values for varying initial currents. ....	41
Figure 2.19. Control algorithm used for an efficient actuator design. ....	43
Figure 2.20. Cable connection using a coil of wire. ....	46
Figure 3.1. Solidworks model of actuator design. ....	53
Figure A.1. Constant current power supply used in most tests.....	63
Figure A.2. 5V power supply used in transient test. ....	63
Figure A.3. Digital multimeter to read potentiometer and thermistor resistance values. .	64
Figure A.4. Digital oscilloscope used in transient test.....	64
Figure A.5. 5k rotary potentiometer with lever arm used most tests. ....	65

Figure A.6. 10K3 thermistor probe (left) and complete thermistor with leads (right).....	65
Figure A.7. Nitinol wires used for testing.....	66
Figure A.8. Nitinol cables of 6 mil diameter wire used for testing.....	66
Figure A.9. Spade lugs used for wire attachment. ....	67
Figure A.10. Nitinol cable with wires wrapped around the end of the spade lug.....	67
Figure A.11. General test setup. ....	68
Figure A.12. Temperature test setup. ....	68
Figure A.13. Thermistor attachment for temperature test.....	69
Figure A.14. Transient test setup.....	69
Figure A.15. 5V circuit loop of transient test setup with oscilloscope 1 attachment.....	70
Figure A.16. Triggering circuit of transient test setup with oscilloscope 2 attachment....	70
Figure A.17. Weight attachment for wire hysteresis test. ....	71
Figure B.1. Wire contraction curve for 5 mil diameter wire.....	73
Figure B.2. Wire contraction curve for 6 mil diameter wire.....	73
Figure B.3. Wire contraction curve for 8 mil diameter wire.....	74
Figure B.4. Wire contraction curve for 10 mil diameter wire.....	74
Figure B.5. Wire contraction curve for 12 mil diameter wire.....	75
Figure B.6. Wire contraction curve for 15 mil diameter wire.....	75
Figure B.7. Wire contraction and extension curves for 5 mil diameter wire. ....	76
Figure B.8. Wire contraction and extension curves for 6 mil diameter wire. ....	76
Figure B.9. Wire contraction and extension curves for 8 mil diameter wire. ....	77
Figure B.10. Wire contraction and extension curves for 10 mil diameter wire. ....	77
Figure B.11. Wire contraction and extension curves for 12 mil diameter wire. ....	78
Figure B.12. Wire contraction and extension curves for 15 mil diameter wire. ....	78
Figure B.13. Current hysteresis as a function of pull force for 5 mil diameter wire. ....	79
Figure B.14. Current hysteresis as a function of pull force for 6 mil diameter wire. ....	79
Figure B.15. Current hysteresis as a function of pull force for 8 mil diameter wire. ....	80
Figure B.16. Current hysteresis as a function of pull force for 10 mil diameter wire. ....	80
Figure B.17. Current hysteresis as a function of pull force for 12 mil diameter wire. ....	81
Figure B.18. Current hysteresis as a function of pull force for 15 mil diameter wire. ....	81

Figure B.19. Current hysteresis as a function of pull force for all wires.....	82
Figure B.20. Work curve for 5 mil diameter wire.....	83
Figure B.21. Work curve for 6 mil diameter wire.....	83
Figure B.22. Work curve for 8 mil diameter wire.....	84
Figure B.23. Work curve for 10 mil diameter wire.....	84
Figure B.24. Work curve for 12 mil diameter wire.....	85
Figure B.25. Work curve for 15 mil diameter wire.....	85
Figure B.26. Wire hysteresis as a function of pull force for 5 mil diameter wire.....	86
Figure B.27. Wire hysteresis as a function of pull force for 6 mil diameter wire.....	86
Figure B.28. Wire hysteresis as a function of pull force for 8 mil diameter wire.....	87
Figure B.29. Wire hysteresis as a function of pull force for 10 mil diameter wire.....	87
Figure B.30. Wire hysteresis as a function of pull force for 12 mil diameter wire.....	88
Figure B.31. Wire hysteresis as a function of pull force for 15 mil diameter wire.....	88
Figure B.32. Wire hysteresis as a function of pull force for all wires. ....	89
Figure B.33. Wire hysteresis as a function of pull force for 6 mil 2-wire cable.....	90
Figure B.34. Wire hysteresis as a function of pull force for 6 mil 3-wire cable.....	90
Figure B.35. Wire hysteresis as a function of pull force for 6 mil 4-wire cable.....	91
Figure B.36. Wire hysteresis as a function of pull force for all 6 mil diameter cables.....	91
Figure B.37. Resistance curve for 5 mil diameter wire for increasing current values.....	92
Figure B.38. Resistance curve for 6 mil diameter wire for increasing current values.....	92
Figure B.39. Resistance curve for 8 mil diameter wire for increasing current values.....	93
Figure B.40. Resistance curve for 10 mil diameter wire for increasing current values....	93
Figure B.41. Resistance curve for 12 mil diameter wire for increasing current values....	94
Figure B.42. Resistance curve for 15 mil diameter wire for increasing current values....	94
Figure B.43. Temperature curves with transition temperature for 5 mil diameter wire. ..	95
Figure B.44. Temperature curves with transition temperature for 6 mil diameter wire. ..	95
Figure B.45. Temperature curves with transition temperature for 8 mil diameter wire. ..	96
Figure B.46. Temperature curves with transition temperature for 10 mil diameter wire. ..	96
Figure B.47. Temperature curves with transition temperature for 12 mil diameter wire. ..	97
Figure B.48. Temperature curves with transition temperature for 15 mil diameter wire. ..	97

Figure B.49. Temperature curves with transition temperature for all wires. ....	98
Figure C.1. Solidworks drawing of actuator base. ....	100
Figure C.2. Solidworks drawing of short lever arm. ....	101
Figure C.3. Solidworks drawing of long lever arm. ....	102
Figure C.4. Solidworks model of actuator design. ....	103
Figure C.5. Complete actuator assembly ready for testing. ....	104
Figure C.6. Nitinol wire attachment to actuator base. ....	104
Figure C.7. Adjustable wire attachment to nitinol wire. ....	105
Figure C.8. Top view of actuator base. ....	105
Figure C.9. Bottom view of actuator base. ....	106
Figure C.10. Top and side views of short and long lever arms. ....	106

## CHAPTER 1. INTRODUCTION

---

### *1.1. PROBLEM STATEMENT*

Before starting this thesis, a prior project had been started to design and manufacture an enhancement glove which would assist movements made in the hands to help with daily activities such as grasping objects. This glove would not be a fully functional hand on its own, but rather assist someone with weak muscles in their hand. The most important part of this project was to determine the method of actuation for each finger. Motors were the easiest solution since many similar projects had been done using motors, but they were discarded as an option given that there were known problems with using motors in an application with limited space. Nitinol was suggested as a possible actuation method given that it had been used in similar applications with success. The problem with using nitinol is that not much was known about how to use nitinol as an actuator. Also, many actuators using nitinol as the method of actuation were incapable of holding loads needed for an enhancement glove.

It was at this point that the thesis was devoted to the research of nitinol wire for the specific purpose of designing an actuator. The purpose of this thesis would be to research characteristics of nitinol wire making it a more practical option for actuation as well as designing a prototype actuator to prove that it is possible to use this material to design actuators that can hold larger loads. For the specific application of an enhancement glove, nitinol is potentially a preferred method of actuation given that it is small, light, and relatively inexpensive when compared to motors. Additionally, given known parameters

to nitinol actuation wire can allow users to design their own specific actuator to meet their own specifications.

## 1.2. BACKGROUND

Nitinol is a nickel-titanium alloy which is considered part of the shape memory alloy class which means that it goes through the shape memory effect as seen in Figure 1.1.

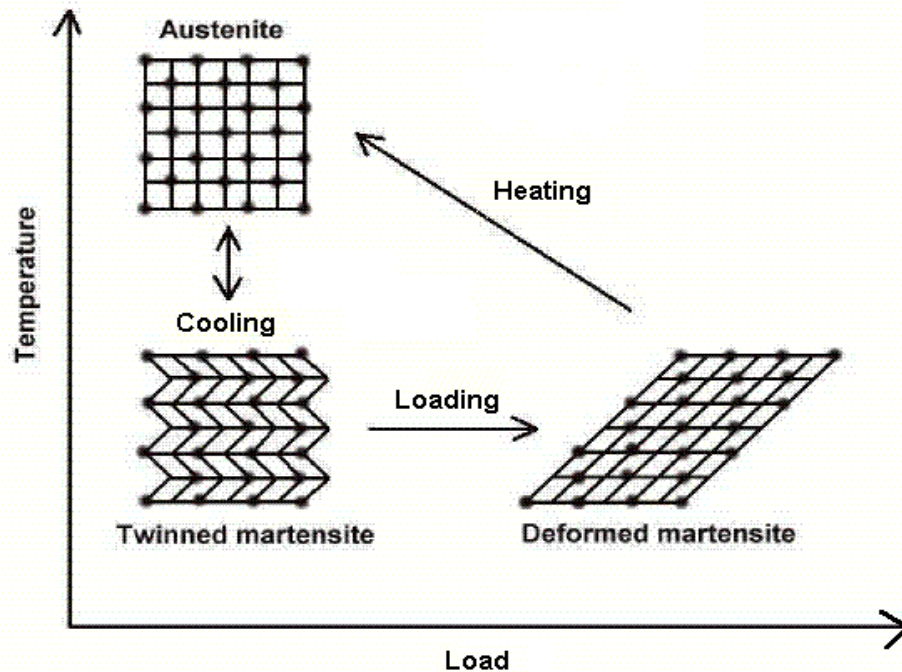


Figure 1.1. Shape memory effect [1].

When the material is held at low temperatures, it is in a very ductile form known as martensite. This allows for the nitinol wire to be bent in any shape. When the material is heated up past its transition temperature, it becomes much more rigid as it enters its austenite form. When nitinol wire enters the austenite state, it returns to its original shape regardless of any deformations that occurred at lower temperatures, therefore it is

referred to as a shape memory alloy. When the material is cooled and re-enters its martensite state, it does not return to its deformed shape until a load is put on the wire [1].

Nitinol covers a wide range of nickel-titanium alloys with different nickel to titanium ratios. Given the specific composition, the characteristics will change. One notable characteristic is the temperature at which nitinol transitions between its martensite and austenite states. This will affect how useful nitinol is in certain situations. For example, in order to use nitinol as an actuator, the transition temperature must be above and differentiable from room temperature so that actuation can be controlled with the addition of heat. Specific samples of nitinol with transition temperatures below room temperature remain in the austenite form and thus can be used because of their rigidity.

The specific nitinol wire used in actuation application is sometimes referred to as Biometal™ and has special shape memory properties. Pieces of Biometal™ wire have an austenite state which is a shorter version of the original wire, and therefore the wire will contract when heat is applied. When the wire contracts, it pulls with a certain amount of force. This pull force can be used as a method of actuation. When the heat is removed, the wire will return to its martensite state which will be the original length of wire granted there is some restoring force in the wire. Unlike other types of nitinol wire, Biometal™ can be cycled millions of times between its martensite and austenite states which make it a desirable material for an actuator. The practical method to heating up Biometal™ wire is to apply a constant current through the wire [2].

For use in this study, a specific nitinol actuation wire called Flexinol® was used. Flexinol® shares many of the same properties as Biometal™, but differs primarily in its transition temperature and pull force, both of which are likely caused by differences in

nickel to titanium ratio. There were two distinctive advantages to using Flexinol® over other nitinol suppliers: published data and minimum order requirements. Images Scientific Instruments, the manufacturer of Flexinol®, provides values for wire resistance, maximum pull force, transition temperature, and time required for actuating the wire. These values offered a great starting point and could be used as a reference as I performed my own tests. Also, Images Scientific Instruments does not have a minimum purchase requirement, meaning that any amount of wire can be purchased at any time. This makes Flexinol® a preferred choice for individuals who only need small quantities of nitinol wire. Other companies can offer lower prices, but large minimum purchases must be met, which is less ideal for prototype designs. Data tables for Flexinol® can be found in Table 1.1 [3].

Table 1.1. Flexinol® wire properties [3].

Diameter Size (Inches)	Resistance (Ohms/Inch)	Maximum Pull Force (grams)	Approximate Current at Room Temperature (mA)	Contraction Time (seconds)	Extension Time (seconds)
0.005	1.8	230	250	1	0.9
0.006	1.3	330	400	1	1.2
0.008	0.8	590	610	1	2.2
0.010	0.5	930	1000	1	3.5
0.012	0.33	1250	1750	1	6.0
0.015	0.2	2000	2750	1	10.0

Nitinol is primarily used in medical applications due to its superelastic properties and high corrosion resistance. Though there are some nitinol actuators currently being produced, they are much less common. The specific nitinol wires used for actuation in this series of tests is claimed to contract approximately 5-6% of its total length [4].



Any remaining background research relevant to the specific tests performed in this thesis will be discussed in the specific section prior to the results.

### ***1.3. NITINOL TESTING OVERVIEW***

At the start of the testing phase, it was important to identify what inputs and outputs would be essential to perform a complete and thorough analysis of nitinol wire. The first two inputs considered were current and wire diameter. The applied current is the most efficient way to heat up nitinol wire which causes it to shorten. The diameter directly affects the geometry of the wire and will thus have an impact on how the wire behaves. There were six wire diameters tested: 5, 6, 8, 10, 12, and 15 thousandths of an inch (mil) diameter wires. Smaller diameter wires were initially considered, but they were not used as it was difficult to clamp the ends of the wire. To simplify the writing of this report, the 6 mil diameter wire will be used as a means to discuss the trends found in all wires. The results for all wires can be found in Appendix B.

After some testing was done, it was determined that pull force should also be analyzed as a third variable. After the removal of current to the nitinol wire, the amount the wire extended was dependent on the applied pull force on the wire. This pull force in the wire had a large effect on the hysteresis in the wire and thus was used as an input to these tests.

Two other inputs that would have been considered were nickel to titanium composition ratio and specific manufacturing process of the wire. These two additional factors will affect how the wire behaves, but given the scope of this thesis, it was determined that doing a complete study of nitinol provided by a single manufacturer

would be sufficient. Unfortunately, not including these inputs limits the numerical results to this specific manufacturer.

To determine the outputs required, it is necessary to know what relevant information is needed for the design of an actuator. The following output variables were measured: wire contraction, temperature, wire hysteresis, current hysteresis, wire resistance, and time constants. First, it is necessary to know the mechanical work that nitinol can provide, which requires knowing the amount of displacement or contraction in the wire as a function of current. Given that nitinol wire is current driven and most electromechanical applications are powered with voltage sources, it is important to know the resistance in the wire. Temperature and time constants of the wire are necessary to determine the maximum internal temperature of an actuator as well as the time required to actuate nitinol. The wire hysteresis and current hysteresis were additional variables that were determined later in the testing process as it became evident that pull force had a large influence on the system outputs.

#### ***1.4. GENERAL TEST SETUP***

The same test setup, with some minor modifications for recording different variables, was used for most of the tests. A detailed schematic of the general setup can be found in Figure 1.2. Each piece of nitinol wire was clamped at the ends using spade lugs which could be easily clamped to a frame. One of the ends of the wire was attached to a replaceable spring that kept the nitinol wire in tension with a certain pull force. This spring was replaced for some tests whenever varying pull forces were desired. A variable constant current power supply was used by attaching two probes at the two ends of the

nitinol wire. This power supply also displayed the voltage drop across the nitinol which could be used to calculate the resistance of the wire during testing. A 5 k $\Omega$  rotary potentiometer was fitted with a lever arm that was attached to the connection between the nitinol wire and spring. Given that nitinol wire only contracts about 5% of its own length, the angular displacement measurement from the potentiometer could be converted to a linear displacement with negligible error. The output resistance from the potentiometer was read by a digital multimeter which was converted to a displacement given the geometry of the test setup.

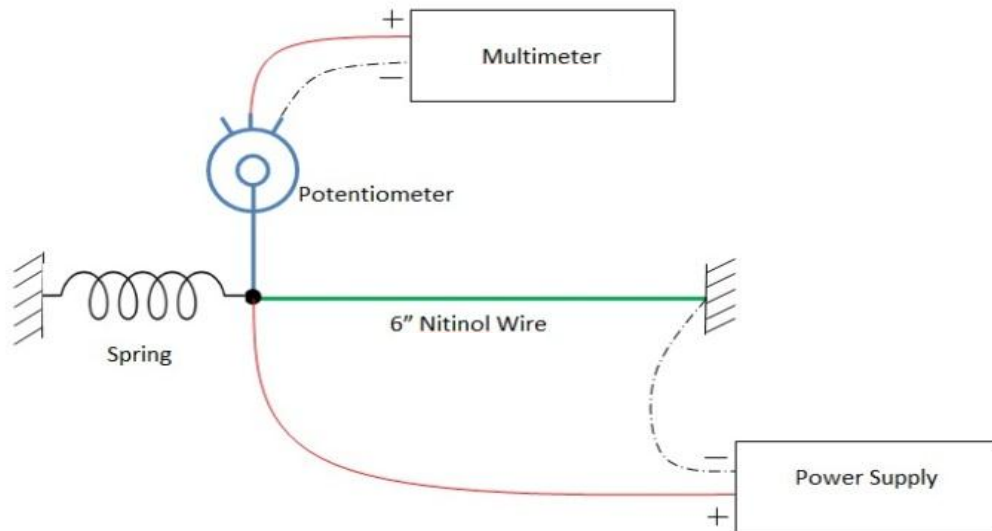


Figure 1.2. General test setup for all tests.

Each individual test has a few minor alterations to record different variables using equipment such as a digital oscilloscope for the transient tests and a 10K3 thermistor, temperature sensor with 10 k $\Omega$  resistance at room temperature, for the temperature tests. Any variations to these tests will be described in the appropriate section prior to discussing the results with a provided schematic. Photographs of the actual setup including wire clamping methods can be found in Appendix A.

## CHAPTER 2. NITINOL WIRE TESTING AND RESULTS

---

### 2.1. WIRE CONTRACTION TEST

#### 2.1.1. PURPOSE OF TEST

When designing an actuator using nitinol, the most important piece of information is knowing the mechanical work that the nitinol wire can produce, or force multiplied by displacement. This set of tests was designed to determine how much nitinol wire contracts when applying a variable current through the wire which is a measure of displacement. Of the characteristics of nitinol, this is probably the most well-known because this material is known for its shape memory effect. The specific wire used in this study should contract approximately 5-6% given the documentation provided by the manufacturer. Also, this wire has a known transition current provided in Table 1.1 which is the current that Flexinol® transitions from martensite to austenite, and thus contracts. These two pieces of information do not take into account how the contraction in the wire varies as a function of current. The desired outcome of this test is an equation that characterizes the contraction in the wire as a function of current along with an associated plot of displacement as a function of current.

#### 2.1.2. SETUP AND PROCEDURE

This test uses the same general setup found in Figure 1.2. Data was collected by slowly increasing the current from a minimum to a maximum through its transition current and recording steady state displacements. This steady state displacement was recorded by directly taking resistance across the potentiometer at steady state and converting it to a displacement given the geometry of the setup. This test was simplified

by normalizing the wire contraction between 0 and 1 to eliminate the error due to wire hysteresis on this test. Wire hysteresis is accounted for in a later test and incorporated into the final displacement model, so this simplification is acceptable. It is worth noting that steady state data was recorded for increasing currents only. Data found from decreasing currents will be discussed in the next set of tests regarding current hysteresis.

### 2.1.3. RESULTS

The raw data recorded for the 6 mil diameter wire can be found in Figure 2.1 along with the regression line, prediction intervals, and control currents, all of which will be discussed in this section. This regression line will be referred to as the contraction curve since the data was collected for increasing current values that cause the wire to contract. The results of wires of other thicknesses are similar and can be found in Appendix B. The first decision that had to be made was the type of regression line used. Two types of

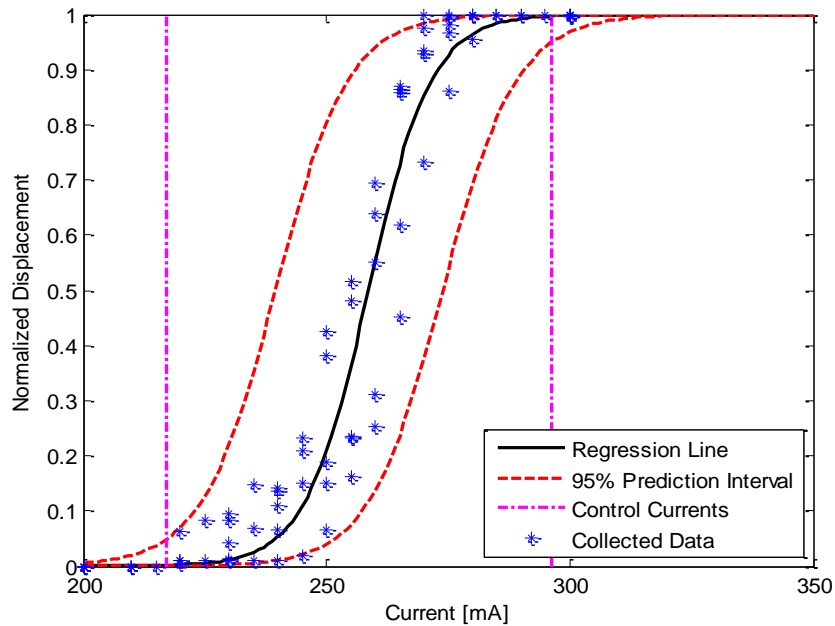


Figure 2.1. Wire contraction curve for 6 mil diameter wire.

regression that were considered were arctangent growth and logistic growth. An arctangent growth curve is non-linear regression line derived from the arctangent function. A logistic growth curve is a type of non-linear regression line used in MINITAB®, a statistical software program where most data analysis was performed. These two regression lines can be found in Equations (2.1) and (2.2):

$$y_{arctangent} = C_2 + (C_1 - C_2) * \left[ \frac{1}{\pi} \tan^{-1} \left( \frac{x - C_3}{C_4} \right) + \frac{1}{2} \right] \quad (2.1)$$

$$y_{logistic} = C_1 + \frac{C_2 - C_1}{1 + e^{(x-C_3)/C_4}} \quad (2.2)$$

Where,  $C_1 \equiv$  the maximum value of y

$C_2 \equiv$  the minimum value of y

$C_3 \equiv$  value of x when y is halfway between  $C_1$  and  $C_2$

$C_4 \equiv$  a measure of spread in the x-direction

$C_1$  and  $C_2$  represent the upper and lower limits in the y-direction which will be set to 1 and 0 since the normalized displacement ranges from 0 to 1. Both of these equations asymptotically approach  $C_1$  as  $x \rightarrow \infty$  and  $C_2$  as  $x \rightarrow -\infty$ . The value of  $C_3$  represents the transition current where the normalized displacement reaches 50% or half of the total contraction.  $C_4$  represents some measure of spread in the x-direction, where larger values of  $C_4$  represent more spread. Both of these equations do a decent job modeling the data, but logistic growth was chosen because it was a better fit for the data collected. Logistic growth regression was chosen as the default regression after this point for any data with

this specific trend. The constants found from these normalized logistic growth regression lines can be found in Table 2.1.

Table 2.1. Constants from wire contraction test.

Wire Diameter [mils]	C1	C2	C3 [mA]	C4 [mA]
5	1	0	213.6	8.66
6	1	0	258.6	6.47
8	1	0	331.7	8.93
10	1	0	437.3	16.92
12	1	0	578.5	26.68
15	1	0	706.6	28.12

The regression line models the average contraction for varying currents, but the data collected from this test has a wide range of values that does not follow the regression line exactly. For example, if a current value of the constant  $C_3$  was applied to a piece of nitinol wire, it is unclear whether or not the wire will be exactly 50% contracted. Prediction intervals were added to reduce the amount of uncertainty in the performance of the wire. In short, these prediction intervals show where 95% of the data is likely to fall. These prediction intervals were obtained using a feature in MINITAB® during the regression analysis. The default prediction intervals provided by MINITAB® were not particularly useful, so a new set of prediction intervals were obtained by linearizing the data, getting prediction intervals on the linear data, and performing a back transformation on those prediction intervals. This process allowed for the two prediction intervals to be logistic growth curves with the same boundaries as the contraction curve, which is more intuitive.

Using these prediction intervals, two control current values were determined which represent the current values where the nitinol wire is either fully extended or contracted. These current values are at the locations where the prediction interval range is 0.05 or 5% of the full contraction distance. These currents allow for a certainty in knowing whether or not the wire has contracted. At the upper control current, the nitinol wire is fully contracted. At the lower control current, the nitinol wire is fully extended. These control currents will be important when creating a control algorithm to decrease reaction times.



## 2.2. CURRENT HYSTERESIS TEST

### 2.2.1. PURPOSE OF TEST

Upon further testing of how current affects the contraction in the wire, it was found that the initial contraction curve does not characterize all contractions in the wire. A study performed by Nitinol Devices and Components (NDC) shows a trend that data collected by heating the wire differs from the data collected by cooling the wire. NDC claims that there will be a gap between these two curves caused by transition temperature hysteresis in the wire [5]. This specific form of hysteresis will be referred to as current hysteresis. In another similar article, NDC published a diagram showing this general trend that accounts for hysteresis which can be found in Figure 2.2 [6]. Through observation, it was

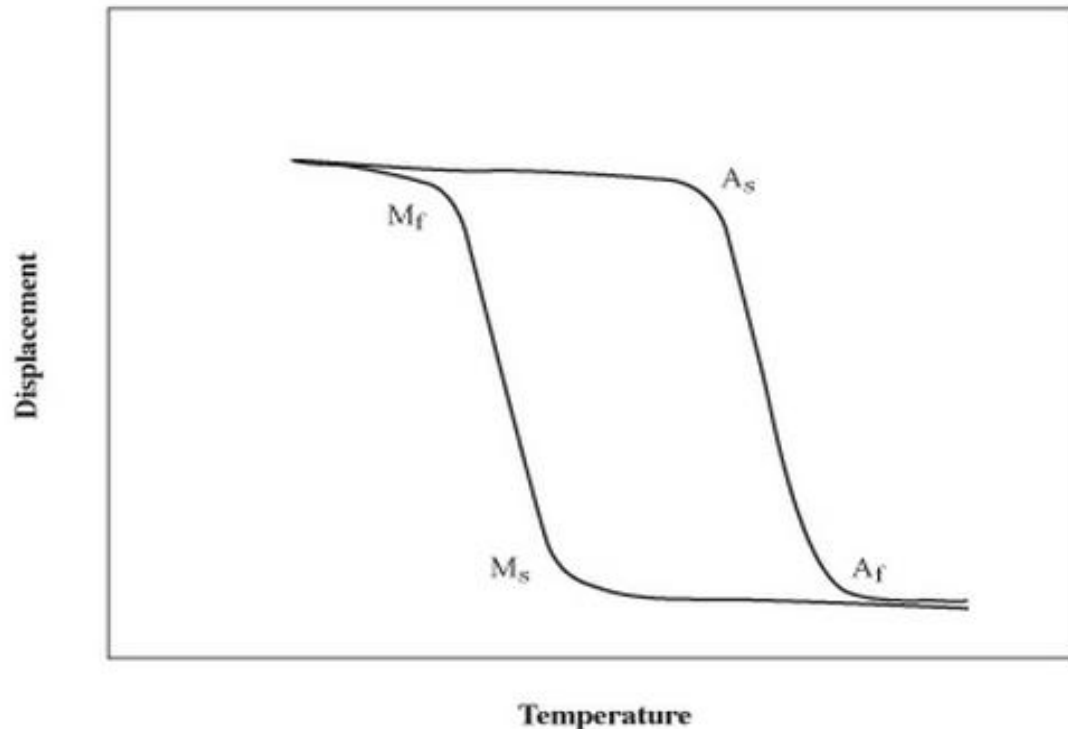


Figure 2.2. Transition temperature hysteresis trend [6].

also found that the pull force in the spring would have an impact on data collected for decreasing current values.

This test was designed to fully characterize wire contraction as a function of current and pull force for both increasing and decreasing currents.

### *2.2.2. SETUP AND PROCEDURE*

This test uses the same general setup found in Figure 1.2. Data was collected by slowly increasing the current from a minimum to a maximum through its transition current and then slowly decreasing the current from a maximum to a minimum through its transition current and recording steady state displacements. Like the wire contraction test, this test was simplified by normalizing the wire contraction to eliminate the error due to wire hysteresis on this test.

Once a set of data was taken using a spring with known pull force, the spring was replaced with another spring with a different pull force. The varying pull force would result in multiple sets of logistic growth curves which could be used to determine the current hysteresis as a function of pull force. Even though the pull force of the spring changes as the nitinol wire contracts, it changes only slightly given that the springs used had relatively low stiffness. If high stiffness springs were used, this change in force would need to be accounted for.

### *2.2.3. RESULTS*

The results for the current hysteresis test performed on 6 mil diameter wire can be found in Figure 2.3. As expected, when data was collected for decreasing currents, a new logistic growth curve was generated confirming the trend found by NDC. This new curve

has the same general shape with a lower transition current. This new curve generated from decreasing current values will be referred to as the extension curve since data is collected for decreasing current values that cause the wire to extend.

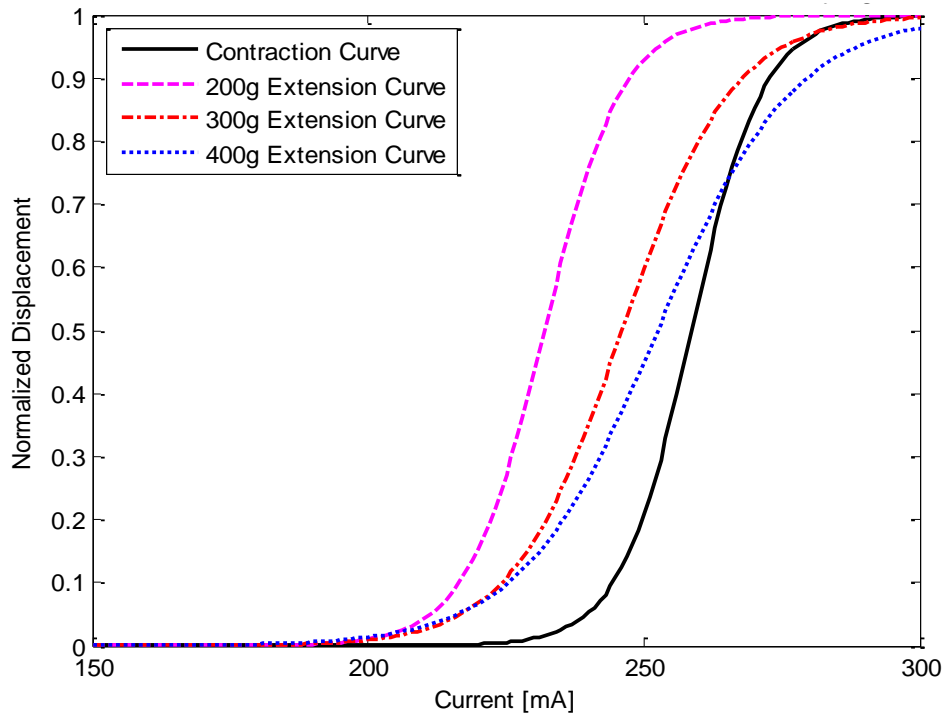


Figure 2.3. Wire contraction and extension curves for 6 mil diameter wire.

The current hysteresis was found to also be a function of the pull force. The larger the pull force on the wire, the smaller the current hysteresis. The important observation is that the transition current for each extension curve approaches that of the initial regression curve, or the contraction curve. Even though the shape of each extension curve changes, it will be assumed that it does not change in order to simplify the final displacement model. Figure 2.4 shows these current hystereses plotted as a function of pull force as a means to approximate the current hysteresis for any pull force. Since the current hysteresis appears to approach zero for large pull forces, an exponential decay

regression line was used. The function for this regression line can be found in Equation (2.3):

$$\Delta I_h = \Delta I_{max} e^{-bF} \quad (2.3)$$

Where,  $\Delta I_h \equiv$  Current Hysteresis [mA]

$F \equiv$  Pull Force [g]

$\Delta I_{max} \equiv$  Maximum Current Hysteresis [mA]

$b \equiv$  Current Hysteresis Decay Rate  $\left[\frac{1}{g}\right]$

The constants for these equations are found in Table 2.2.

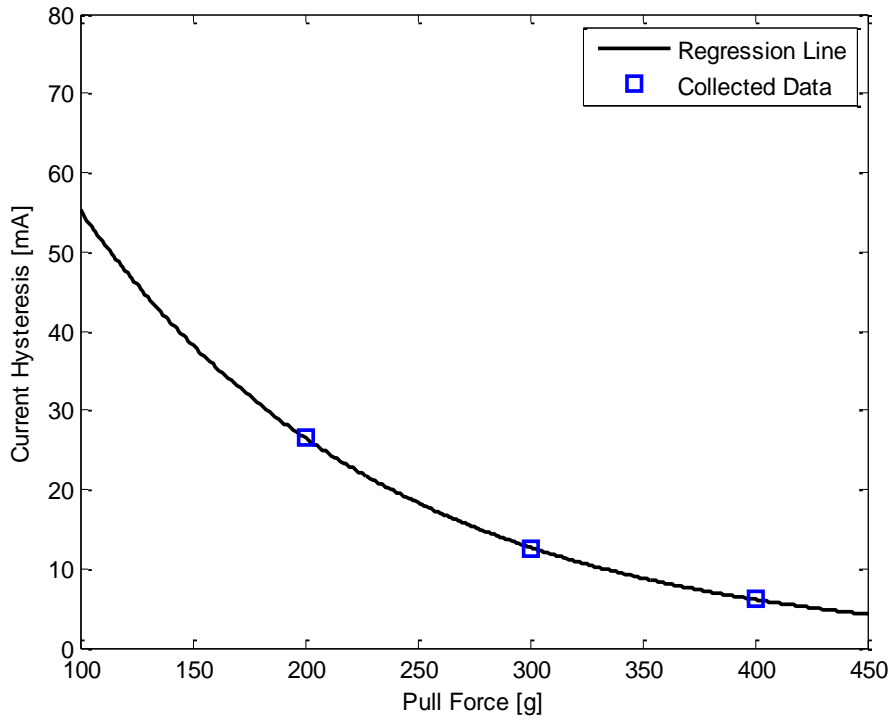


Figure 2.4. Current hysteresis as a function of pull force for 6 mil diameter wire.

## 2.3. WIRE HYSTERESIS TEST

### 2.3.1. PURPOSE OF TEST

Given that the previous tests were normalized to eliminate the effects of wire hysteresis, a separate set of tests was needed to determine the amount of wire hysteresis. Wire hysteresis is a measure of the total contraction that does not occur when a specific pull force is applied to the wire. When shape memory wire is cooled down from the austenite state to the martensite state, some pull force is required to restore the wire to its original length; without a substantial restoring force, wire hysteresis occurs. This set of tests was designed to determine the wire hysteresis as a function of pull force.

### 2.3.2. SETUP AND PROCEDURE

Two setups were used for this set of tests. The first of these is the general test setup found in Figure 1.2. The second setup was used to apply a constant pull force to the wire. This pull force was applied by attaching a weight to one end of the nitinol wire with the other end fixed. By letting the weight hang off one end, the wire would be pulled with a constant force determined by the mass of the weight. A schematic of this second setup can be found in Figure 2.5.

To accurately determine the wire hysteresis for different pull forces, the contraction in the wire was measured immediately after applying a pull force to



Figure 2.5. Test setup for wire hysteresis test.

the wire using the second setup for this test. Applying this force would extend the wire slightly if there was any hysteresis in the wire. Since the wire always contracts to the same length, the amount the wire contracted would represent a restoring displacement associated with the pull force applied prior to contraction. The wire hysteresis could be found by subtracting the restoring displacement from the total contraction displacement. This process was done for each wire at varying initial pull forces.

### 2.3.3. RESULTS

For each wire, as this pull force increased, the restoring displacement increased and the wire hysteresis decreased. This means that larger pull forces result in larger contractions, which result in more mechanical work. Figure 2.6 shows the wire hysteresis

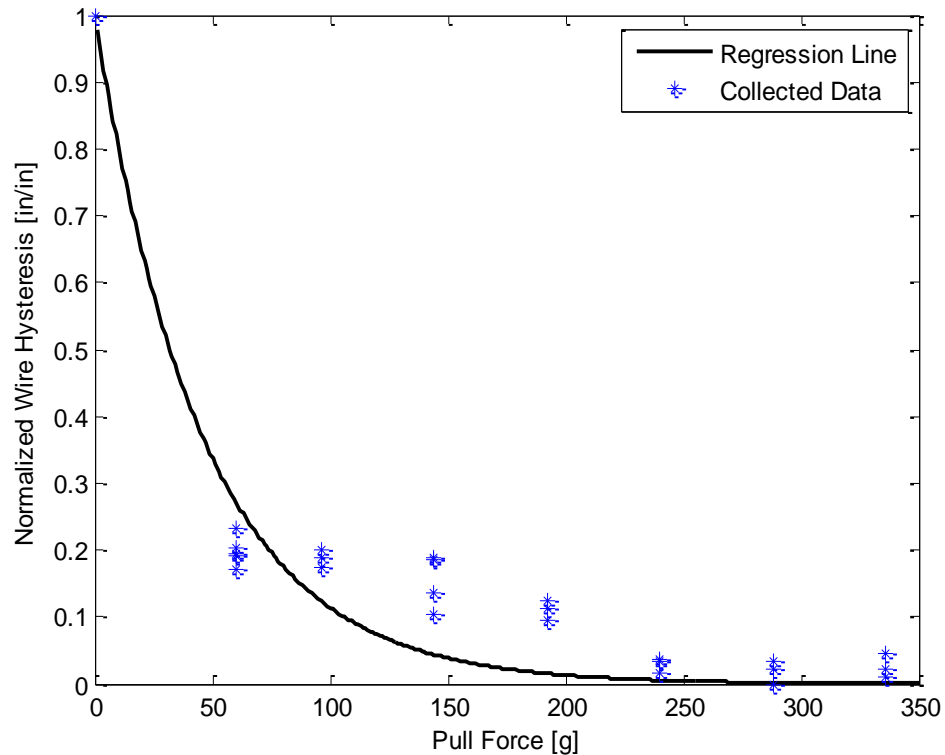


Figure 2.6. Wire hysteresis as a function of pull force for 6 mil diameter wire.

as a function of pull force for the 6 mil diameter wire. This curve was also normalized between 0 and 1 to match the scale for the wire contraction test which also was normalized between 0 and 1. Using this scale allowed for easy development of the final displacement model.

An exponential decay regression line was fit to the data in order to determine the amount of hysteresis that would be found in the wire for any applied pull force. The function for this regression line can be found in Equation (2.4):

$$\Delta l_h = \Delta l_{max} e^{-aF} \quad (2.4)$$

Where,  $\Delta l_h \equiv$  Wire Hysteresis  $\left[ \frac{in}{in} \right]$

$$\Delta l_{max} = 0.066 \left[ \frac{in}{in} \right]$$

$F \equiv$  Pull Force [g]

$a \equiv$  Wire Hysteresis Decay Rate  $\left[ \frac{1}{g} \right]$

The constants for these equations are found in Table 2.2. The value for  $\Delta l_{max}$  was found from the results of these tests.

One note to make is that the pull forces used in this study are in units of grams and kilograms. This has been done for two specific reasons. First, the specifications provided by the manufacturer had pull forces using these units, so the same units were used throughout my tests. Additionally, the nitinol wire is supporting a load generated by the addition of a mass at the end of the wire. This mass is often in units of grams. To convert these to a conventional unit of force, they need to be multiplied by the numerical value for gravity.

## 2.4. FINAL DISPLACEMENT MODEL

Given the results from the wire contraction, current hysteresis, and wire hysteresis tests, a final model was made to fully characterize nitinol actuation displacement as a function of pull force and current. A graphical representation of the final displacement model can be found in Figure 2.7.

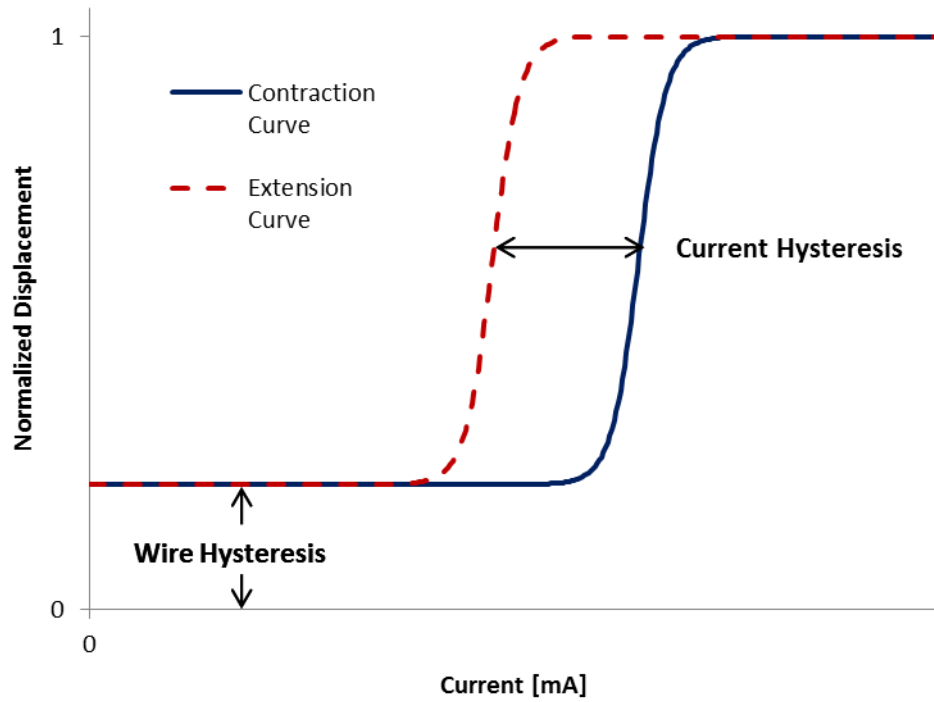


Figure 2.7. Final displacement model.

The logistic growth equations for the contraction and extension curves are shown in Equations (2.5) and (2.6):

$$\Delta l_{contract} = \Delta l_{max} + \frac{\Delta l_h - \Delta l_{max}}{1 + e^{((I-I^*)/c)}} \quad (2.5)$$

$$\Delta l_{extend} = \Delta l_{max} + \frac{\Delta l_h - \Delta l_{max}}{1 + e^{((I-I^*+\Delta I_h)/c)}} \quad (2.6)$$



Where,  $\Delta l_{max} = 0.066 \left[ \frac{in}{in} \right]$

$$\Delta l_h = \Delta l_{max} e^{-aF} \equiv \text{Wire Hysteresis} \left[ \frac{in}{in} \right]$$

$$\Delta I_h = \Delta I_{max} e^{-bF} \equiv \text{Current Hysteresis [mA]}$$

$$F \equiv \text{Pull Force [g]}$$

$$I \equiv \text{Current [mA]}$$

$$\Delta I_{max} \equiv \text{Maximum Current Hysteresis [mA]}$$

$$I^* \equiv \text{Transition Current [mA]}$$

$$C \equiv \text{Current Spread [mA]}$$

$$a \equiv \text{Wire Hysteresis Decay Rate} \left[ \frac{1}{g} \right]$$

$$b \equiv \text{Current Hysteresis Decay Rate} \left[ \frac{1}{g} \right]$$

The required constants are found in Table 2.2. The value for  $\Delta l_{max}$  was found from the results of these tests.

These equations were created using the standard form of the logistic growth regression line including factors for wire hysteresis and current hysteresis. All the constants used in these equations were derived from regression lines derived from the three previous tests.  $I^*$  and  $C$  come from Figure 2.1,  $\Delta I_{max}$  and  $b$  come from Figure 2.4, and “ $a$ ” comes from Figure 2.6.

The final displacement model is the means to know contraction in the wire as a function of both current and pull force. Given that the pull force is known for this model, the mechanical work can be determined by multiplying the force by displacement.

Knowing this allows for the design of an actuator with custom specifications for mechanical work.

Table 2.2. Constants for final displacement model.

Wire Diameter [mils]	$\Delta I_{max}$ [mA]	$I^*$ [mA]	$C$ [mA]	$a$ [g <sup>-1</sup> ]	$b$ [g <sup>-1</sup> ]
5	152.3	213.6	8.66	0.01708	0.00860
6	115.1	258.6	6.47	0.02172	0.00735
8	265.1	331.7	8.93	0.00725	0.00542
10	199.8	437.3	16.92	0.00434	0.00080
12	335.5	578.5	26.68	0.00313	0.00039
15	393.5	706.6	28.12	0.00186	0.00018

## **2.5. MAXIMUM PULL FORCE**

### **2.5.1. PURPOSE OF TEST**

The final displacement model provides enough information to determine the mechanical work of nitinol wire granted that the pull force does not exceed the physical limitations of the wire. For designing an actuator, it is important to know the maximum mechanical work that the actuator can exert, meaning the correlation between work and pull force must be known. Through careful analysis of what would be necessary in actuator design, it was determined that three distinct force values would be necessary for each wire: The maximum force before wire contraction starts to decrease ( $F_{max}$ ), the minimum force to produce no wire contraction when the wire is heated ( $F_0$ ), and the maximum force before wire failure ( $F_f$ ). This test would be done as a means to find these three force values for each diameter wire.

### **2.5.2. SETUP AND PROCEDURE**

One single setup was used for this test similar to the second setup used in the wire hysteresis test where a pull force was applied to the wire found in Figure 2.5. The pull force was applied by attaching a weight to one end of the nitinol wire with the other end fixed. By letting the weight hang off one end, the wire would be pulled with a constant force determined by the mass of the weight. Additionally, a constant current power supply was attached to the ends of the nitinol wire so the wire could contract while a constant pull force was applied.

To start the process of obtaining the three force values, the wire was contracted by applying a constant current through the wire with a mass attached at one end. This mass

was then increased until there was a noticeable difference in the amount the nitinol wire contracted, denoting the applied force  $F_{max}$ . The mass was then increased further until there was no noticeable contraction, denoting the applied force  $F_0$ . The wire was then removed from the power supply and the mass was increased until the wire failed, denoting the applied force  $F_f$ .

### 2.5.3. RESULTS

Figure 2.8 shows these three forces plotted against wire diameter. Each of these three forces could be converted to a stress by dividing them by the cross sectional area of the wire. This stress should be constant from wire to wire, meaning that force should be linearly proportional to cross sectional area. Since area is a function of diameter squared, pull force will also be a function of diameter squared, which is why a quadratic

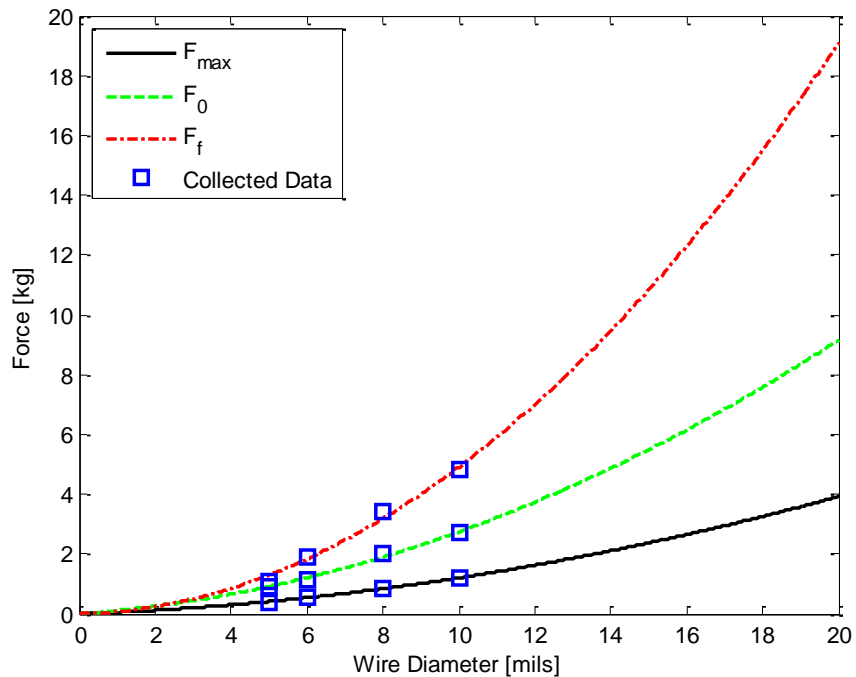


Figure 2.8. Force curves for any wire diameter.

regression line was used. The quadratic regression equations for the three forces are shown in Equations (2.7) - (2.9):

$$F_{max} = u_{max}d^2 + v_{max}d \quad (2.7)$$

$$F_0 = u_0d^2 + v_0d \quad (2.8)$$

$$F_f = u_f d^2 + v_f d \quad (2.9)$$

Where  $u$  and  $v$  are constants for each wire,  $d$  is the wire diameter in mils, and  $F$  is the pull force in grams. The constants for these equations can be found in Table 2.3.

Table 2.3. Constants for force curves.

Subscript	$u$ [g/mil <sup>2</sup> ]	$v$ [g/mil]
<i>max</i>	7.565	44.808
<i>0</i>	18.355	90.615
<i>f</i>	46.272	28.259
<i>max_w</i>	9.466	43.467

To interpret Figure 2.8, for any wire diameter, pull forces under  $F_{max}$  are desired as they do not reduce the amount the nitinol wire will contract. Pull forces between  $F_{max}$  and  $F_0$  can be used, but will contract less. Pull forces between  $F_0$  and  $F_f$  will result in no contraction and pull forces exceeding  $F_f$  will result in wire failure. One thing to note is that the 12 and 15 mil diameter wires were not tested due to limited resources and the large forces required for failure. Given the accurate trends in the data for the other diameter wires, these forces can be extrapolated from the regression curves.

This curve alone does not explain at what force maximum mechanical work can be expected. One can predict that the maximum mechanical work will occur somewhere

between  $F_{max}$  and  $F_0$ , much closer to  $F_{max}$ . In order to know the maximum mechanical work, the work needs to be plotted as a function of pull force. The mechanical work is found by simply multiplying force by displacement. The displacement of nitinol wire between pull forces of  $F_{max}$  and  $F_0$  was modeled to be linear since the test results do not suggest a more complicated trend. This displacement also includes the effects of wire hysteresis, which is almost negligible for larger forces. The work curve for 6 mil wire can be found in Figure 2.9.

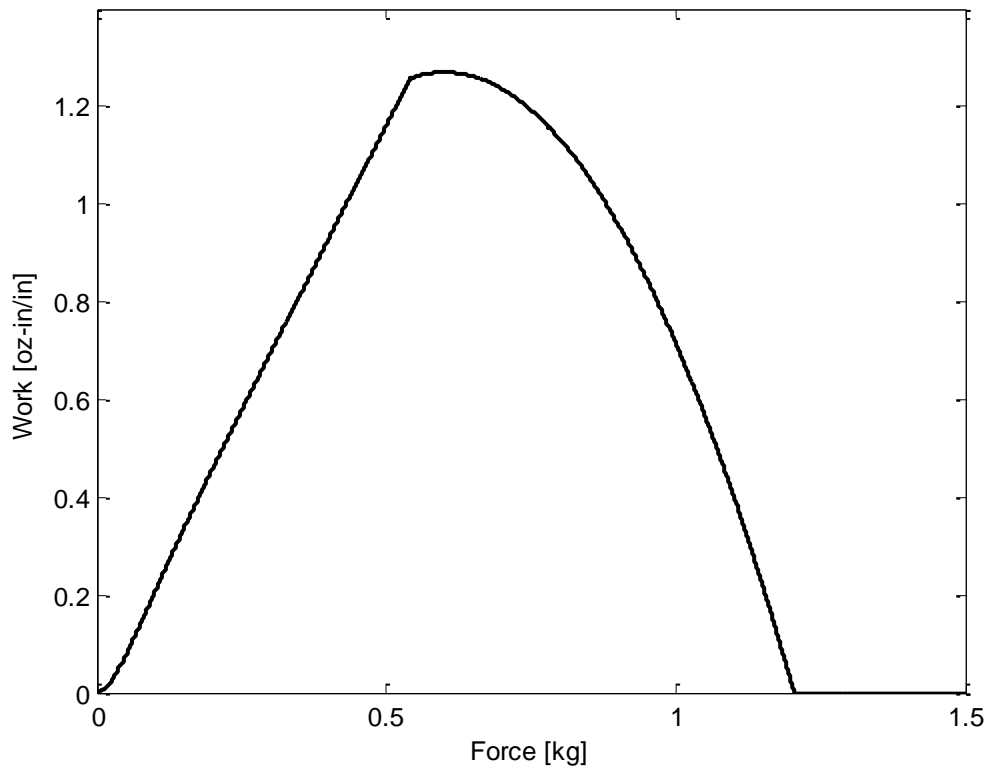


Figure 2.9. Work curve for 6 mil diameter wire.

As seen in the figure, maximum mechanical work occurs at a pull force slightly above  $F_{max}$ . Additionally, a numerical value for mechanical work can be found in oz-in/in,

which is important to know for design considerations. The numerical values for maximum mechanical work and the force required for maximum mechanical work, denoted as  $F_{max\_w}$ , can be found in Table 2.4.

Table 2.4. Maximum force and work values for all wires.

Wire Diameter [mils]	$F_{max}$ [g]	$F_{max\_w}$ [g]	Maximum Work [oz-in/in]
5	413	457	0.968
6	541	602	1.270
8	843	953	1.981
10	1205	1381	2.833
12	1627	1881	3.832
15	2374	2784	5.586

In a similar fashion to Equations (2.7) - (2.9), a quadratic regression can be developed for the force resulting in mechanical work as seen in Equation (2.10).

$$F_{max\_w} = u_{max\_w}d^2 + v_{max\_w}d \quad (2.10)$$

Where  $u$  and  $v$  are constants for each wire,  $d$  is the wire diameter in mils, and  $F$  is the pull force in grams. The constants for these equations can be found in Table 2.3. For comparison, Figure 2.10 shows all four forces plotted against wire diameter. This figure shows graphically that maximum mechanical work occurs when a pull force slightly above  $F_{max}$  is used.

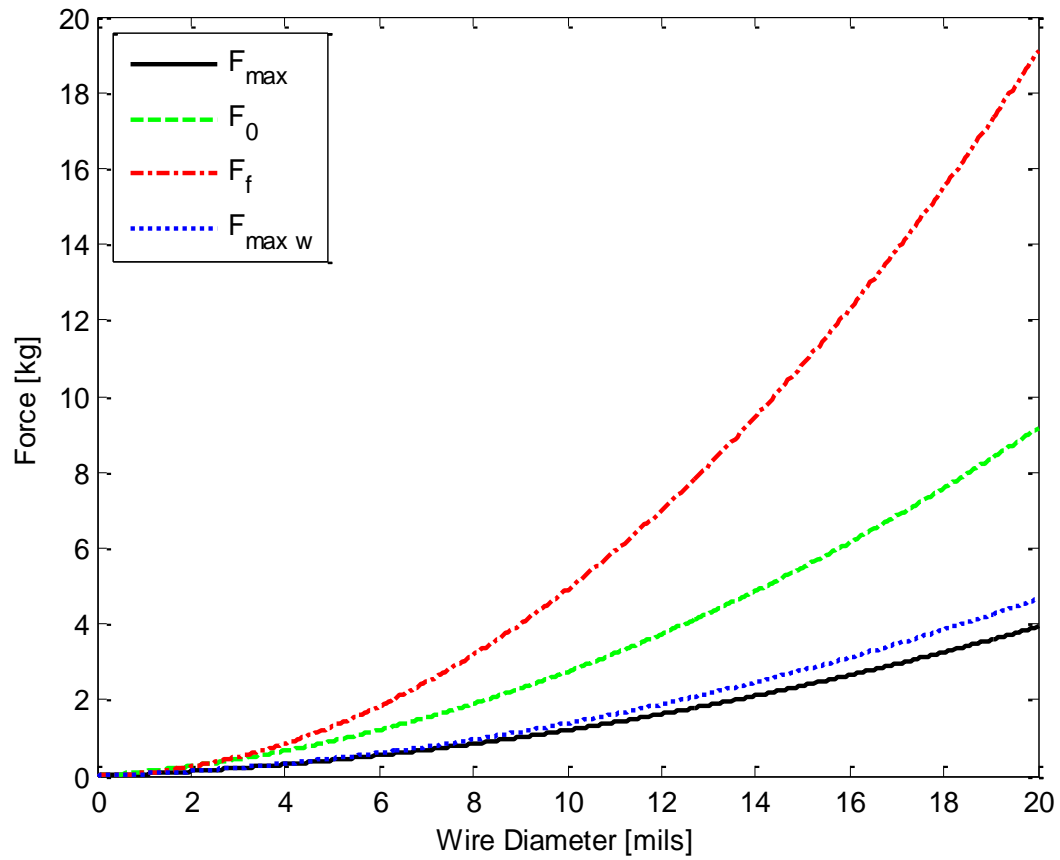


Figure 2.10. Force curves for any wire diameter including  $F_{max\_w}$ .



## **2.6. VARIABLE WIRE RESISTANCE**

### **2.6.1. PURPOSE OF TEST**

The data table provided with Flexinol® suggests that there is one constant value for the resistance of a strand of nitinol wire, but given the change of crystalline structure, it seems that the resistance of nitinol should change as it transitions from martensite to austenite, and vice versa. Through observations from previous tests, this trend was confirmed. It is important to know the resistance of the wire because most electromechanical systems are powered with a constant voltage source rather than a constant current source. If a voltage source is used to provide power to a nitinol actuator, it is very important to know these resistance values since nitinol is current driven. The desired output of this test is an equation for the resistance of the wire as a function of current.

### **2.6.2. SETUP AND PROCEDURE**

Since the resistance of the nitinol wire can be determined by dividing the voltage across the wire by the current through the wire, a separate test was not needed to obtain data for the resistance in each wire. The setup and procedures from the wire contraction test and current hysteresis tests were used to collect the resistance data. The constant current power supply is capable of also measuring the voltage drop across the power supply, so additional equipment was not required.

### **2.6.3. RESULTS**

Observations early on in the testing process suggested that there would be two distinct resistance values for each wire, but analysis of the results showed that there is a

similar logistic growth trend in resistance values as a function of current that occurs through the transition current. Figure 2.11 shows the regression curve for the wire resistance in the 6 mil diameter wire that is associated with increasing current values that cause the wire to contract.

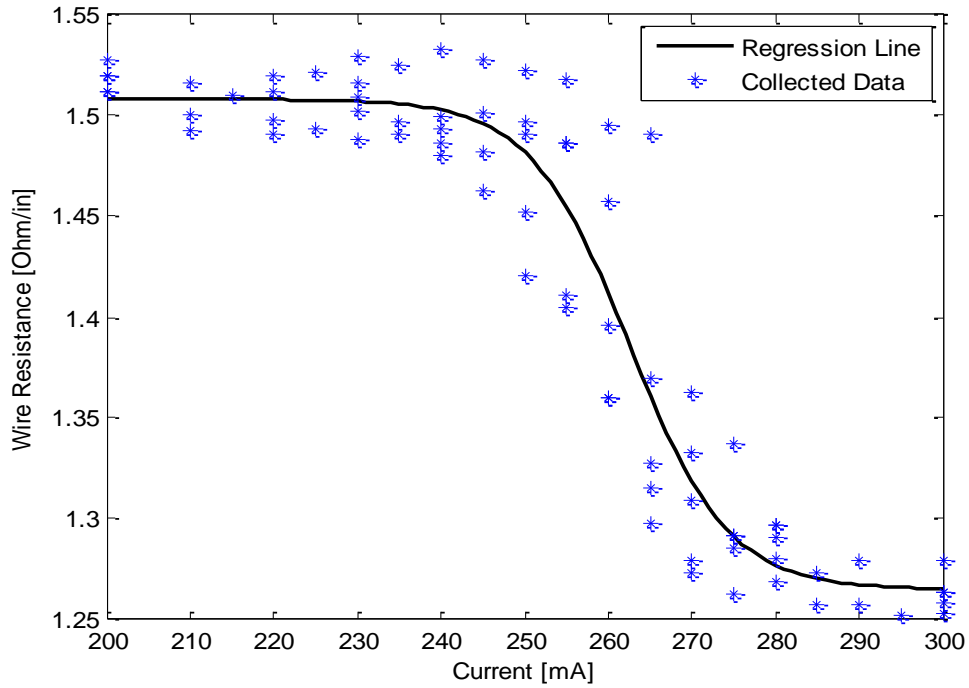


Figure 2.11. Resistance curve for 6 mil diameter wire for increasing current values.

When this curve is compared to the logistic growth curve for wire contraction, the transition current and shape appear to be almost the same, so the same constants can be used for the resistance regression giving Equations (2.11) and (2.12):

$$R_{contract} = R_{min} + \frac{R_{max} - R_{min}}{1 + e^{((I-I^*)/c)}} \quad (2.11)$$

$$R_{extend} = R_{min} + \frac{R_{max} - R_{min}}{1 + e^{((I-I^*+\Delta I_h)/c)}} \quad (2.12)$$

Where,  $\Delta I_h = \Delta I_{max} e^{-bF} \equiv$  Current Hysteresis [mA]

$F \equiv$  Pull Force [g]

$I \equiv$  Current [mA]

$\Delta I_{max} \equiv$  Maximum Current Hysteresis [mA]

$I^* \equiv$  Transition Current [mA]

$C \equiv$  Current Spread [mA]

$b \equiv$  Current Hysteresis Decay Rate  $\left[\frac{1}{g}\right]$

$R_{min} \equiv$  Minimum Resistance [ $\Omega$ ]

$R_{max} \equiv$  Maximum Resistance [ $\Omega$ ]

The required constants are found in Table 2.2 and Table 2.5.

Table 2.5. Resistance values for varying wire diameter.

Wire Diameter [mils]	$R_{max}$ [ $\Omega$ /in]	$R_{min}$ [ $\Omega$ /in]
5	2.131	1.823
6	1.501	1.266
8	0.812	0.692
10	0.544	0.467
12	0.359	0.310
15	0.292	0.269

Same as the final displacement model,  $I^*$  and  $C$  come from Figure 2.1, and  $\Delta I_{max}$  and  $b$  come from Figure 2.4. The two new variables  $R_{min}$  and  $R_{max}$  come from Figure 2.11.

## **2.7. TEMPERATURE TEST**

### **2.7.1. PURPOSE OF TEST**

In practice, nitinol wire is actuated by applying a current through the wire, but in theory, it is actuated by temperature; current is a means to heat up the wire to a specific temperature. From a design standpoint, it is important to know the temperature an actuator will reach so the rest of the system can be designed with that in mind. The temperature of the wire is a function of resistance and current,  $I^2R$ , as this is the heat dissipation of the wire to the atmosphere. If nitinol had a constant resistance, one would expect temperature to be a quadratic function in terms of current. Given that nitinol has two distinct resistances, the temperature vs. current curve should have a parabolic shape on either side of the transition current where the concavity for larger currents is smaller given the decrease in resistance.

In addition to knowing the transition temperature, it is important to know the temperature of the wire as a function of current to be used as a design consideration. Anything the wire is in contact with must have a melting point substantially higher than the maximum temperature the wire will reach. This is very crucial if plastics are used as an actuator chassis because they have relatively low melting points when compared to metals. The outcome of this test is to have an equation for wire temperature as a function of current.

### **2.7.2. SETUP AND PROCEDURE**

To measure the temperature of the wire, a small 10K3 thermistor was wrapped around the nitinol wire with the entire probe being in contact with the wire. 10K3 thermistors get

their name from having a resistance of 10 k $\Omega$  at room temperature. This specific type of thermistor is able to sense temperatures up to 100°C, which is higher than the transition temperature of Flexinol®. By attaching the thermistor leads to a multimeter, the resistance can be measured and converted to a temperature using calibration constants provided by the manufacturer. The nitinol wire is held in tension using a spring, and the nitinol wire is heated up using a constant current power supply with leads attached to the two ends of nitinol wire. A schematic of this test setup can be found in Figure 2.12.

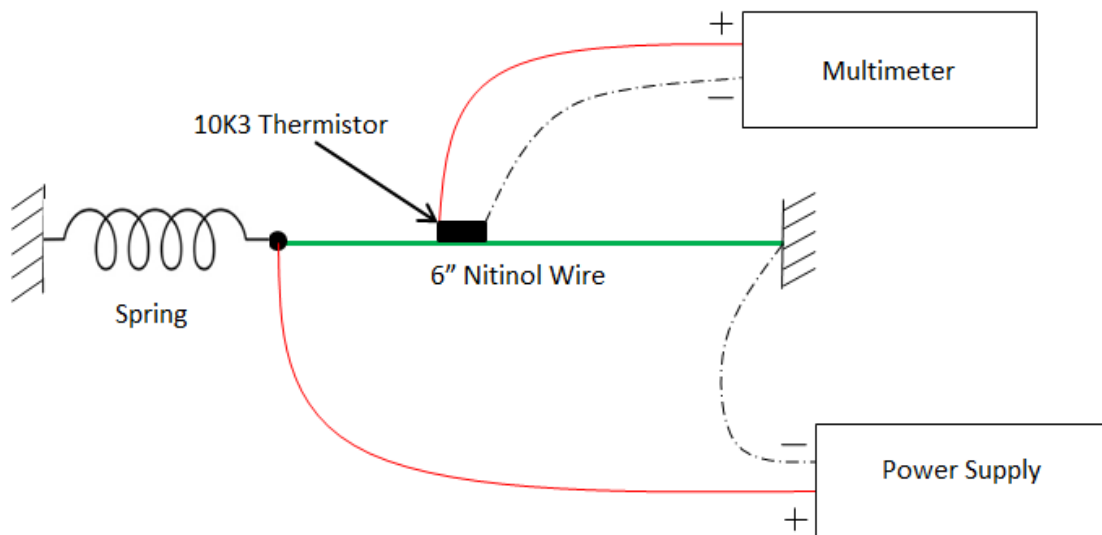


Figure 2.12. Test setup for temperature test.

Data was collected by slowly increasing the current from a minimum to a maximum through its transition current and recording the steady state resistance of the thermistor which could be converted to a temperature. Data was also collected for decreasing currents, but this did not result in an additional regression line.

### 2.7.3. RESULTS

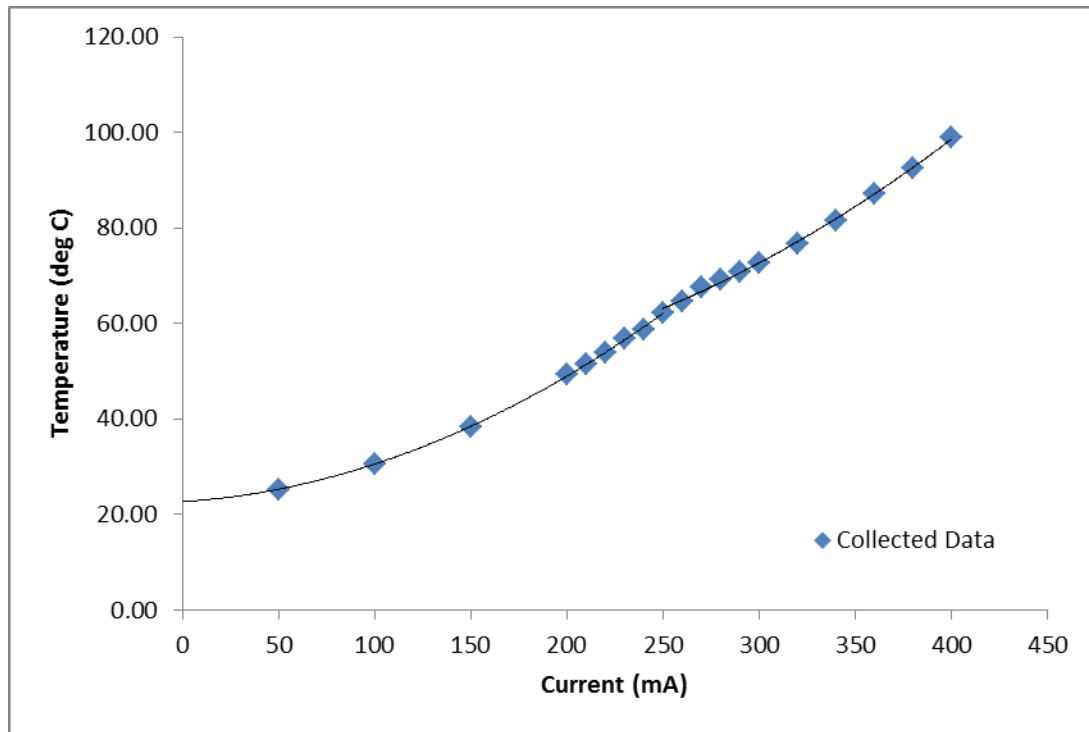


Figure 2.13. Initial temperature data with double parabolic regression.

When initial tests were performed for measuring the temperature, a distinct double parabolic function was seen confirming what would be expected in theory. A set of data with a double parabolic regression can be seen in Figure 2.13. In practice though, having two functions to define the temperature for a single wire is too much. It turns out that a single cubic curve can be used to approximate the temperature for a reasonable range of currents for each wire. This cubic function for temperature is represented by Equation (2.13) that was generated using MINITAB®:

$$T = T_1 I^3 + T_2 I^2 + T_3 I + T_4 \quad (2.13)$$

Where  $T_1$ ,  $T_2$ , and  $T_3$  are cubic, quadratic, and linear coefficients determined by the cubic regression and  $T_4$  is the constant term which is fixed at room temperature. For this regression,  $T_4$  was fixed at 23.5 °C. Table 2.6 shows these constant values for all wire diameters.

Table 2.6. Temperature curve constants using the compensated regression curves.

Wire Diameter [mils]	$T_1$ [°C/mA <sup>3</sup> ]	$T_2$ [°C/mA <sup>2</sup> ]	$T_3$ [°C/mA]	$T_4$ [°C]
5	-8.40E-07	9.18E-04	0.0475	23.5
6	-4.75E-07	5.64E-04	0.0555	23.5
8	-1.23E-07	2.92E-04	0.0489	23.5
10	-8.62E-08	2.05E-04	0.0274	23.5
12	-6.59E-08	1.52E-04	0.0100	23.5
15	-4.42E-08	1.12E-04	0.0050	23.5

Given that all nitinol samples used in these tests have a relatively small diameter when compared to the diameter of the thermistor probe, it was known there would be some error in this method of data collection. This error would result in each wire having a different transition temperature. In theory, each wire should have the same transition temperature, so this error was compensated by adjusting the cubic regression for each wire so that the transition temperatures were the same. The maximum transition temperature was used as the true value since errors in temperature measurements are most likely to decrease the recorded temperature. Each regression line was then compensated by changing the linear component,  $T_3$ , so that the true transition temperature would occur at the transition current for each wire. The smaller diameter wires needed the most compensation since it was harder to get an accurate reading on such small diameter wires. Figure 2.14 shows the temperature curves for the 6 mil diameter wire which yield

a final transition temperature of 67.4 °C. This figure shows the compensated and uncompensated regression lines, where the compensated regression line adjusts the linear term to reduce the effects of thermistor measurement error. It is worth noting that the values in Table 2.6 use the compensated values for  $T_3$ .

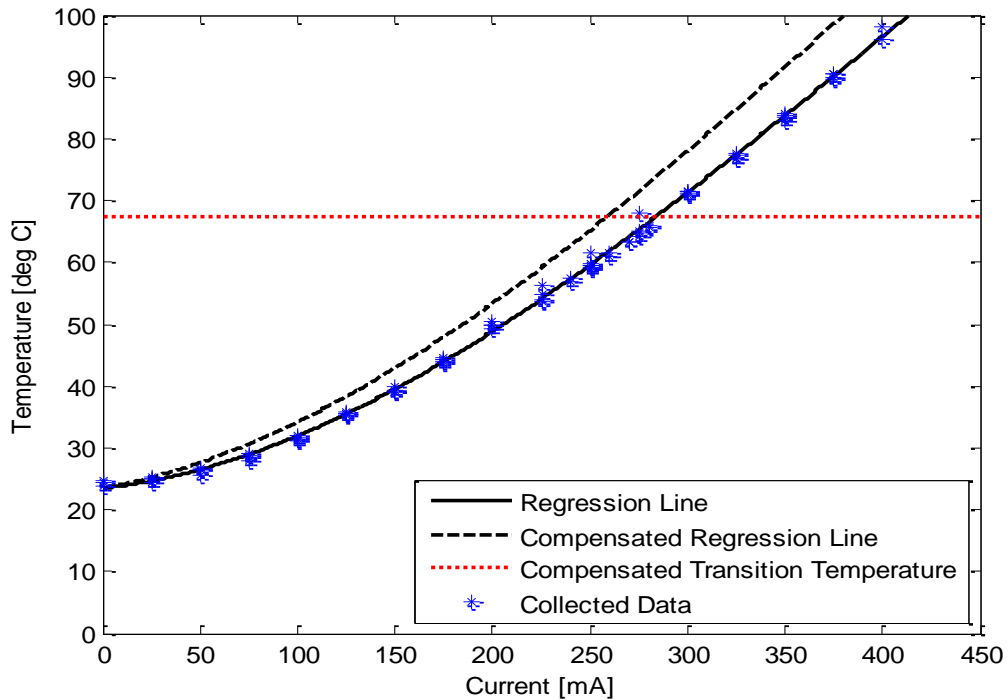


Figure 2.14. Temperature curves with transition temperature for 6 mil diameter wire.

Knowing the transition temperature can help determine the nickel to titanium ratio. More research was done by NDC to create a correlation between nitinol transition temperature and Nickel to Titanium ratio as seen in Figure 2.15. It is estimated that this ratio is about 0.98 for the samples of wire tested. This ratio will definitely affect the transition temperature of nitinol, but it may also have an impact on other characteristics such as wire time constants and max pull force.



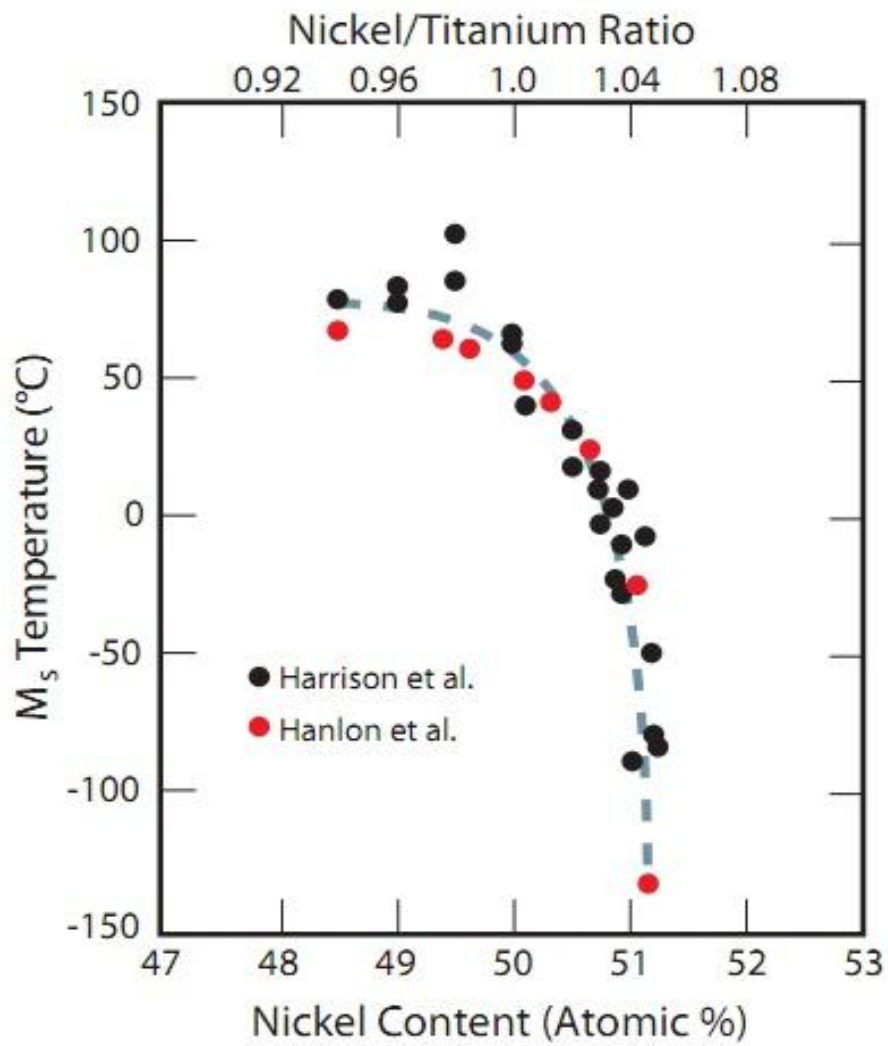


Figure 2.15. Transition current as a function of Nickel to Titanium ratio [5].

## **2.8. TRANSIENT TEST**

### **2.8.1. PURPOSE OF TEST**

Thus far, all presented results relate to steady state values with no regards to any transient effects. Of all the transient effects, it is more useful to know how the nitinol contracts as a function of time. This following test was designed to determine the time constants for each of the wires so that total reaction times could be determined. Through observation, it was also found that each wire would not immediately contract when current was applied. This is due to the fact that it takes time for the wire to reach the transition temperature when it starts contracting. It was theorized that if the wires were partially heated, they would contract much more quickly. This test would be repeated for each wire changing the initial current prior to wire contraction and recording the results.

### **2.8.2. SETUP AND PROCEDURE**

This test used the same general setup as the wire contraction test with the addition of two oscilloscope probes that were used for triggering and data collection. The first set of oscilloscope probes was put across the power supply which was used to trigger data collection. The second set of oscilloscope probes was placed as part of a circuit made with the potentiometer leads. Since the oscilloscope measures voltage drops and not resistance, a small circuit was created by placing a 2.7 k $\Omega$  resistor in series with the potentiometer leads and a 5V voltage drop between the two resistances. The second set of oscilloscope probes was then placed across the resistor in this circuit. The voltage measured by the second oscilloscope is representative of the length of the wire and can be used to record changes in length with respect to time. A 330 $\mu$ F capacitor was placed in

parallel with the resistor to smooth out any noise. A schematic of this test setup can be found in Figure 2.16.

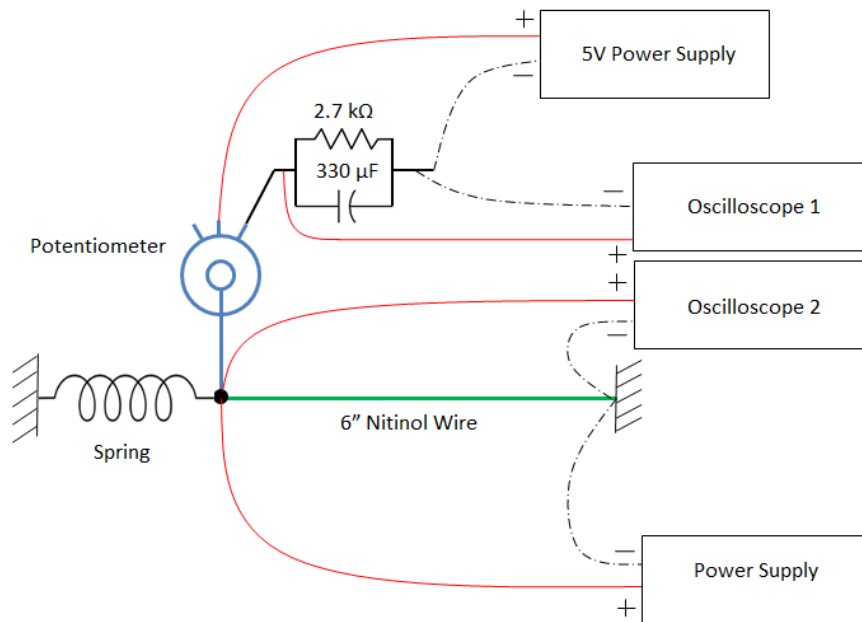


Figure 2.16. Test setup for transient test.

To determine the time constants for each wire, a constant current was applied to each wire while the oscilloscope recorded the transient effects. The time required to fully contract the wire would be representative of twice the time constant at a 95% contraction level. The time constant in the wire is the equivalent of the time required for a step response to cause the wire to contract 63.2% of its total contraction displacement. Even though the response of the wire had a slightly second ordered nature to it, it was assumed that the behavior was first ordered to simplify the model. This slight second ordered trend is due to a small lag in contraction as the temperature changes. This test was also performed by cooling wires down by removing the current applied to the wire and recording the transient effects. Each wire has two time constants, one for the increasing

currents and one for decreasing currents. Each of the transient tests was repeated with adjusting the initial current to pre-heat the wire before contraction and extension.

### 2.8.3. RESULTS

Table 2.7. Contraction and extension time constants.

Wire Diameter [mils]	Contraction Time Constant [s]	Extension Time Constant [s]
5	1.472	1.102
6	1.087	1.100
8	1.157	2.009
10	1.261	3.521
12	1.343	5.841
15	1.782	9.936

Table 2.7 shows the two time constants for each wire. It is important to note that all transient results were at room temperature without the aid of any fluid bath or air convection to decrease the time required to cool the wire. Given that methods for cooling down the wire could result in inconsistent results from wire to wire, using still air was used as a means to compare the results to each other.

The time constant alone does not give enough information about how long it takes for a piece of nitinol wire to contract or extend once current is applied or removed. Figure 2.17 and Figure 2.18 show the time to contraction and time to extension for each wire at varying initial currents. In all cases, pre-heating the wire resulted in a decrease in total reaction time. These figures do not show the total contraction and extension times, but rather the time prior to contraction or extension.

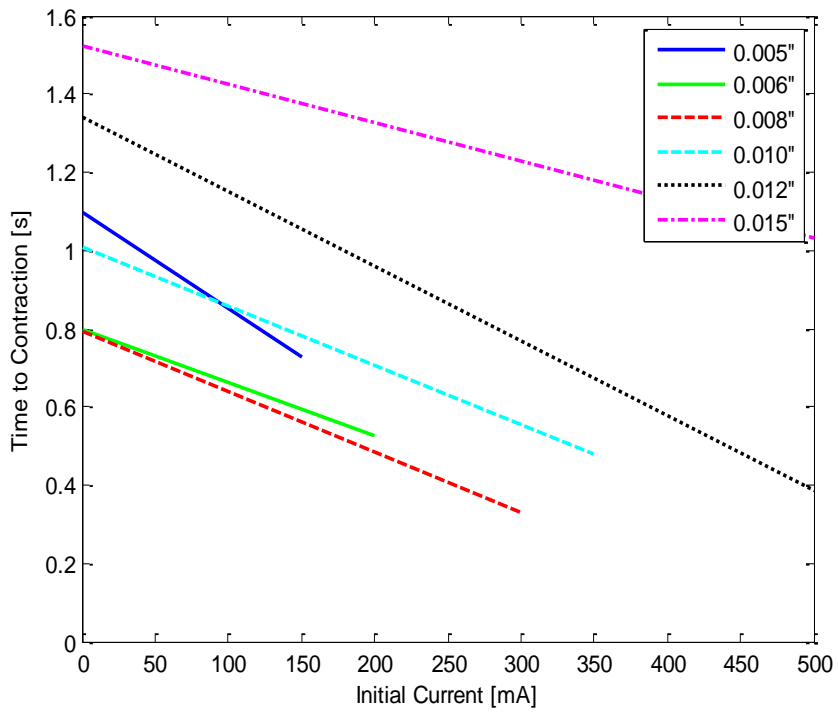


Figure 2.17. Time to contraction values at varying initial currents.

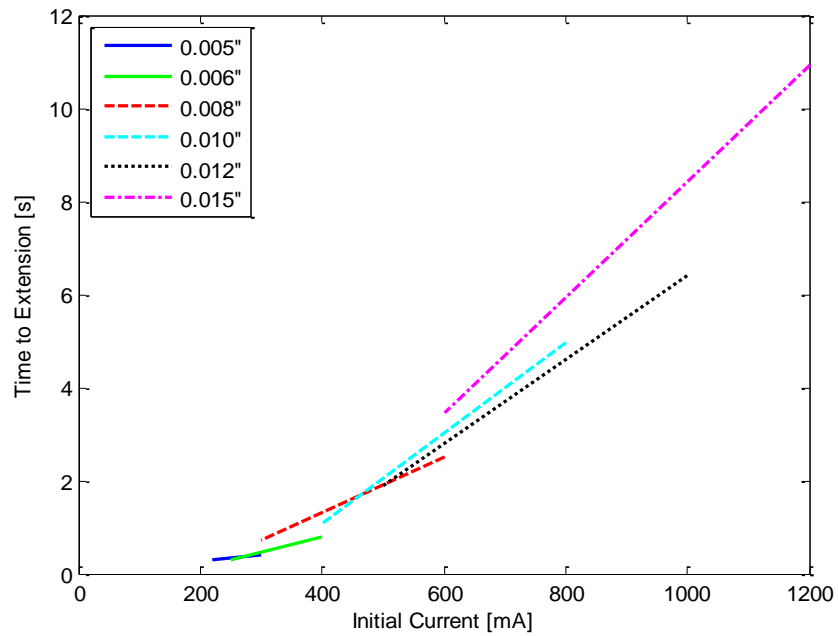


Figure 2.18. Time to extension values for varying initial currents.

In order to find the total contraction and extension times, Equations (2.14) and (2.15) must be used:

$$t_{contract} = 2\tau_{contract} + t_{tc} \quad (2.14)$$

$$t_{extend} = 2\tau_{extend} + t_{te} \quad (2.15)$$

Where,  $t_{contract} \equiv$  Total Contraction Time [s]

$t_{extend} \equiv$  Total Extension Time [s]

$\tau_{contract} \equiv$  Contraction Time Constant [s]

$\tau_{extension} \equiv$  Extension Time Constant [s]

$t_{tc} \equiv$  Time to Contraction [s]

$t_{te} \equiv$  Time to Extension [s]

Given these equations and the trends seen in the results, the quickest theoretical reaction time for each wire will be equal to twice the time constant of the wire assuming that the time to contraction/extension is zero. This quick reaction time can be obtained by developing a control algorithm for actuating nitinol wire where the wire is pre-heated prior to wire contraction and extension.

## 2.9. CONTROL ALGORITHM

Given that decreasing the starting current prior to actuation can reduce reaction times, one might ask how to design the most efficient control algorithm to reduce reaction times to a minimum. Using the control currents and current hysteresis found through the wire contraction tests along with the time constants found through the transient tests, a precise control algorithm can be constructed. A crude graphical model of this control algorithm can be found in Figure 2.19.

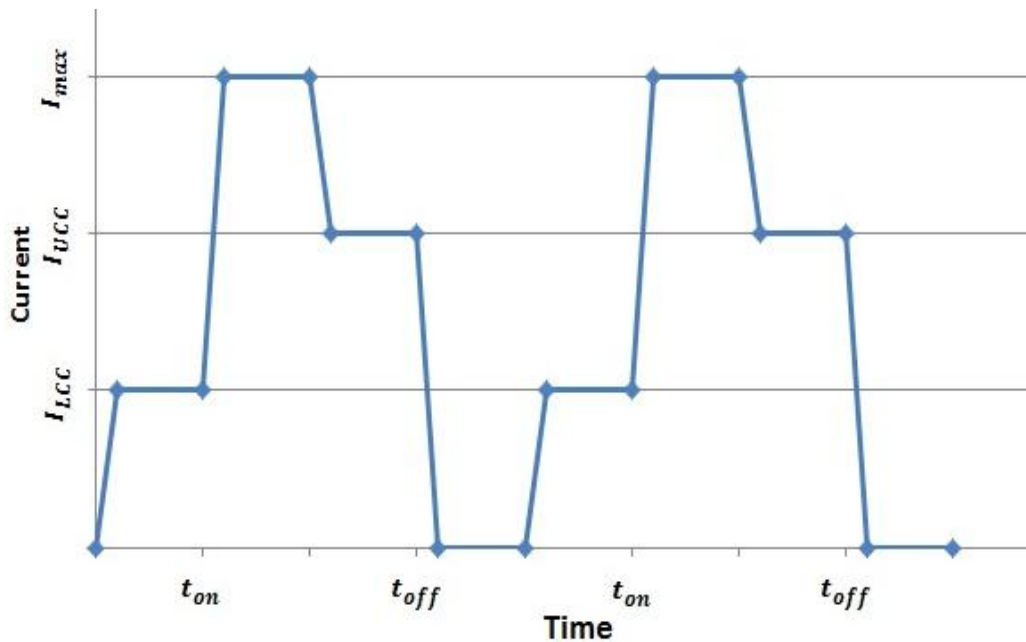


Figure 2.19. Control algorithm used for an efficient actuator design.

In this figure, the current is adjusted between four distinct current values: maximum current ( $I_{max}$ ), upper control current ( $I_{UCC}$ ), lower control current ( $I_{LCC}$ ), and off. The upper control current is found directly from the prediction interval of the initial wire contraction test. The lower control current is found by subtracting the current hysteresis from the control current found in the initial wire contraction test. This will account for

any current hysteresis caused by small pull forces. The maximum current is found through the temperature curves so that a certain temperature is not exceeded in the nitinol wire. A maximum current is selected primarily to ensure the nitinol wire does not exceed a certain temperature. Though no temperature was determined to be the absolute maximum, it is advised not to exceed 120 °C. Table 2.8 shows these currents used in the control algorithm.

Table 2.8. Current values for control algorithm.

Wire Diameter [mils]	$I_{\max}$ [mA]	$I_{UCC}$ [mA]	$I_{LCC} + \Delta I_h$ [mA]
5	355	277	160
6	438	296	217
8	542	396	262
10	727	576	317
12	1004	742	405
15	1253	852	576

Note that  $I_{\max}$  is based on a maximum temperature of 120 °C and  $I_{LCC} + \Delta I_h$  is the lower control current before subtracting the current hysteresis. This current hysteresis will be a function of the pull force as previously mentioned.

The control algorithm is performed by going through the following steps:

1. When the nitinol wire is fully extended at room temperature, the current through the wire is raised to the lower control current. This will heat up the wire without causing any actuation to occur.
2. When the nitinol wire needs to be contracted, the current through the wire is raised to the maximum current for the wire. This will rapidly heat up the wire through its transition temperature resulting in a quick response.



3. Once the wire is fully contracted, the current through the wire is lowered to the upper control current. This will cool down the wire without causing any extension to occur.
4. When the wire needs to be extended, all power is removed from the wire. This will rapidly cool down the wire through its transition temperature resulting in a quick response.
5. Repeat process as necessary.

If this process is used, a nitinol actuator will have a relatively quick response limited only by the time constant of the wire itself.

## **2.10. CABLE FABRICATION AND TESTING**

### **2.10.1. PURPOSE OF CABLES**

For mechanical applications where large pull forces are required, a single piece of nitinol wire will not be enough. Cable fabrication becomes a desired approach and offers some advantages to single large diameter wires. Cables are much more flexible than a single strand and can be used in applications such as pulley systems. An extra advantage is that creating a cable of smaller wires allows for easier clamping of the wire. For a single strand, a clamp must hold onto a small wire with a very large force, whereas for a cable of wires, a single long strand can be wrapped into a coil providing loops of nitinol that can be used for clamping. Figure 2.20 shows the end of a nitinol cable where this coil was looped around the large end of a spade lug and crimped to create a rigid connection.



Figure 2.20. Cable connection using a coil of wire.

Given the shape memory property of nitinol, it is very easy to make a cable. By twisting several strands of nitinol together and heating them up to their austenite state while held in tension, they will stay in that same shape when cooled down to their martensite state. As long as there is always some tension in the cable when they are

heated up, they will continue to hold their shape making braiding of wires unnecessary. Photographs of nitinol cables can be found in Appendix A.

### 2.10.2. CABLE TESTING

Some of the tests in this study were repeated using cables to see how they performed when compared to single cables of similar cross sectional area. Not all tests could be replicated due to limited resources, but enough tests could be performed to see a general trend in how cables behave compared to single strands. All cables used in this study were made from strands of 6 mil diameter nitinol wire.

### 2.10.3. CABLE TRANSIENT TEST

The first test that was done on cables was the transient test to determine the time required for cables to contract. Due to hysteresis in the cables not accounted for when these tests were conducted, extension time constants were not found for cables. Two cables were used: 3 strands and 8 strands of 6 mil wire. Table 2.9 shows the results from this test along with some results from the single strand transient test for comparison. The effective diameter of each cable was calculated by determining the total cross sectional area of the cable and finding the diameter required for a single strand to have the same

Table 2.9. Contraction time constants for 6 mil wire diameter cables.

Wire Diameter [mils]	Number of Strands	Effective Diameter [mils]	Contraction Time Constant [s]
6	3	10.39	1.186
6	8	16.97	2.196
10	1	10	1.261
15	1	15	1.782

cross sectional area. It appears that the time constant for each cable is approximately the same as the time constant for a single wire of equal cross section.

#### 2.10.4. CABLE RESISTANCE

Rather than find the logistic growth equations for variable resistance as a function of current, it was more practical to note the maximum and minimum resistance of each cable and compare that to the resistance values of single strands. In theory, if each strand is perfectly insulated from the rest of the other strands, the resistance of the cable can be modeled as several single strands in parallel. Table 2.10 shows the resistance values for 1,2,3,4, and 8 strands of 6 mil wire. This table also provides the theoretical resistance of the cable if all single wires are perfectly insulated. For small cables with few strands of wire, the resistance can be easily estimated by modeling the cable as single insulated wires. For larger cables with 4 or more strands, the resistance starts to stray from this model which is likely due to interaction between the individual wires.

Table 2.10. Resistances for 6 mil diameter cables with varying number of strands.

Number of Strands	$R_{\max}$	$R_{\max\_ideal}$	$R_{\min}$	$R_{\min\_ideal}$
1	1.501	1.501	1.266	1.266
2	0.741	0.751	0.662	0.633
3	0.457	0.5	0.458	0.422
4	0.411	0.375	0.386	0.3165
8	0.222	0.188	0.2011	0.1583

#### 2.10.5. CABLE HYSTERESIS

The wire hysteresis test was also performed on some cables to see the trends in hysteresis as more strands are added to a cable. Table 2.11 shows the constant “a” found

from these tests for the 2, 3 and 4 strand cables tests along with the results from the single strand wire hysteresis test for comparison. Unlike the other cable tests performed, these results suggest that cables have larger amounts of hysteresis when compared to single wires of similar cross sectional area. This is likely due to the interaction, specifically friction, between the individual wires in a cable. This hysteresis can be overcome by applying a larger pull force.

Table 2.11. Constants from wire hysteresis test for single strands and cables.

Wire Diameter [mils]	Number of Strands	a [g-1]
5	1	0.017075
6	1	0.021721
8	1	0.007255
10	1	0.004343
12	1	0.003125
15	1	0.001862
6	2	0.002535
6	3	0.002405
6	4	0.00182

#### 2.10.6. CABLE CONSLUSIONS

Since it appears that cables behave similarly to single wires, many of the results obtained for single wires can also be applied to cables. These characteristics offer a wide range of options when compared to using a single wire in an actuator design. The specific tests that will not be able to be directly applied to cables are any tests that include hysteresis since cables appear to have larger hysteresis than single wires.

## ***2.11. INTERPRETATION OF TEST RESULTS***

If the wires used during this study were directly applied to a nitinol actuator, the results obtained could be directly applied as well. Unfortunately, given that the nickel to titanium ratio is unknown and may affect the tests performed, the results presented may not be numerically accurate for other brands of wires. On the other hand, all trends found in this study should hold true for any nitinol wire. As discussed in the temperature test section, wires with a nickel to titanium ratio of about 0.98 are more likely to have numerical results similar to the ones found in this study, but this has not been confirmed. Additionally, the method of fabrication of the wire itself may affect the behavior of each wire. This unknown factor is expected to be the cause of inconsistent data found in this study.

Before using nitinol wire for your own personal application, it is recommended to perform some of the same tests done in this thesis, in particular the wire contraction test and the maximum pull force test. Tests including hysteresis can be ignored as long as the nitinol wire is pulled with a constant pull force which is the same as the force it is likely to see during actuation. These tests can be performed by using a similar test setup and following the procedure outlined in each test section. The equations derived in this thesis will be applicable for any nitinol wire, but the constants found through regression lines differ from this study. Once these tests are completed, any nitinol wire can be used for the design of a custom actuator.

## **CHAPTER 3. ACTUATOR DESIGN AND TESING**

---

### ***3.1. INTRODUCTION***

Each wire alone is capable of performing mechanical work which is found by determining the maximum contraction and pull force in the wire. This mechanical work in theory is constant, which becomes a limitation because both contraction and pull force cannot be increased simultaneously. However, either a larger pull force or larger displacement can be obtained by incorporating the wire into some system with mechanical advantage. If more displacement is desired, the maximum pull force must decrease, and vice versa. This offers a much wider range of options when using nitinol for actuation. Since nitinol only shortens about 5-6% of its length, it is likely that more displacement will be desired. If a larger pull force is desired, larger diameter wires or even cables can be used. For this research study, it was our goal to design a prototype actuator that can prove the concept that nitinol wire could be placed in a system with mechanical advantage to obtain larger displacements when compared to a single wire.

### ***3.2. CONCEPTS***

Two concepts for designs were chosen after looking into different ways to obtain mechanical advantage. The first concept was to have a system of pulleys, where the end of one cable would be attached to the pulley thus gaining some additional displacement for each pulley introduced. Since nitinol cables were found to be flexible, they would be able to wrap around pulleys with ease. The second concept was to use lever arms to gain mechanical advantage. If the fulcrum of each lever was offset from center, additional displacements could be obtained. Of these two designs, the lever arm approach was

chosen for two reasons: easy to prototype and easy to adjust. The second aspect in particular is important because it allows for different mechanical advantage settings by changing the pivot of each lever.

### **3.3. DESIGN**

When starting with the design of this prototype actuator, a set of approximate specifications were developed:

1. Must be able to obtain a mechanical advantage of at least 2:1.
2. Must use a wire/cable that is no longer than 6" to minimize size.
3. Should be no more than 1" thick, 3" wide, and 8" long.
4. Should have adjustable pivot point for levers.

These specifications were merely a starting point that was used to start the design. Since this actuator was developed to prove concept rather than be used in a specific project, there were no absolute specifications for size, weight, or material used.

One important design consideration that was considered is how the external load to the actuator would be applied. Nitinol can provide tensile loads, but not compressive loads. If a nitinol actuator needed to actuate for both tensile and compressive loads, some sort of internal restoring force would need to be placed at the end of the nitinol wire to keep it constantly in tension. For this prototype, it was assumed that all forces will be tensile, which allows for a less intricate design. This means that this nitinol actuator would behave more like a muscle, which is typical of nitinol applications.



A final design was made after a couple of iterations which can be seen in Figure 3.1. Part drawings for each of the machined components and photographs of the overall actuator design can be found in Appendix C.

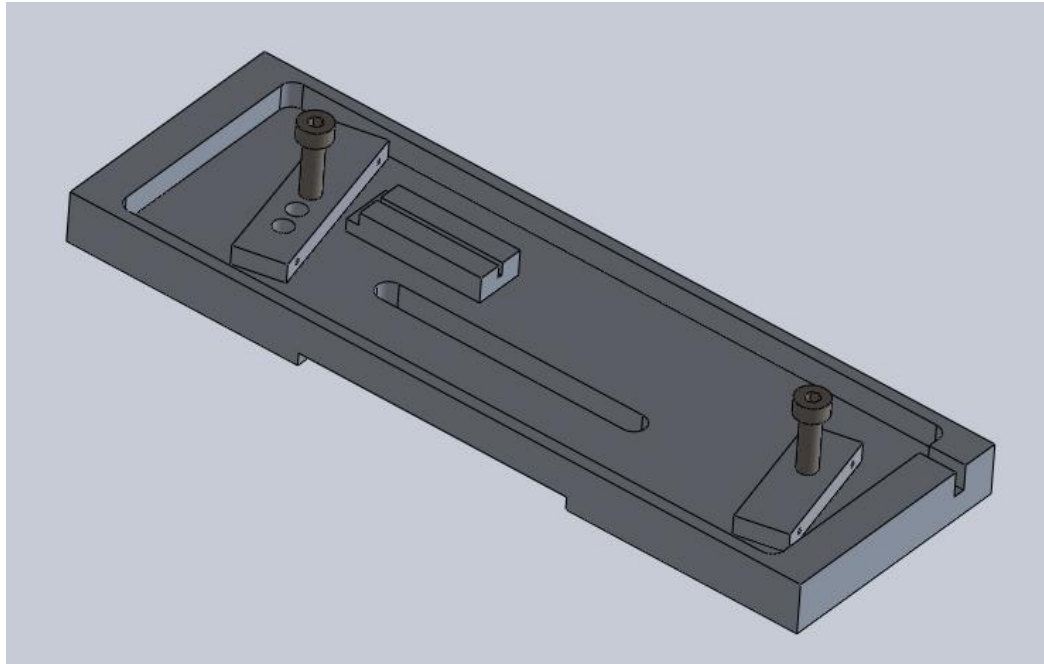


Figure 3.1. Solidworks model of actuator design.

The entire actuator was made using 6061 Multipurpose Aluminum mainly because of the ease to machine. This allowed for an easy fabrication process which is helpful when designing a prototype. The actuator itself has two lever arms, one with a set mechanical advantage of 2:1, and another with an adjustable mechanical advantage of 1:1, 2:1, and 5:1. This adjustment allows for a total mechanical advantage of 2:1, 4:1, or 10:1. These lever arms are attached to the frame of the actuator by using stainless steel shoulder screws. Each lever arm also has two small holes for wires or cables to go through. Since it is assumed all forces resisting the actuator will be tensile, wires can be placed in-between each lever arm rather than using a rigid link. A combination of music wire and

fishing line were used between the individual lever arms. The inside of the frame has one protrusion which is used to fix one end of nitinol wire by wedging it in the slot approximately the width of the spade lugs used to clamp the ends of the wire. The actuator also has a slot through the base to allow for wires to go through so they can remain out of the way.

The manufactured components of the actuator can be assembled with any nitinol wire being used. During the testing process, a nitinol cable with 8 strands of 6 mil wire and a single strand of 8 mil wire were used. This was done to show that the actuator works for both wires and cables.

### **3.4. ACTUATOR TESTING AND RESULTS**

The main goal of testing the actuator was to determine the feasibility of gaining mechanical advantage using this design. This was tested by putting a current through the nitinol wire/cable and measuring the contraction in the wire/cable as well as the total actuator displacement. For consistency, 4 inches of wire/cable were always used for actuation. Additionally, the current used was repeatedly 1800mA and 400mA for the

Table 3.1. Results from actuator testing.

Wire or Cable	Weight [g]	Wire/Cable Contraction [in]	Theoretical Wire Hysteresis [in]	Wire Contraction and Hysteresis [%]	Actuator Displacement [in]	Theoretical Mechanical Advantage	Actual Mechanical Advantage
Cable	400	0.1875	0.089	104.8%	0.375	2:1	2:1
Cable	200	0.125	0.153	105.4%	0.375	4:1	3:1
Wire	100	0.125	0.128	95.8%	0.25	2:1	2:1
Wire	100	0.125	0.128	95.8%	0.4375	4:1	3.5:1
Cable	1100	0.0625	0.013	28.7%	0.125	2:1	2:1

cable and wire respectively. The summarized results from these tests can be found in Table 3.1.

The majority of the values in these results were values recorded directly from the test itself. Wire and cable are labels for a single strand of 8 mil wire and an 8 strand cable of 6 mil wire. The weight is representative of the pull force on the actuator. The pull force on the wire/cable will be the weight multiplied by the mechanical advantage of the actuator. The wire/cable contraction and actuator displacement were directly measured by recording the position of the lever arms before and after actuation. The theoretical mechanical advantage is dependent on the shoulder screw placement on the second lever arm and the actual mechanical advantage is found by dividing the actuator displacement by the wire contraction.

The wire hysteresis was found by using Equation (2.4) and using the constant “a” found in Table 2.2. Given that some loads used in this test were relatively small, this value was needed to account for any contraction that didn’t take place. The wire hysteresis in the cables was approximated for finding the hysteresis in each wire assuming an evenly distributed load through the 8 wires. The remaining column in the results which is wire hysteresis plus wire contraction is a means to compare the results to the theoretical displacements in the wire using the results previously in this thesis.

The first four rows of the results are representative of showing that this prototype actuator works in specific instances where small forces are applied. The last row however shows very large inconsistencies when compared to the rest of this thesis. This deviation from theory is due to friction in the shoulder screws caused by large applied loads. If the

weight used to apply a load was increased much more than 1100g, the wire would not contract at all.

### **3.5. FUTURE IMPROVEMENTS TO DESIGN**

The biggest flaw of this design is that it only works well for small pull forces due to the friction in the lever arm pivot points. This is not a flaw to the specific design used, but rather a flaw of using lever arms in general. In order for this design to work well for larger loads, some sort of bearing or lubrication would need to be used. Bearings would be the ideal solution if they can also handle somewhat substantial lateral loads.

A second flaw with this design which would be a way to improve the actuator is the material used. Aluminum is a great material for prototyping, but it is also conductive, which is an issue if a current is being used as the means to heat up the nitinol wire. For this specific actuator, small sheets of index paper were used to insulate the wire from the aluminum base which works quite well. A better approach would be to have the protrusion in the base be made from a non-conductive material like a ceramic.

In all, the prototype actuator designed has some flaws, but it was able to prove the concept that an actuator can be designed using nitinol actuation wire.

### **3.6. DESIGN OF A CUSTOM ACTUATOR**

When designing a custom actuator, the following steps need to be taken:

1. Determine the mechanical work required from the actuator in oz-in. This value can be found by directly multiplying the required displacement,  $x$ , by the force expected for normal operation of the actuator,  $f$ .

2. Determine the length of wire that will be used in the actuator,  $l$ . Divide the mechanical work by this length to obtain a mechanical work in units of oz-in/in.
3. If a cable is going to be used rather than a single strand, determine the number of strands that will be used in the cable,  $n$ . Divide the mechanical work by this number to obtain the mechanical work in units of oz-in/in for each strand. It is recommended to start the number of strands at one and iterate.
4. Using the mechanical work found in step 3, select a wire diameter that can obtain this mechanical work. This can be done by consulting the work curve found in Figure 2.9 of the text for 6 mil wire as well as Figure B.20 - Figure B.25 in Appendix B for all other diameters. A wire should be selected that has a maximum mechanical work larger than the desired mechanical work. If no wires are capable of obtaining this mechanical work, redo step 3 and increase the number of strands,  $n$ .
5. Once a wire diameter is selected, use the appropriate force curve to determine the force required to obtain this mechanical work,  $F$ . Of the two forces that can obtain this mechanical work, it is recommended to use the smaller one. This force will be in units of kilograms, but it should be converted to the same units used for  $f$ . Kilograms were chosen for this plot as a means for consistency with the rest of the thesis and with the Flexinol® datasheet.
6. The mechanical advantage needed for the actuator,  $m$ , will be the force required for the nitinol wire,  $F$ , divided by the actuator force,  $f$ . A value greater than 1 means that this mechanical advantage will result in an actuator obtaining larger displacements than the wire itself.

This process can be summarized by two design Equations (3.1) and (3.2):

$$W = \frac{fx}{nl} \quad (3.1)$$

$$m = \frac{F}{f} \quad (3.2)$$

Where,  $f \equiv$  Force expected for normal operation of the actuator [oz]

$x \equiv$  Required Displacement for actuator [in]

$n \equiv$  Number of strands in cable

$l \equiv$  Length of wire used [in]

$W \equiv$  Mechanical Work per strand  $\left[ \frac{\text{oz-in}}{\text{in}} \right]$

$F \equiv$  Force per strand of wire derived from work curve [kg]

$m \equiv$  Mechanical Advantage

In these equations,  $f$  and  $x$  are the actuator specifications. The values of  $n$  and  $l$  can be tuned as necessary until a successful design is achieved. The mechanical advantage can be implemented in any manner as long as there are no significant losses due to friction.

Also it is worth noting that the units for force were kept as grams and kilograms to stay consistent with the rest of the results in this thesis. This mass unit can be multiplied by the numerical value for gravity to obtain a traditional unit of force.

### 3.6.1. DESIGN EXAMPLE

As an example, consider an actuator that needs to lift a 250g weight one inch. This results in a required mechanical work of 250 gram-in or 8.82 oz-in. If a single 4 inch

strand of 6 mil diameter is used, using Equation (3.1), a mechanical work of 2.20 oz-in/in is required per strand of wire. Using Table 2.4 as a reference, the maximum mechanical work a single strand can provide is 1.27 oz-in/in, which is insufficient. By iterating the design to have a cable with 2 strands of wire, Equation (3.1) generates a mechanical work of 1.10 oz-in/in, which is less than  $F_{max_w}$  for 6 mil diameter wire. Figure 2.9 shows that approximately 0.4 kg, or 400 g of pull are needed on each strand of the cable. Using Equation (3.2), a mechanical advantage of 1.6 is required.

As an end result, if a 4 inch 2-strand cable of 6 mil diameter wire is put in an actuator system with a mechanical advantage of 1.6, the actuator would be able to lift a 250g weight an inch. This process can be applied to different custom actuator designs.

## **CONCLUSION**

Through a careful analysis and testing of nitinol wire, it was determined that an actuator could in fact be designed using nitinol as the method of actuation. This actuator design can be made by following a step by step procedure that incorporates the results from the tests performed. Also, it has been determined that a careful control algorithm can be implemented to decrease reaction times resulting in a more efficient design. Given this, nitinol wire can be implemented in any actuator design, allowing for customizable specifications giving nitinol actuation an edge to other methods for certain applications.



## LIST OF REFERENCES

- [1] Ryhänen, J., 1999, "Biocompatibility evaluation of nickel-titanium shape memory metal alloy," Ph.D. thesis, University of Oulu, Rautaruukki, OY, Raahel, Finland. pp. 26-27.
- [2] Biometal™. Toki Corporation, Japan. 1987. VHS.
- [3] "Flexinol® Wire". Images SI Inc., 15 April 2013.  
<http://www.imagesco.com/nitinol/wire.html>.
- [4] "Nitinol/Flexinol® Actuator Wire". Images SI Inc., 11 July 2013.  
<http://www.imagesco.com/articles/nitinol/04.html>.
- [5] Duerig, T., Pelton A., and Trepanier C., 2011, "Nitinol," ASM International, SMST e-Elastic newsletter. pp. 2-3, 22-23.
- [6] "Nitinol Facts". Nitinol Devices and Components, 11 July 2013.  
<http://www.nitinol.com/nitinol-university/nitinol-facts>.

## **APPENDIX A. TEST SETUP AND EQUIPMENT PHOTOS**



Figure A.1. Constant current power supply used in most tests.

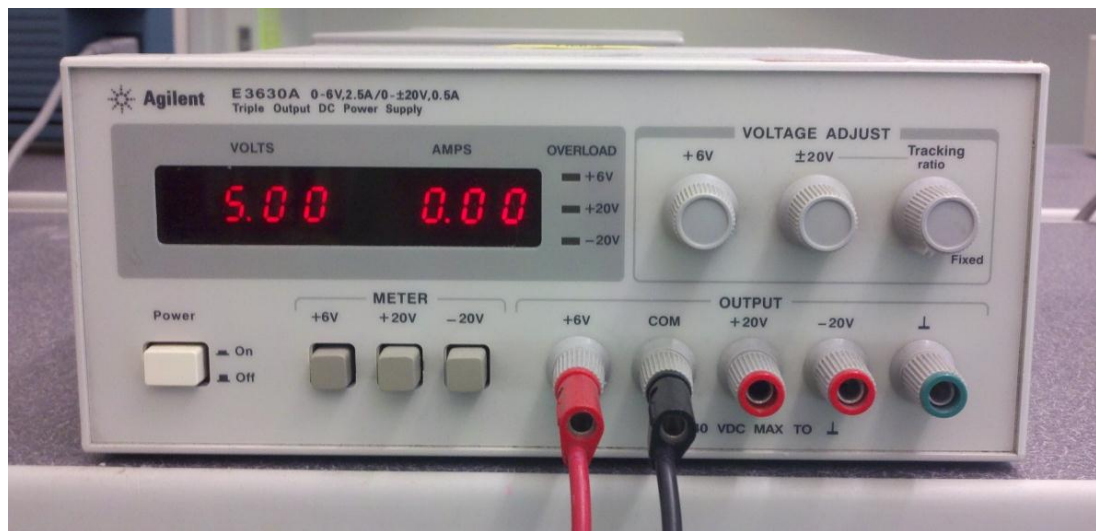


Figure A.2. 5V power supply used in transient test.

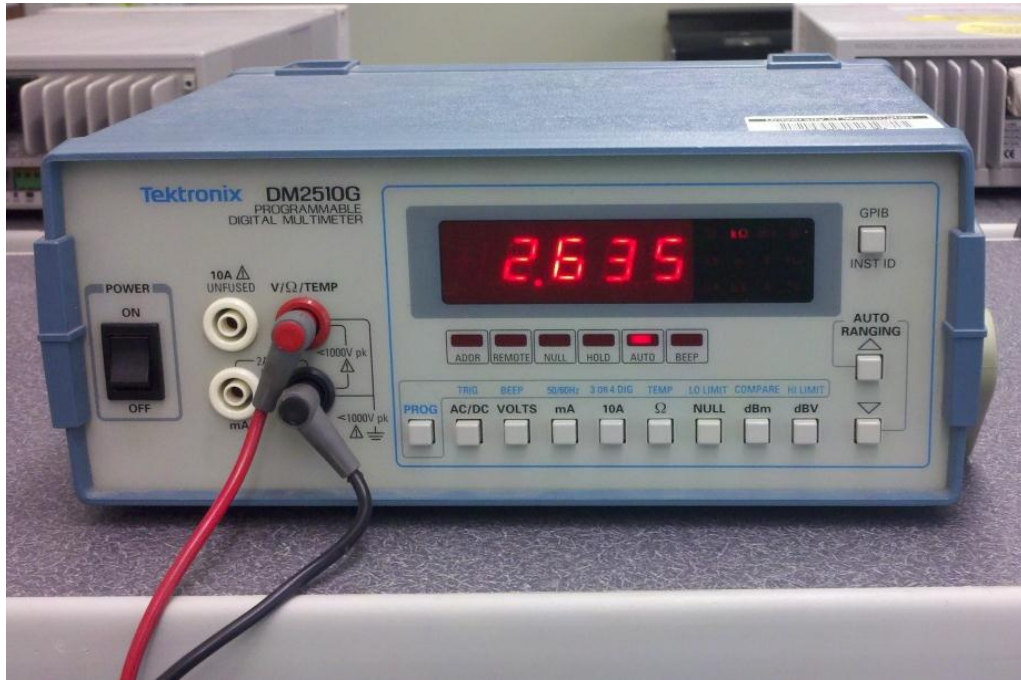


Figure A.3. Digital multimeter to read potentiometer and thermistor resistance values.

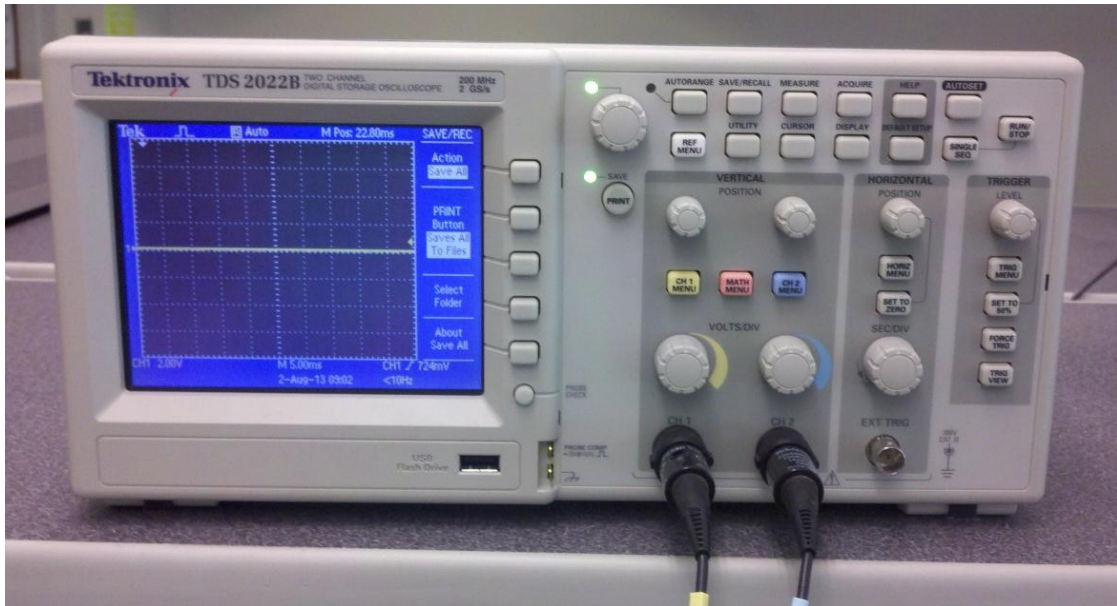


Figure A.4. Digital oscilloscope used in transient test.



Figure A.5. 5k rotary potentiometer with lever arm used most tests.

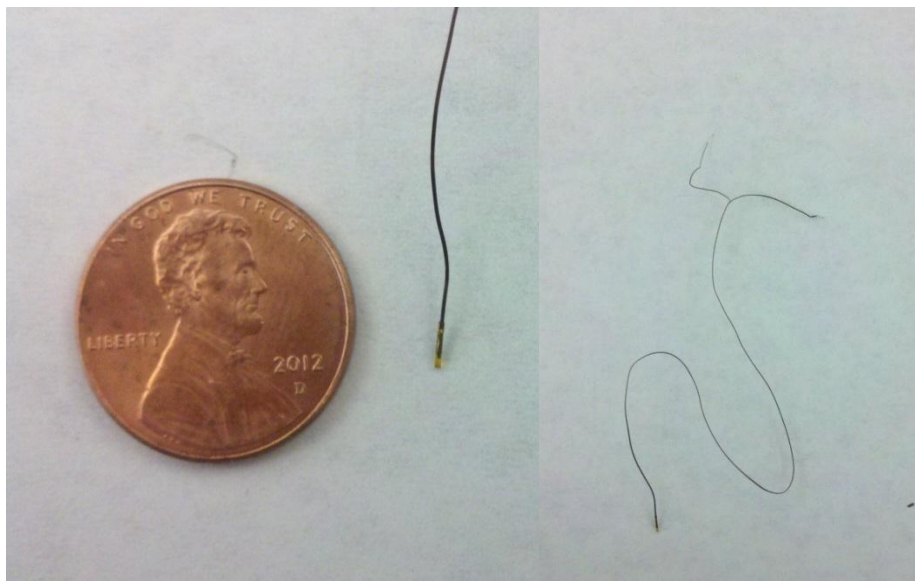


Figure A.6. 10K3 thermistor probe (left) and complete thermistor with leads (right).



Figure A.7. Nitinol wires used for testing.

From left to right: 5, 6, 8, 10, 12, and 15 mil diameter.



Figure A.8. Nitinol cables of 6 mil diameter wire used for testing.

From left to right: 8, 4, 3, and 2 strand cables; 6 mil diameter wire on right.

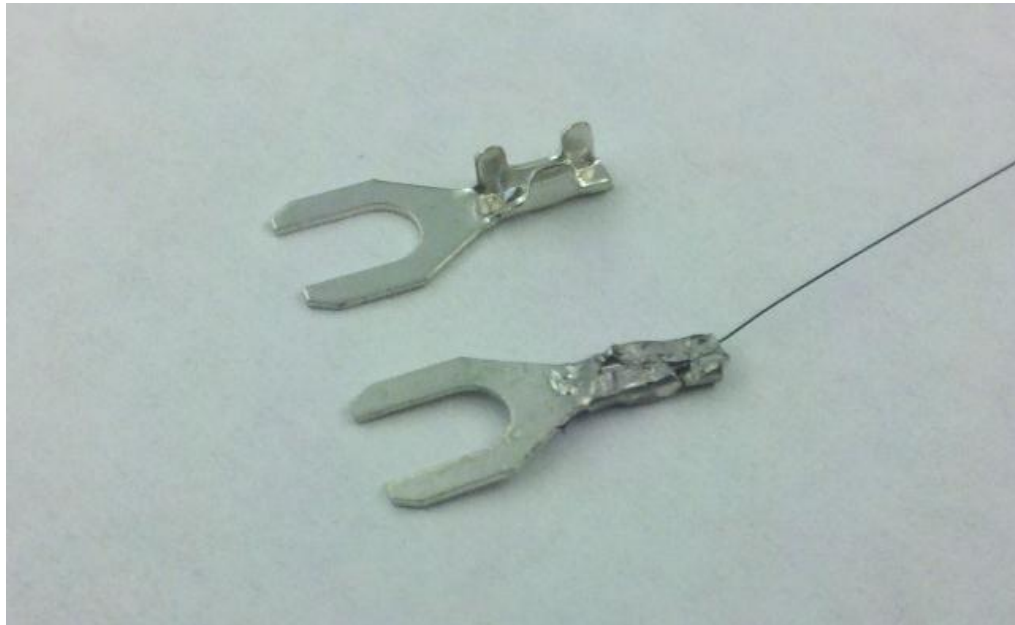


Figure A.9. Spade lugs used for wire attachment.



Figure A.10. Nitinol cable with wires wrapped around the end of the spade lug.

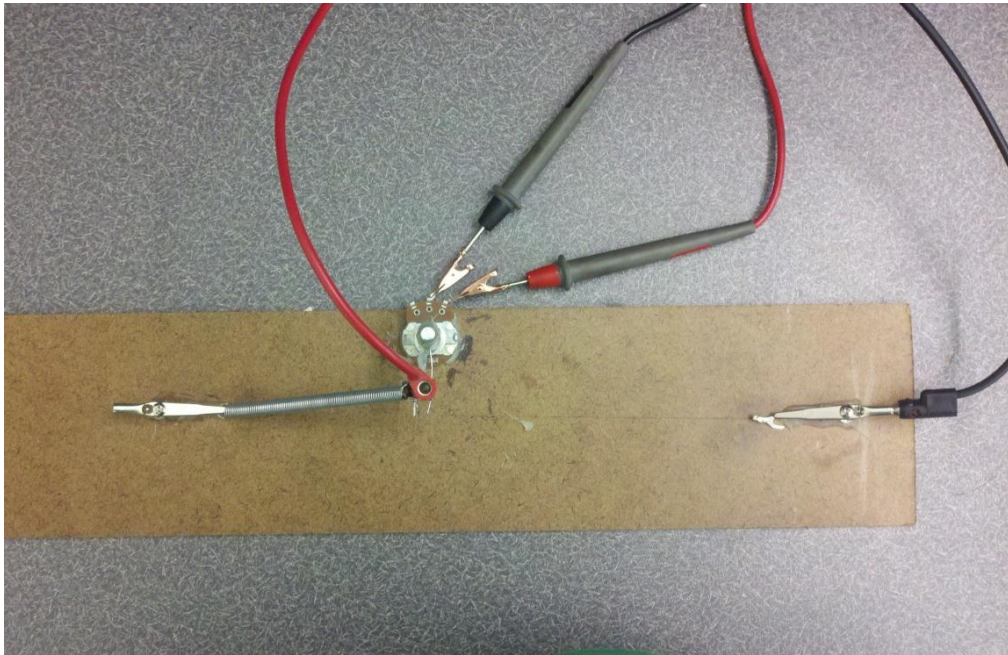


Figure A.11. General test setup.

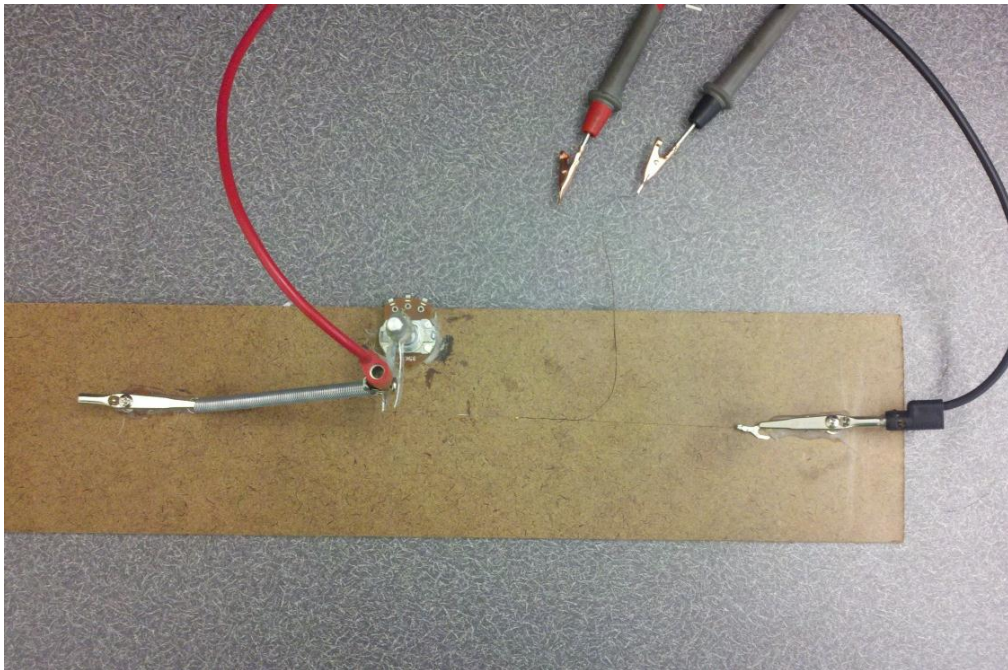


Figure A.12. Temperature test setup.



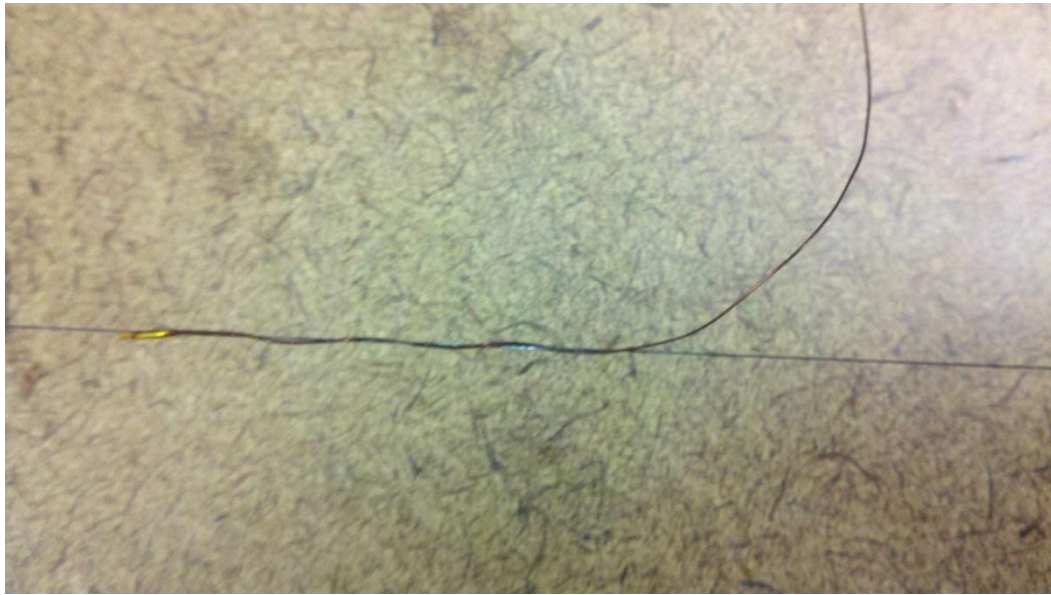


Figure A.13. Thermistor attachment for temperature test.

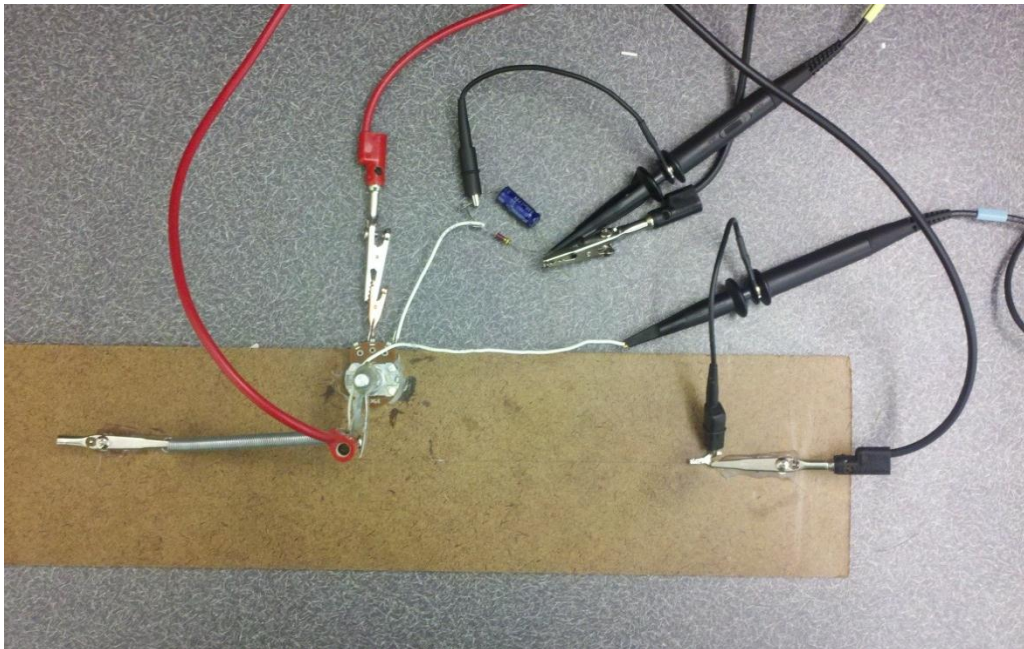


Figure A.14. Transient test setup.

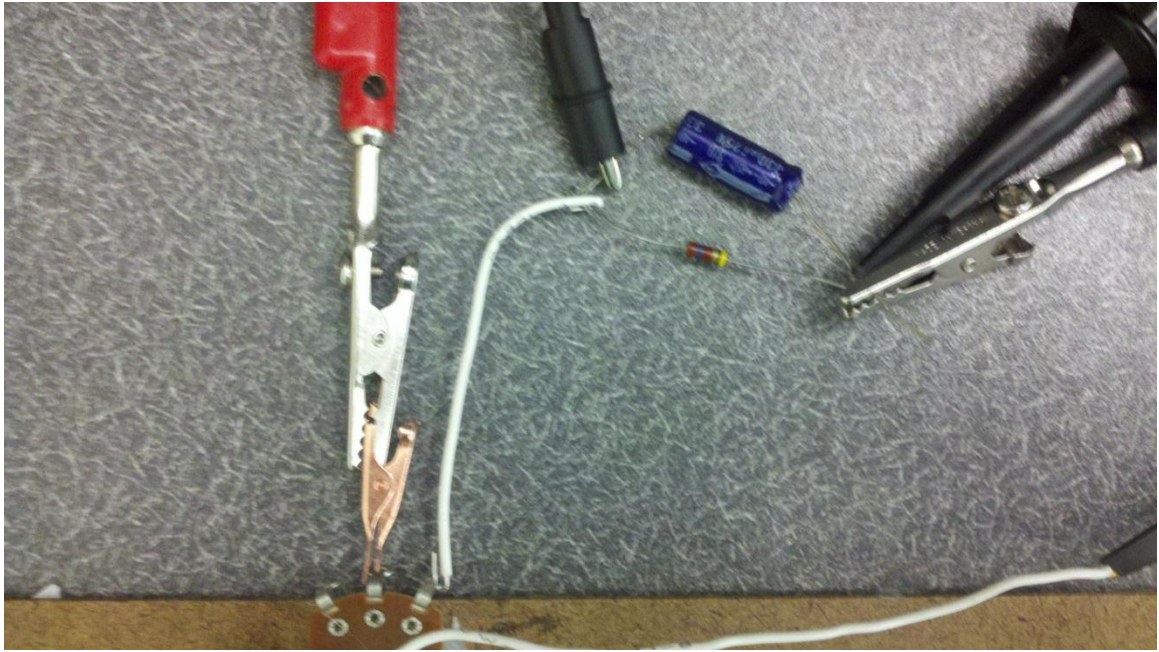


Figure A.15. 5V circuit loop of transient test setup with oscilloscope 1 attachment.

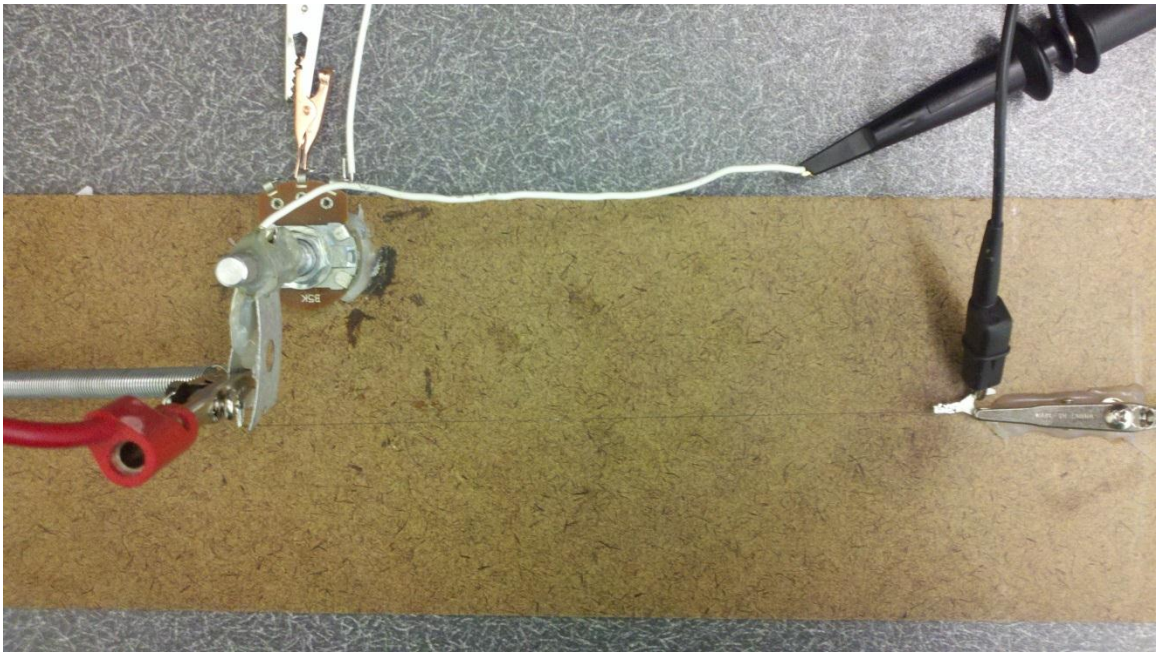


Figure A.16. Triggering circuit of transient test setup with oscilloscope 2 attachment.



Figure A.17. Weight attachment for wire hysteresis test.

**APPENDIX B. RESULTS FROM TESTS FOR ALL WIRES**

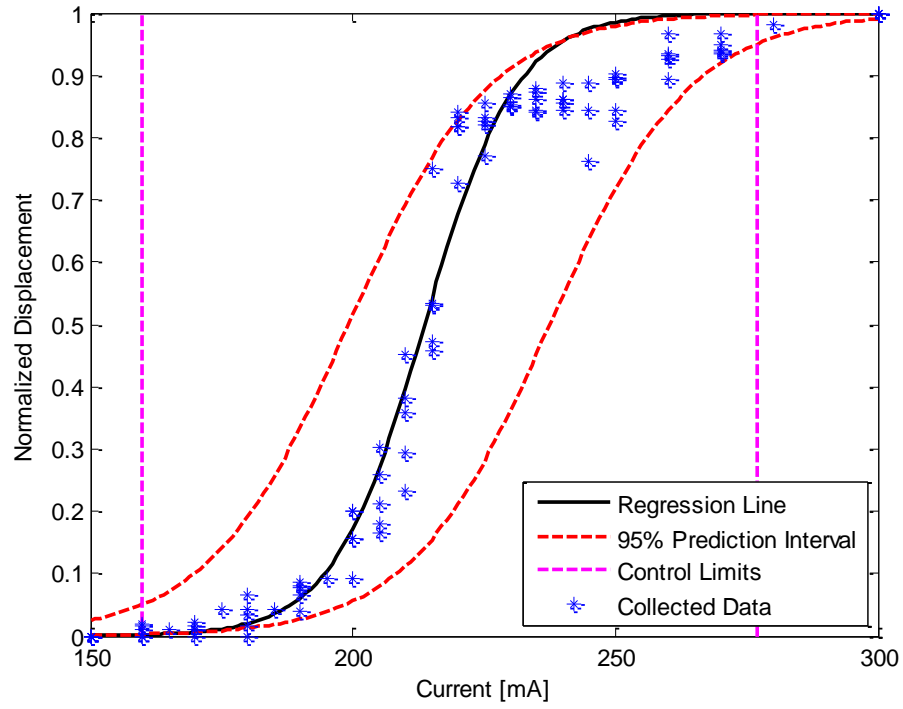


Figure B.1. Wire contraction curve for 5 mil diameter wire.

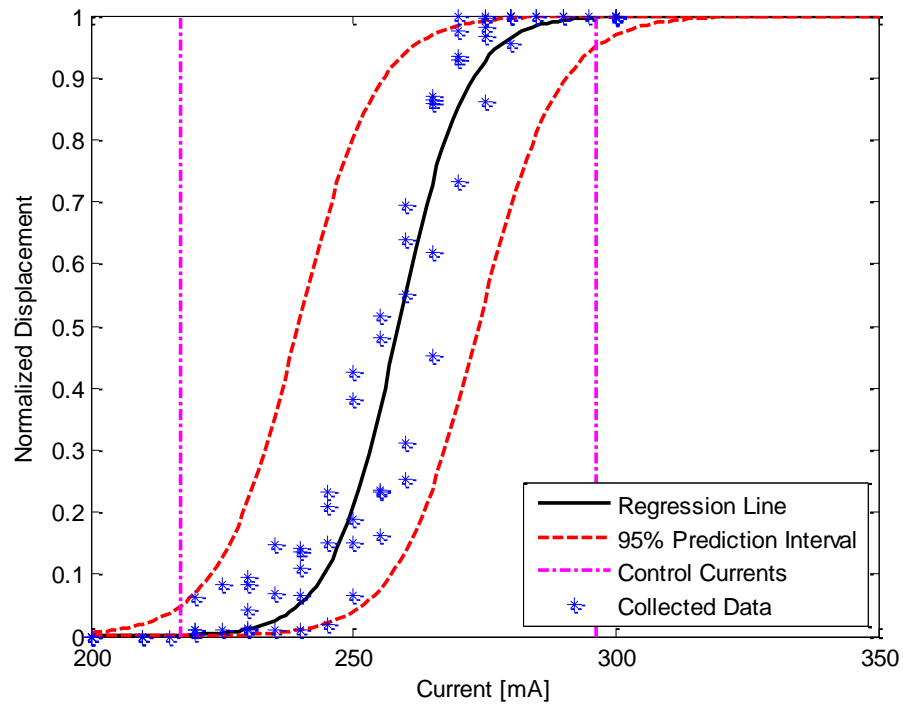


Figure B.2. Wire contraction curve for 6 mil diameter wire.

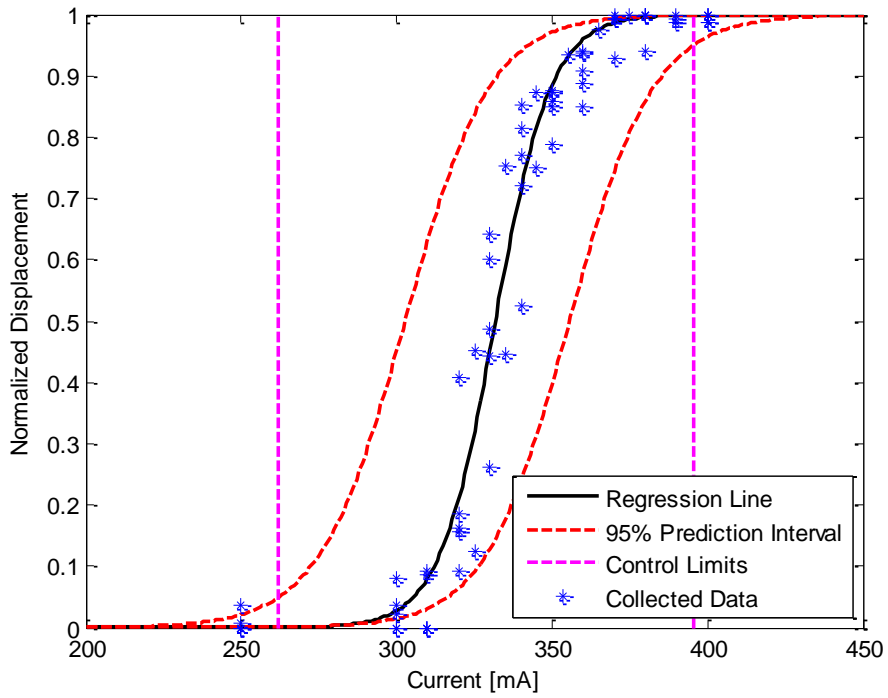


Figure B.3. Wire contraction curve for 8 mil diameter wire.

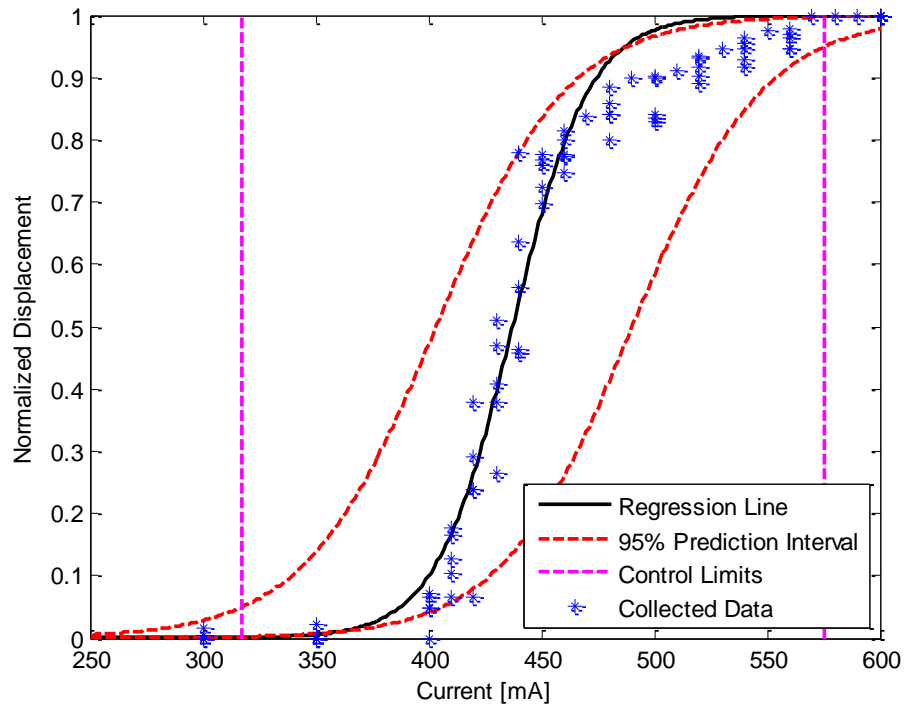


Figure B.4. Wire contraction curve for 10 mil diameter wire.

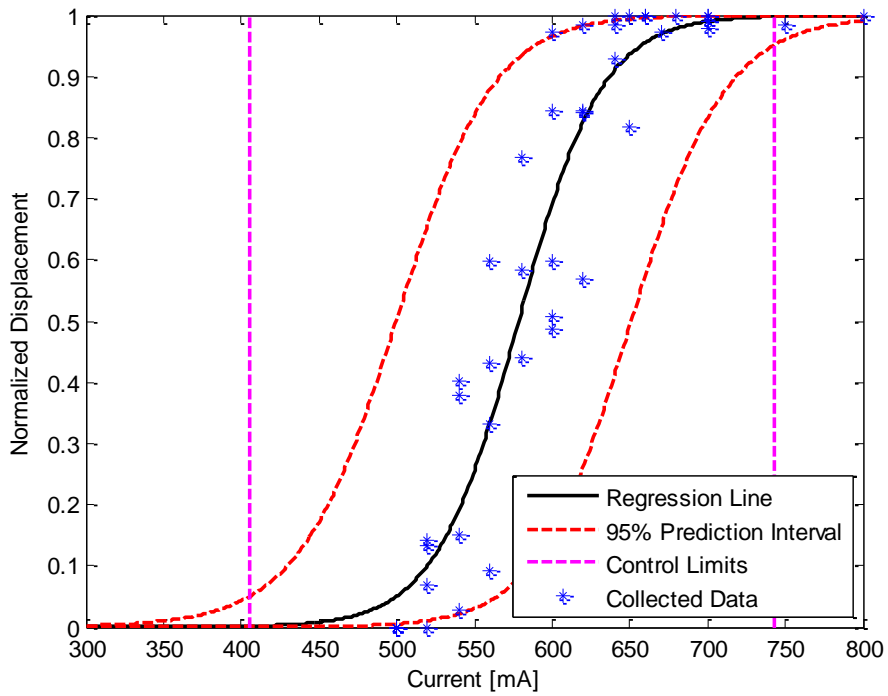


Figure B.5. Wire contraction curve for 12 mil diameter wire.

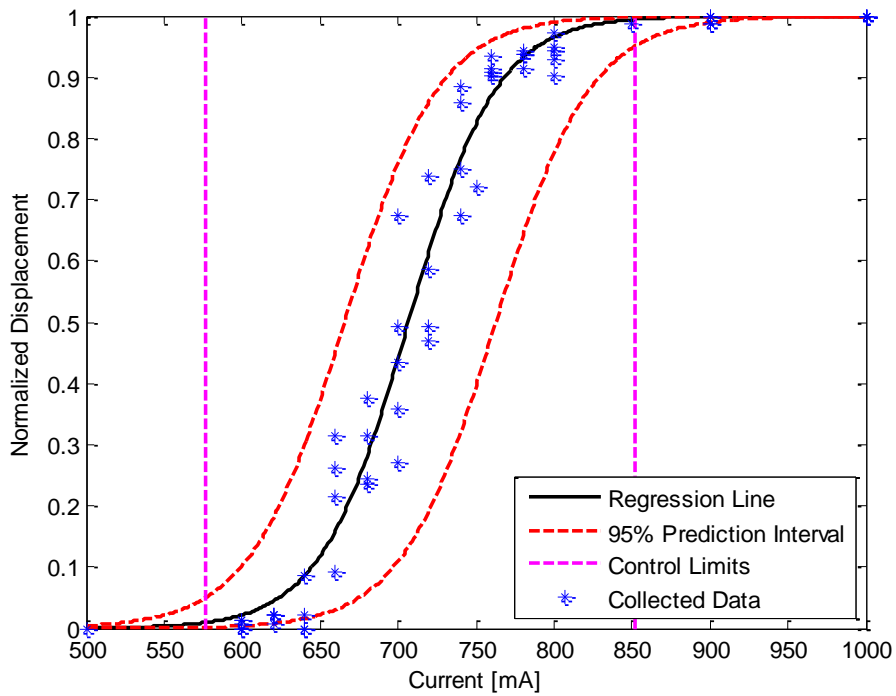


Figure B.6. Wire contraction curve for 15 mil diameter wire.

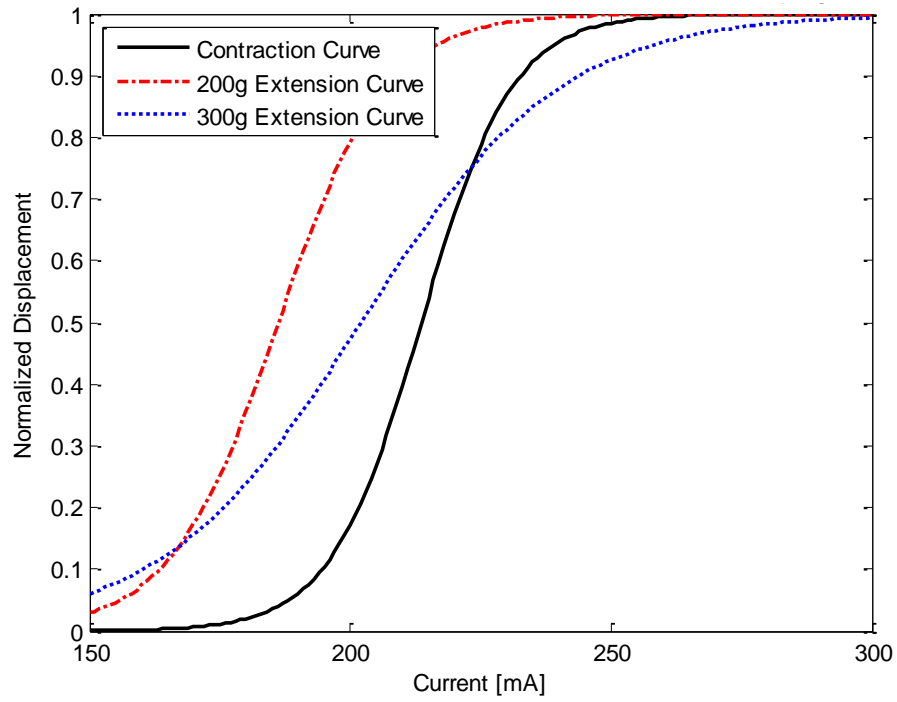


Figure B.7. Wire contraction and extension curves for 5 mil diameter wire.

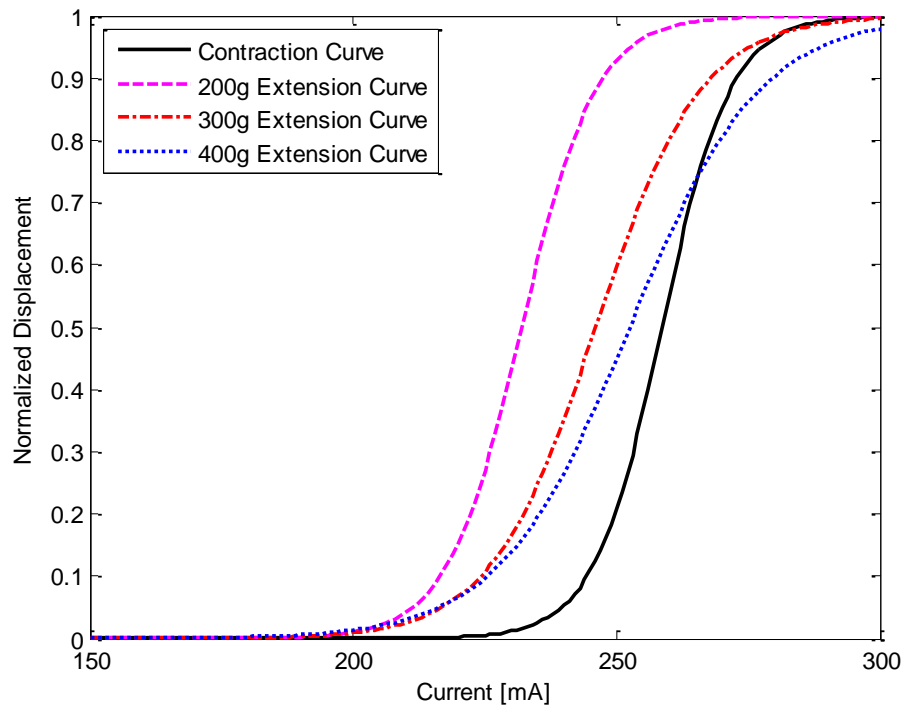


Figure B.8. Wire contraction and extension curves for 6 mil diameter wire.



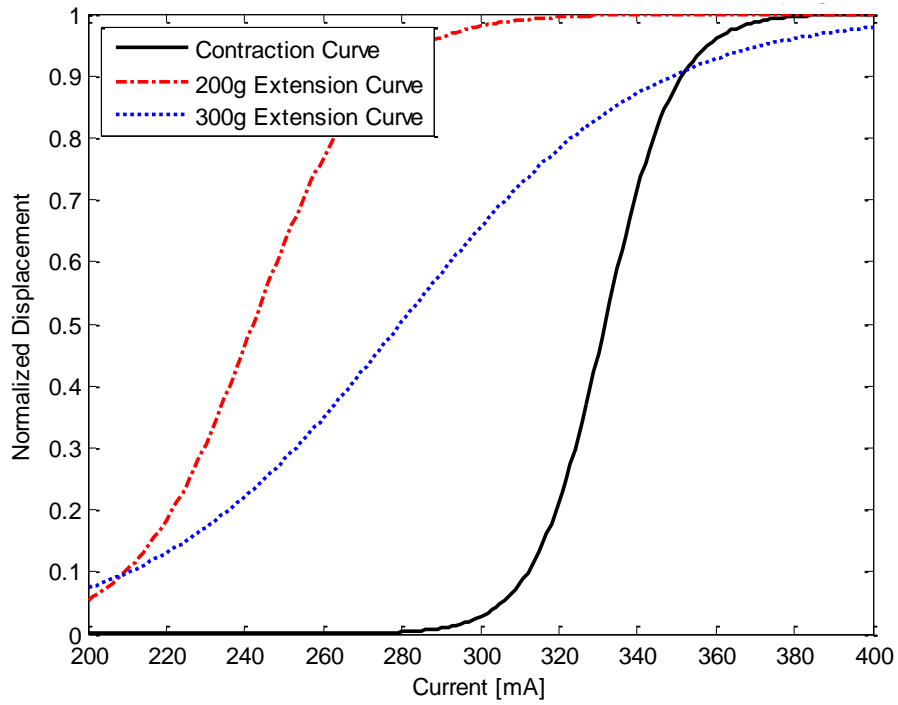


Figure B.9. Wire contraction and extension curves for 8 mil diameter wire.

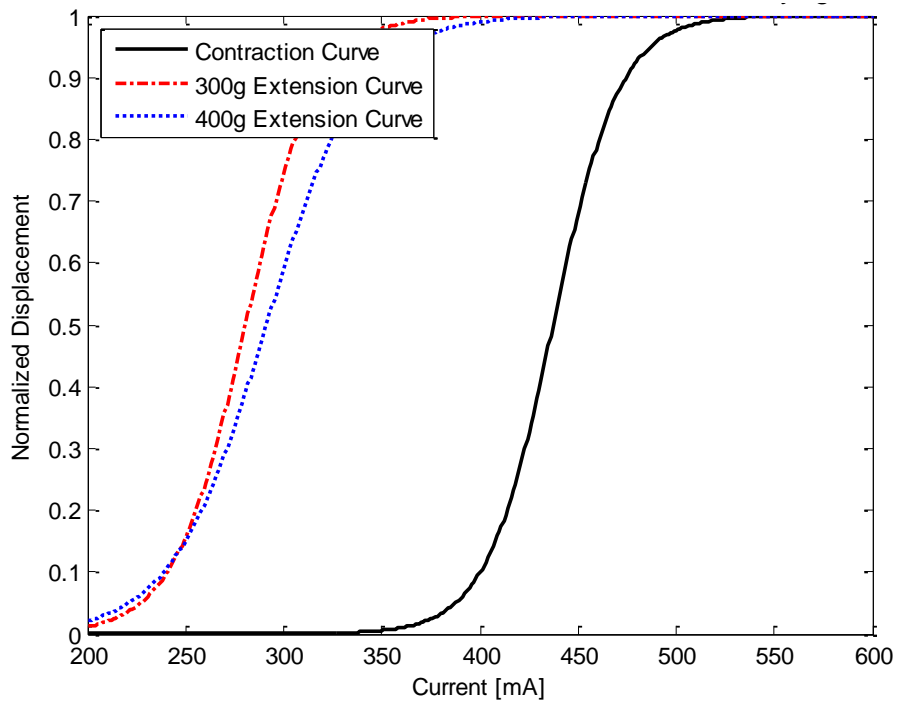


Figure B.10. Wire contraction and extension curves for 10 mil diameter wire.

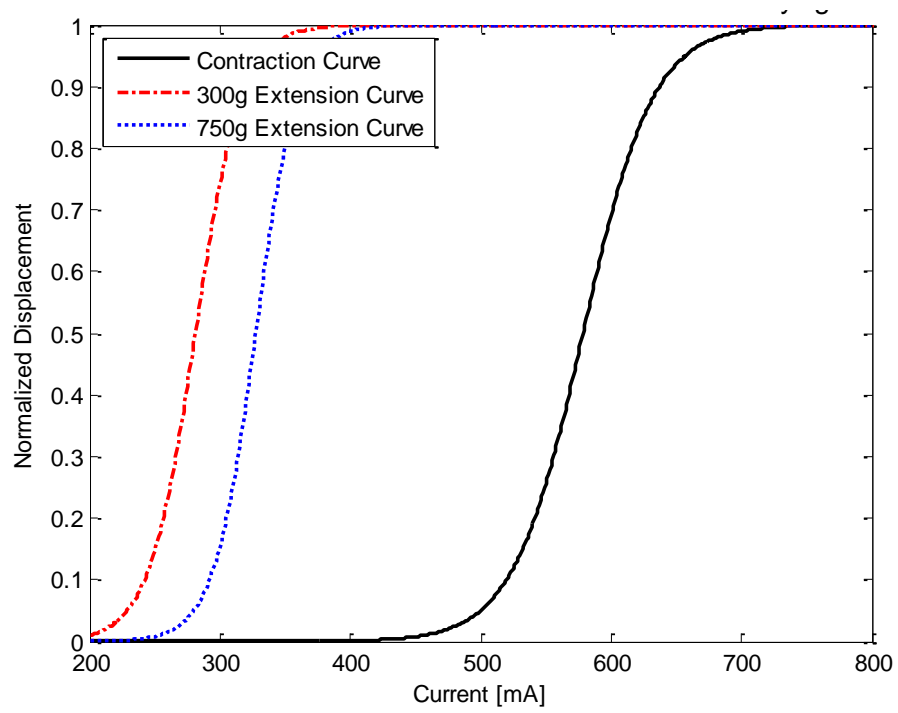


Figure B.11. Wire contraction and extension curves for 12 mil diameter wire.

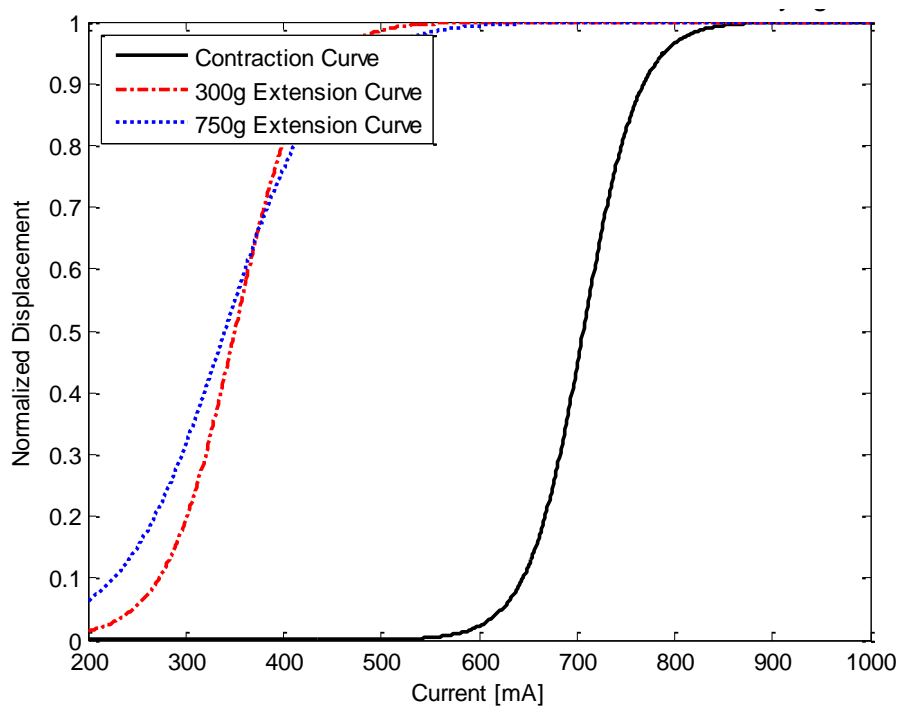


Figure B.12. Wire contraction and extension curves for 15 mil diameter wire.

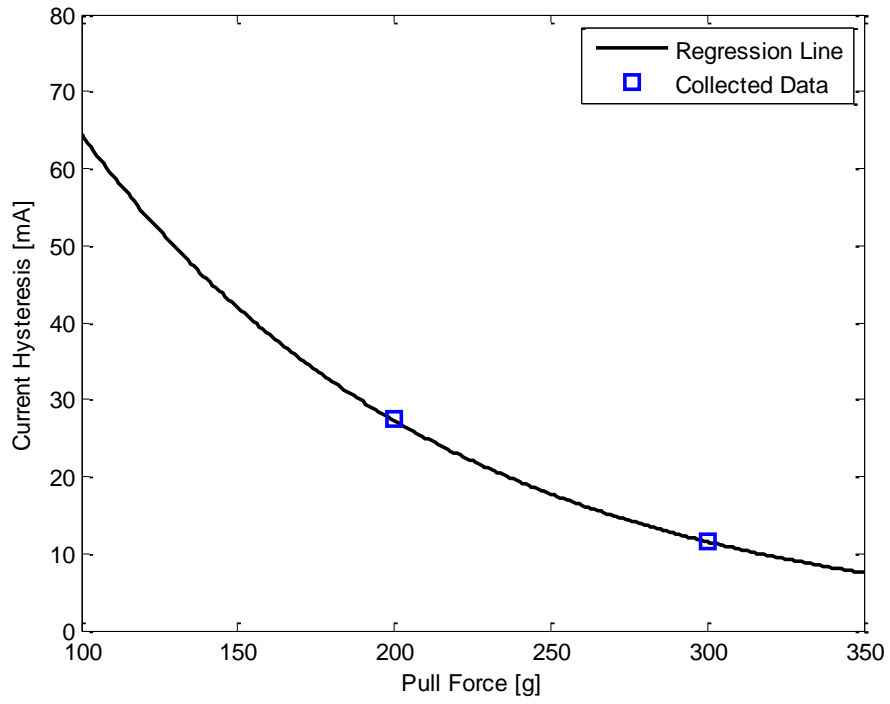


Figure B.13. Current hysteresis as a function of pull force for 5 mil diameter wire.

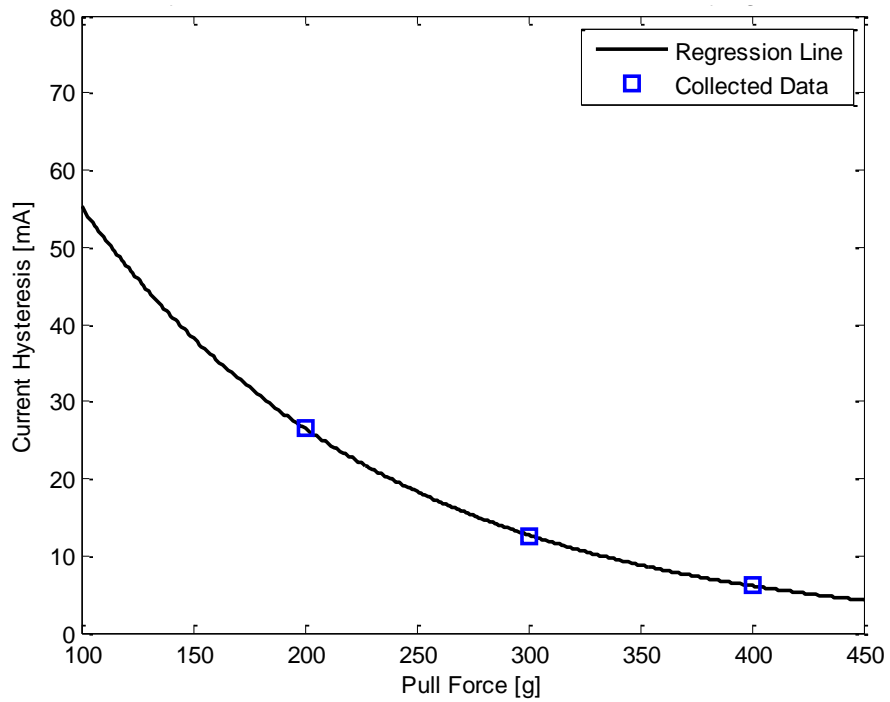


Figure B.14. Current hysteresis as a function of pull force for 6 mil diameter wire.

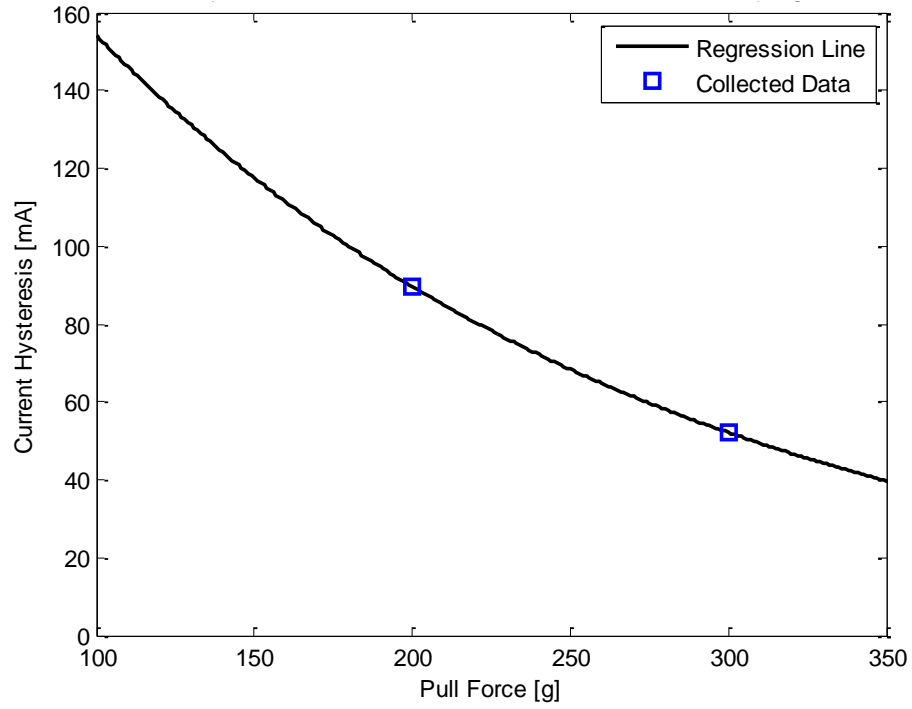


Figure B.15. Current hysteresis as a function of pull force for 8 mil diameter wire.

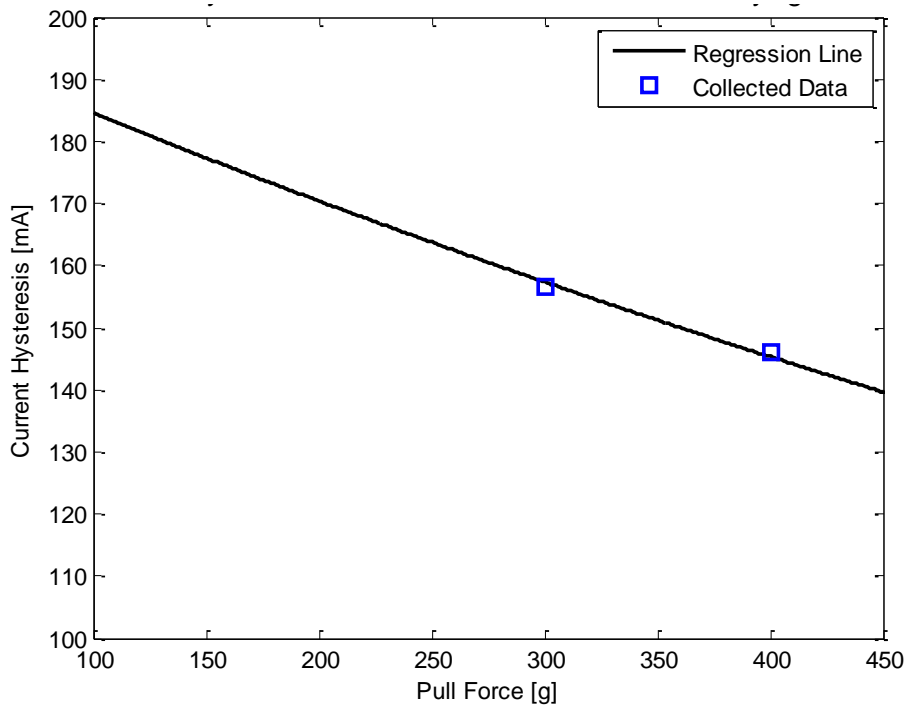


Figure B.16. Current hysteresis as a function of pull force for 10 mil diameter wire.

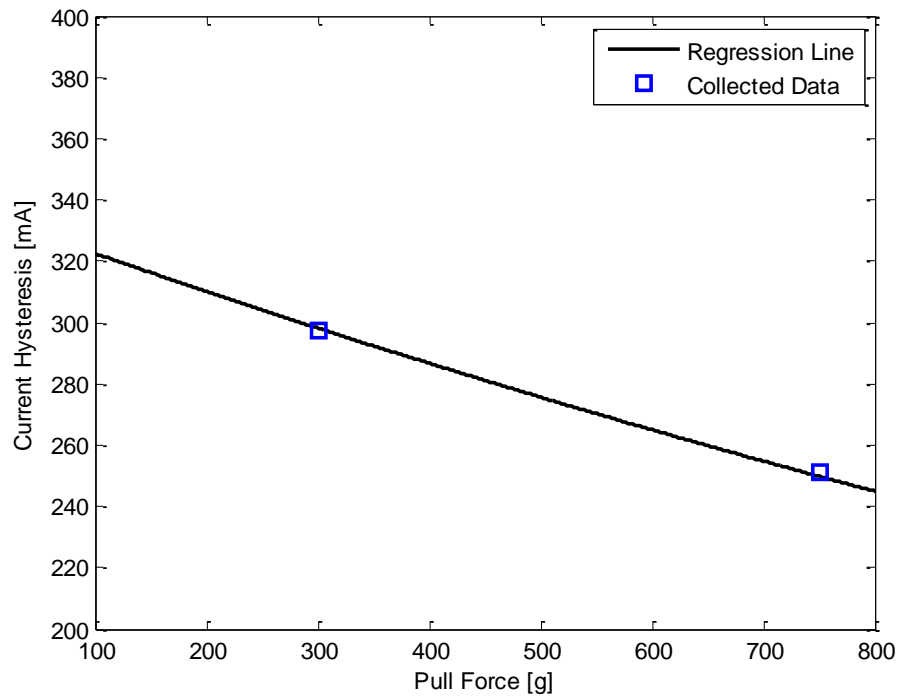


Figure B.17. Current hysteresis as a function of pull force for 12 mil diameter wire.

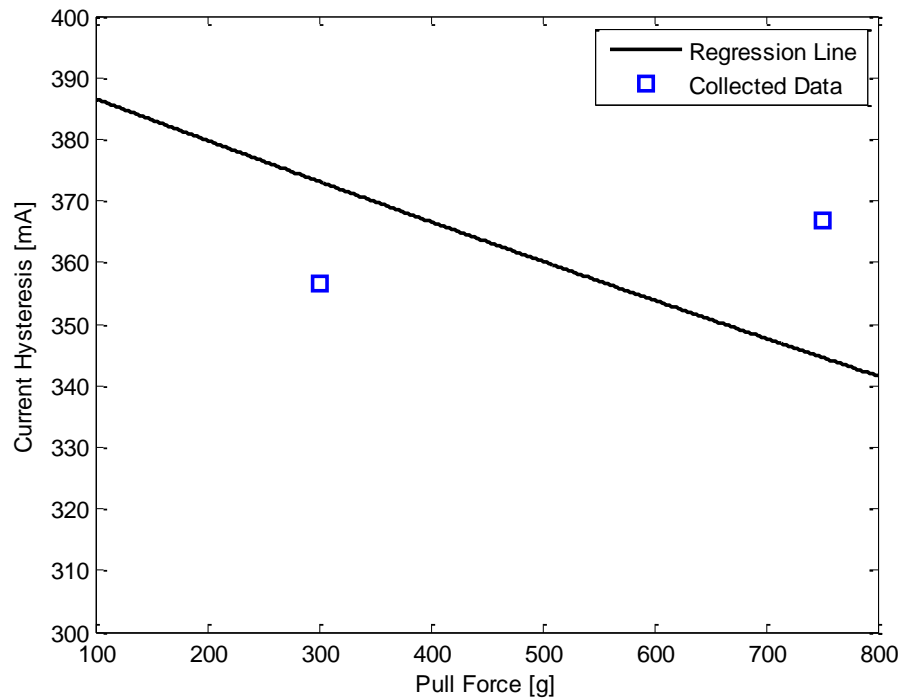


Figure B.18. Current hysteresis as a function of pull force for 15 mil diameter wire.

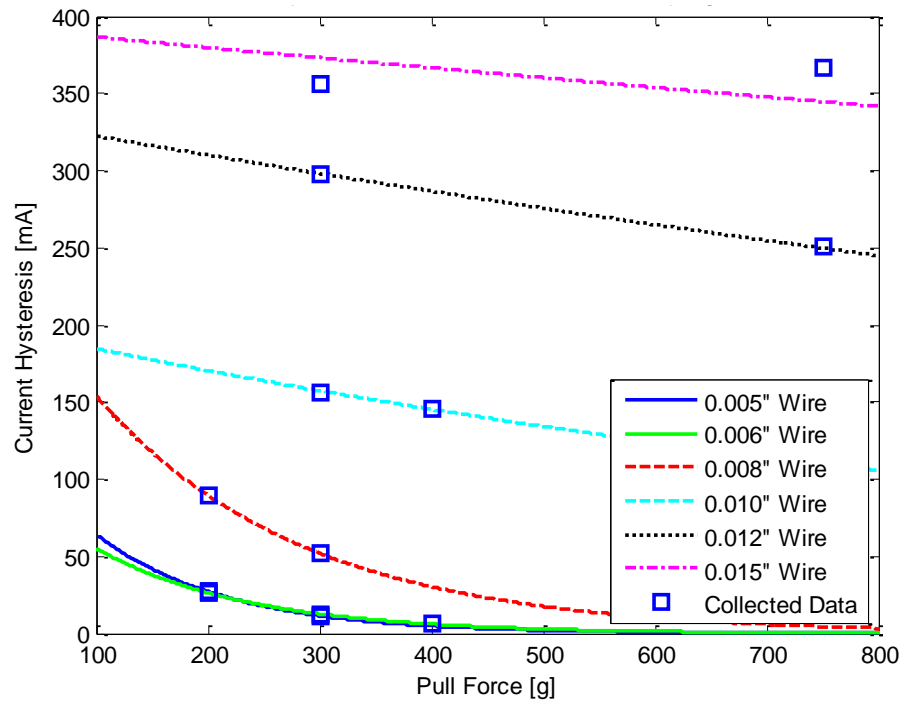


Figure B.19. Current hysteresis as a function of pull force for all wires.

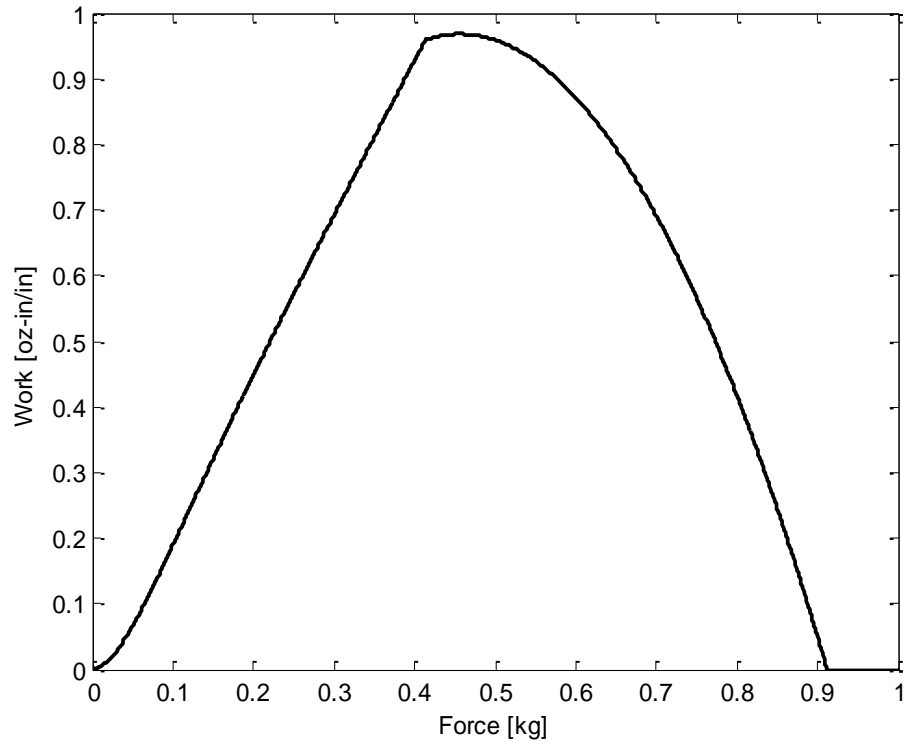


Figure B.20. Work curve for 5 mil diameter wire.

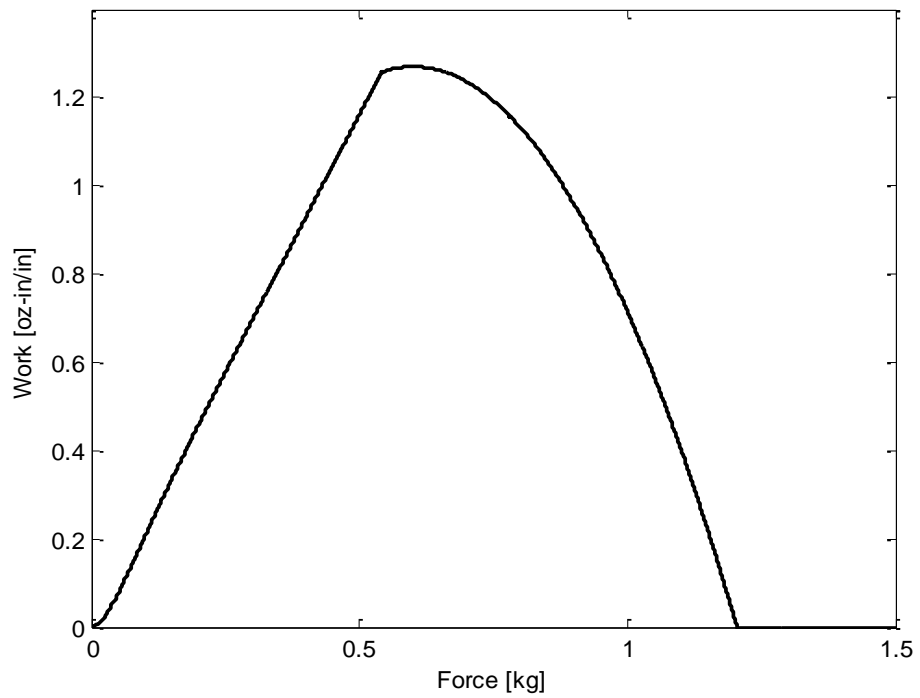


Figure B.21. Work curve for 6 mil diameter wire.

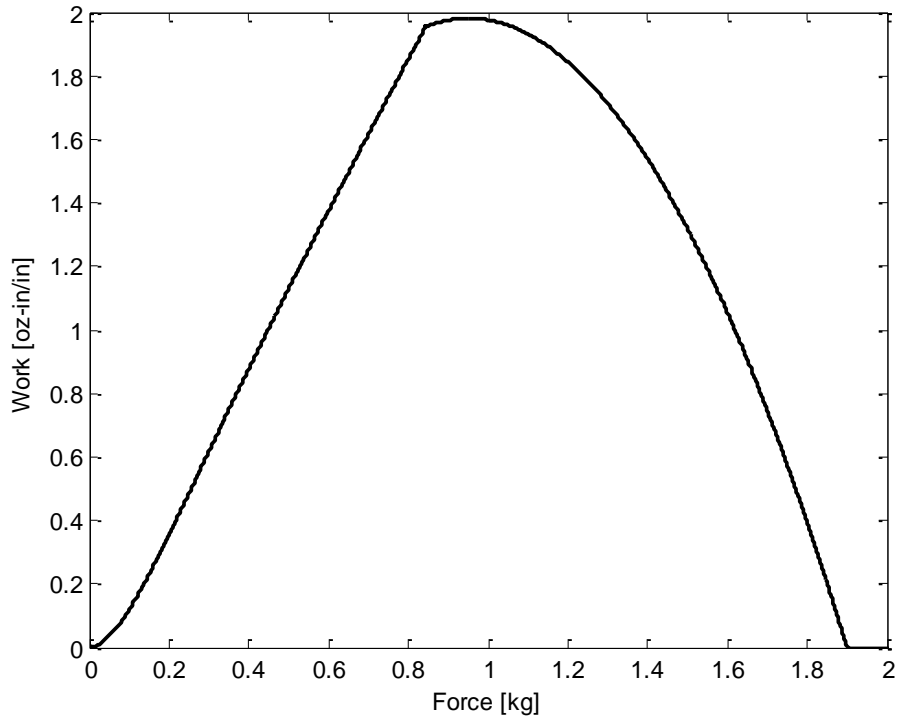


Figure B.22. Work curve for 8 mil diameter wire.

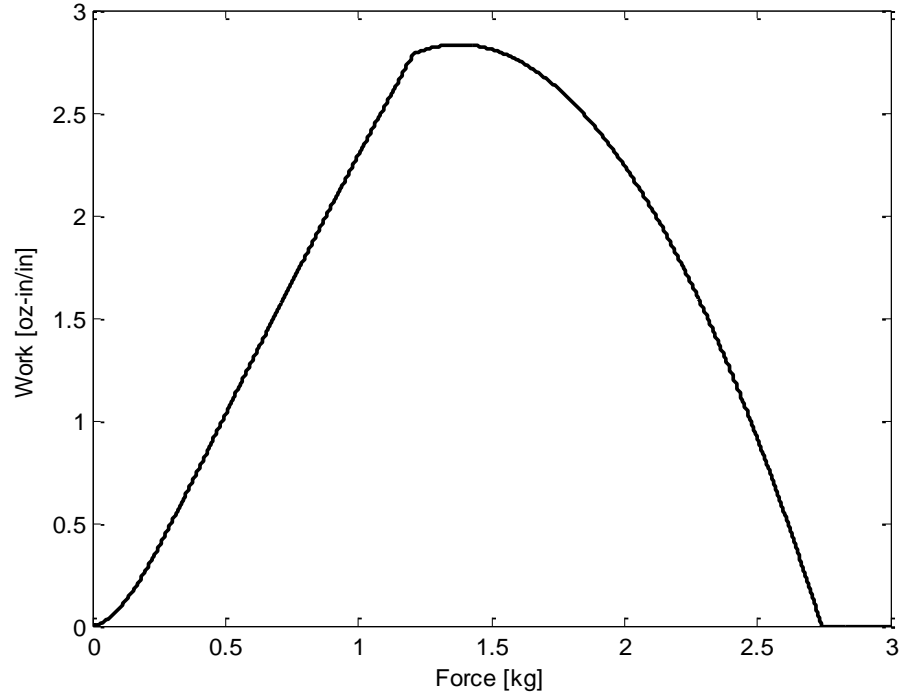


Figure B.23. Work curve for 10 mil diameter wire.



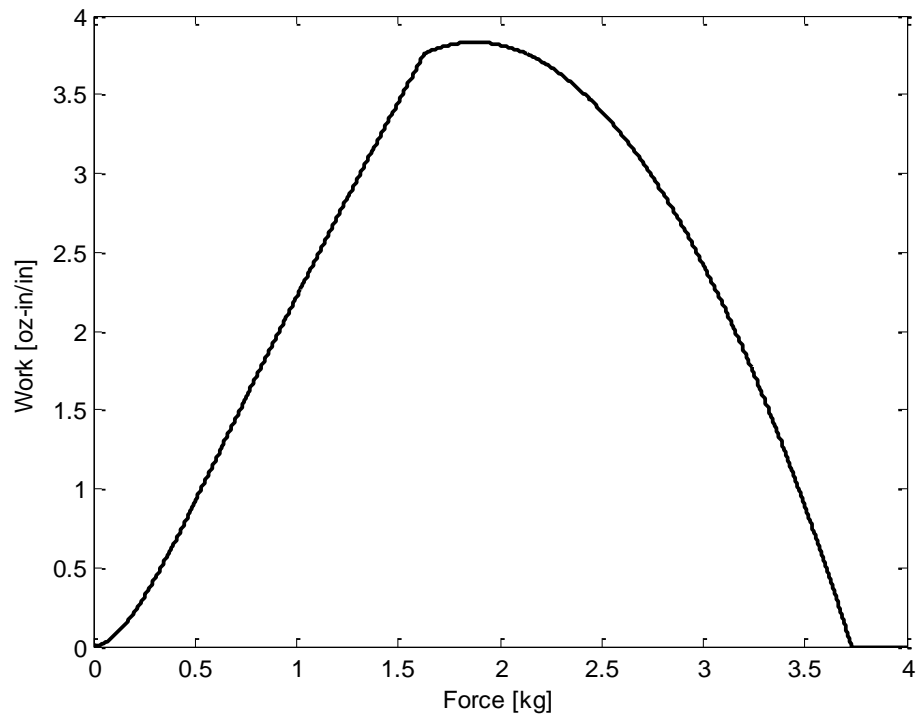


Figure B.24. Work curve for 12 mil diameter wire.

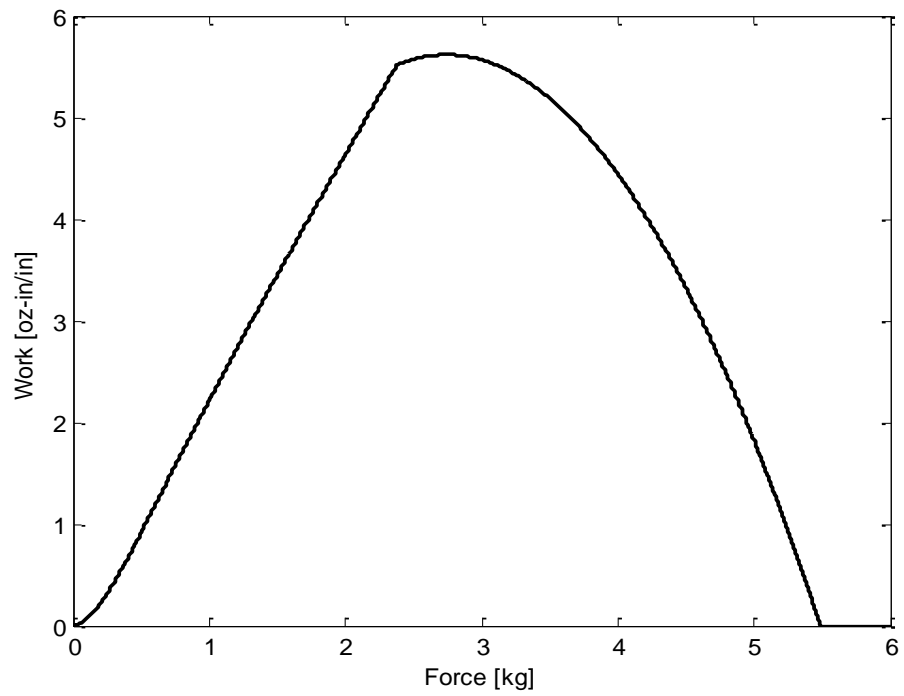


Figure B.25. Work curve for 15 mil diameter wire.

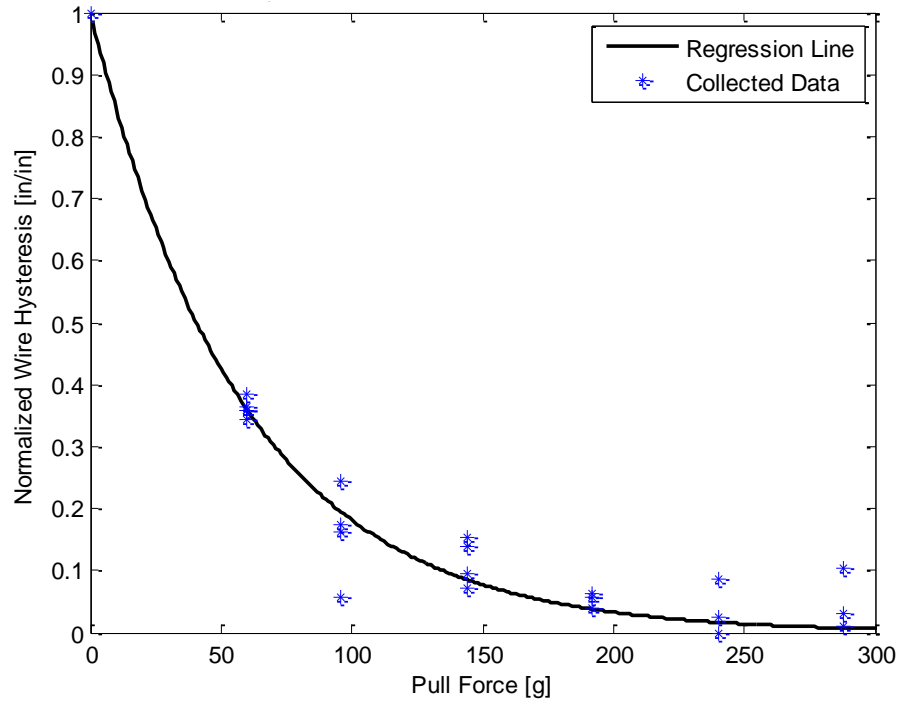


Figure B.26. Wire hysteresis as a function of pull force for 5 mil diameter wire.

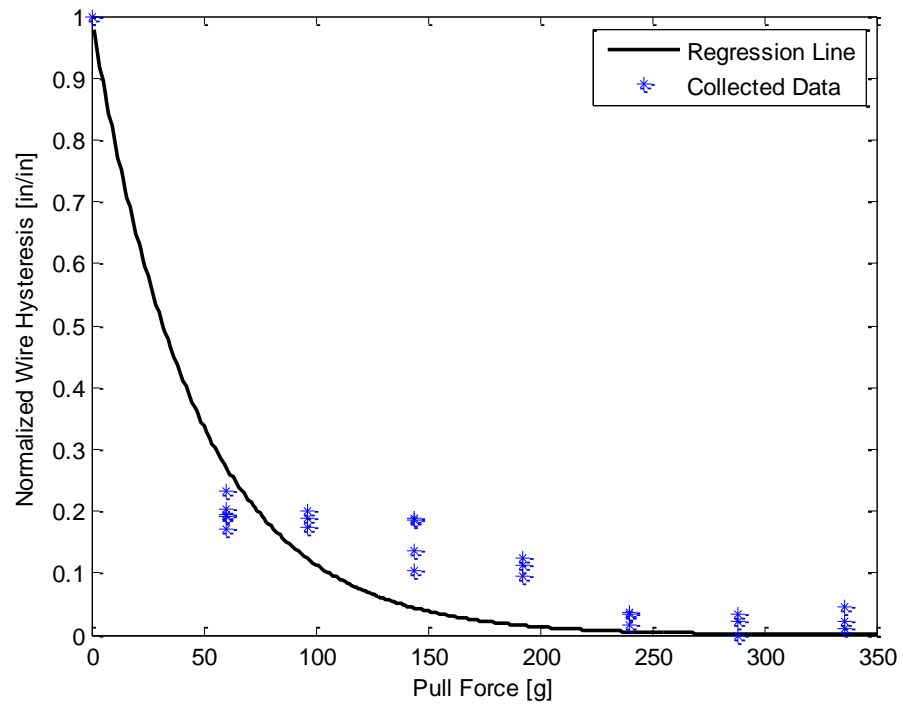


Figure B.27. Wire hysteresis as a function of pull force for 6 mil diameter wire.

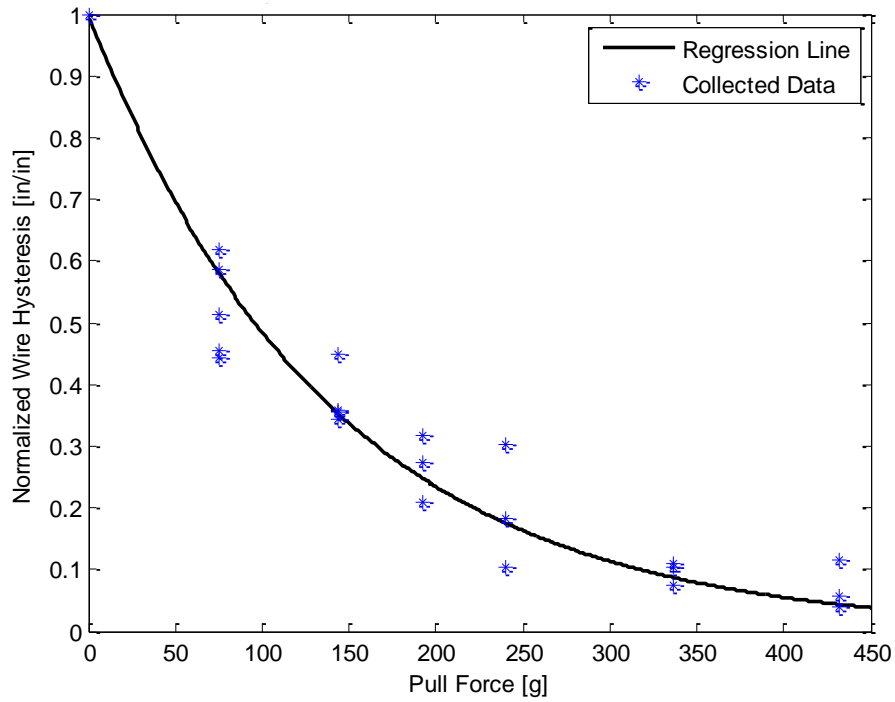


Figure B.28. Wire hysteresis as a function of pull force for 8 mil diameter wire.

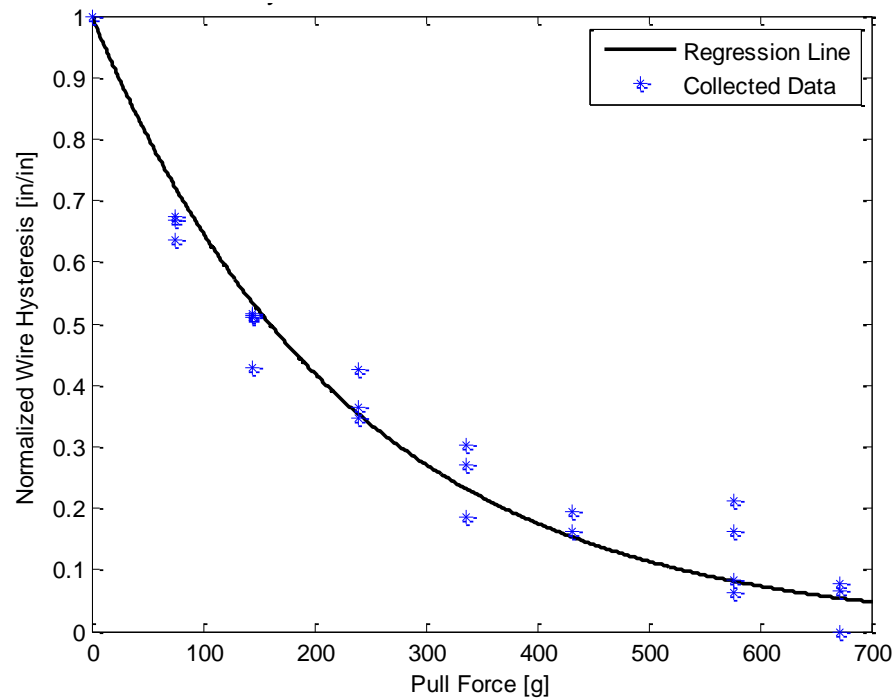


Figure B.29. Wire hysteresis as a function of pull force for 10 mil diameter wire.

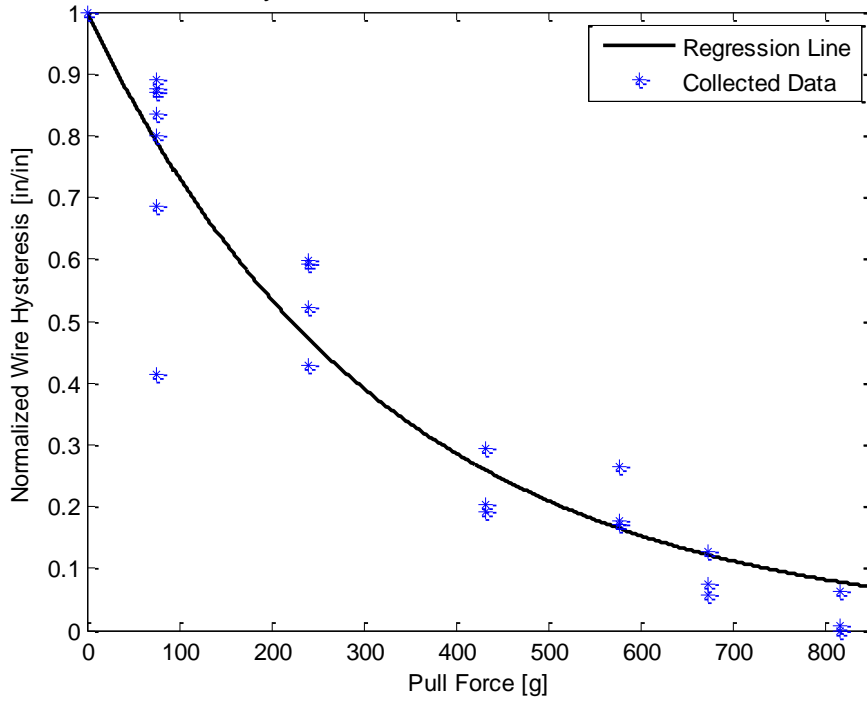


Figure B.30. Wire hysteresis as a function of pull force for 12 mil diameter wire.

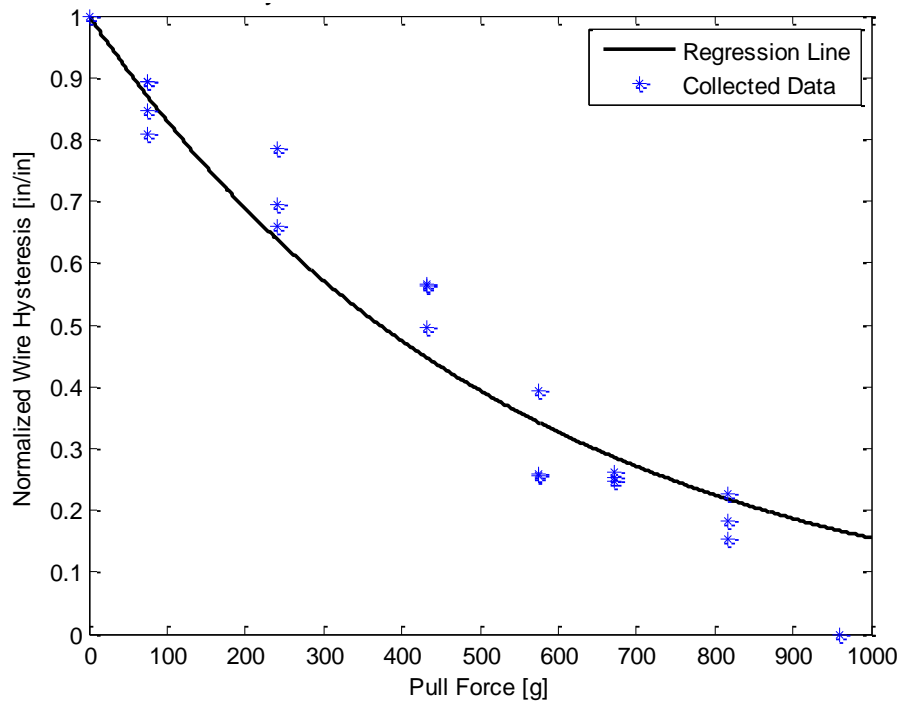


Figure B.31. Wire hysteresis as a function of pull force for 15 mil diameter wire.

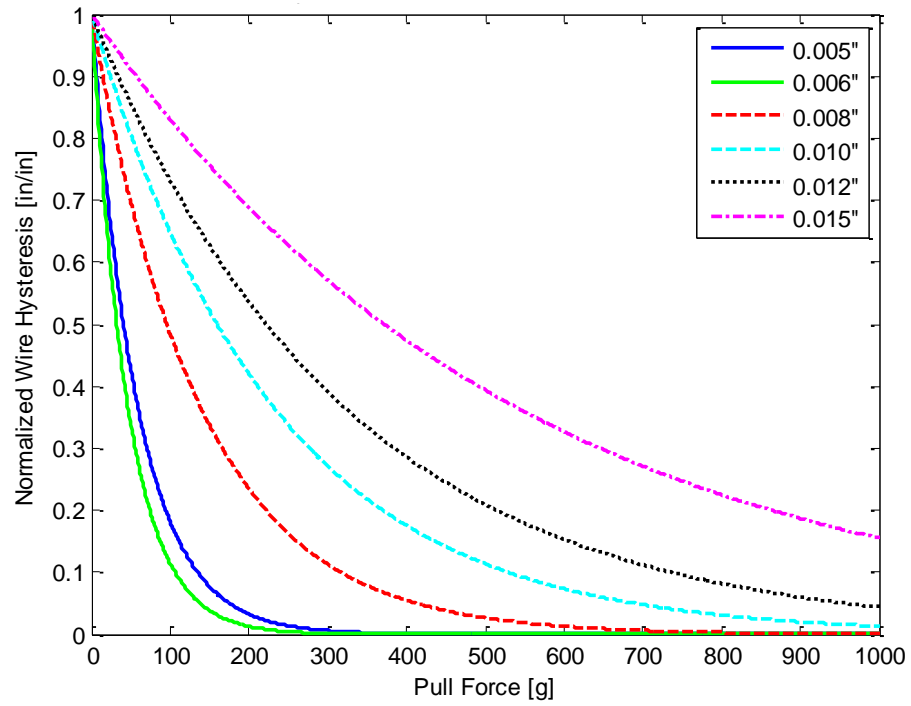


Figure B.32. Wire hysteresis as a function of pull force for all wires.

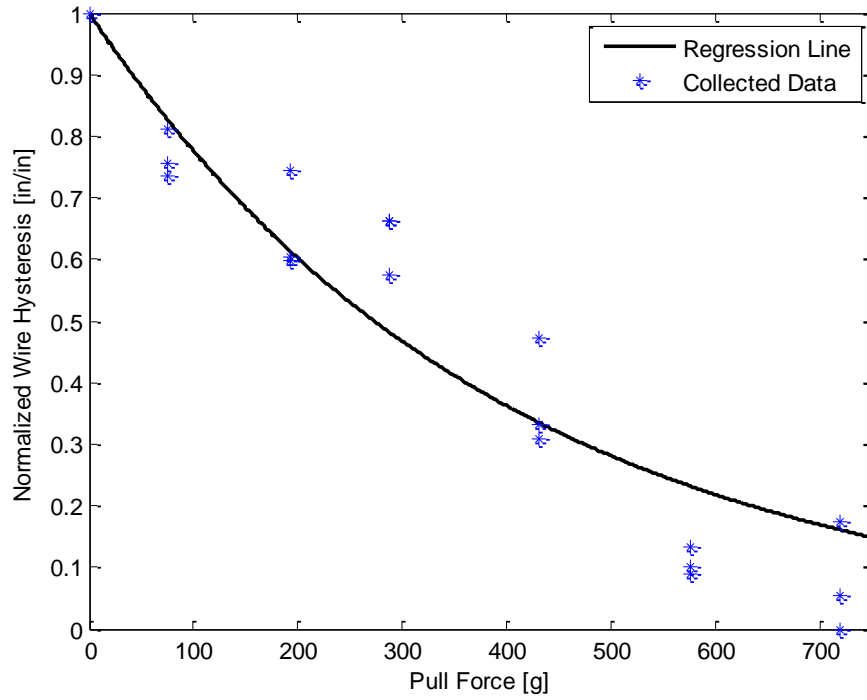


Figure B.33. Wire hysteresis as a function of pull force for 6 mil 2-wire cable.

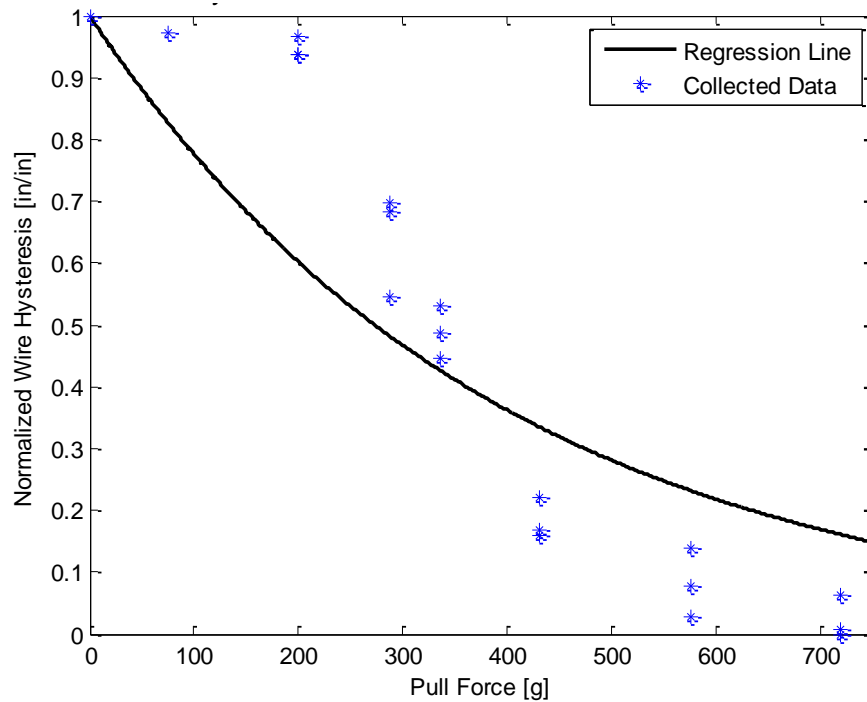


Figure B.34. Wire hysteresis as a function of pull force for 6 mil 3-wire cable.

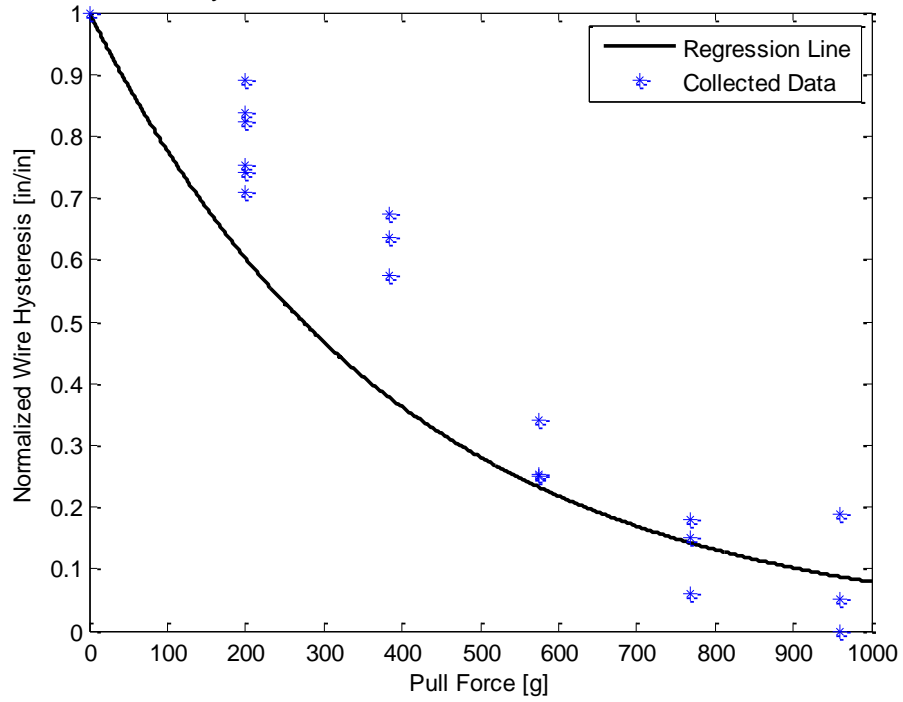


Figure B.35. Wire hysteresis as a function of pull force for 6 mil 4-wire cable.

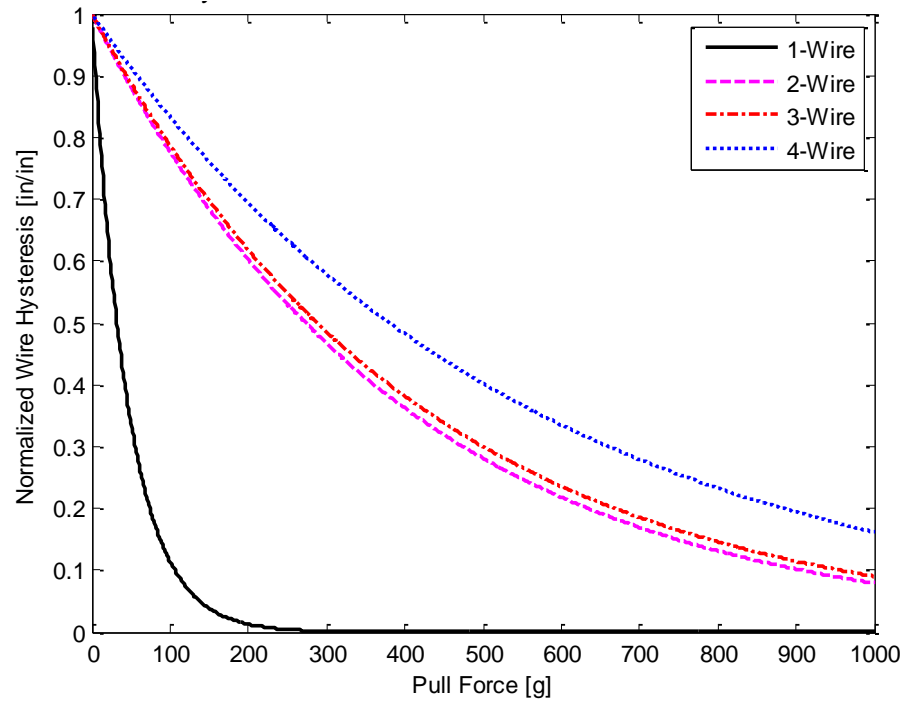


Figure B.36. Wire hysteresis as a function of pull force for all 6 mil diameter cables.

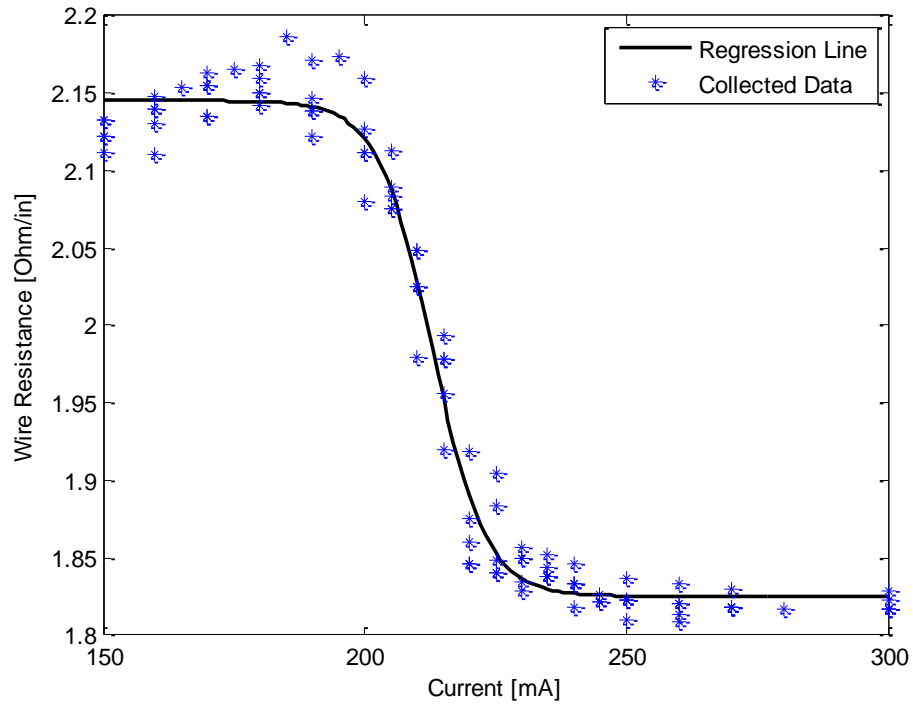


Figure B.37. Resistance curve for 5 mil diameter wire for increasing current values.

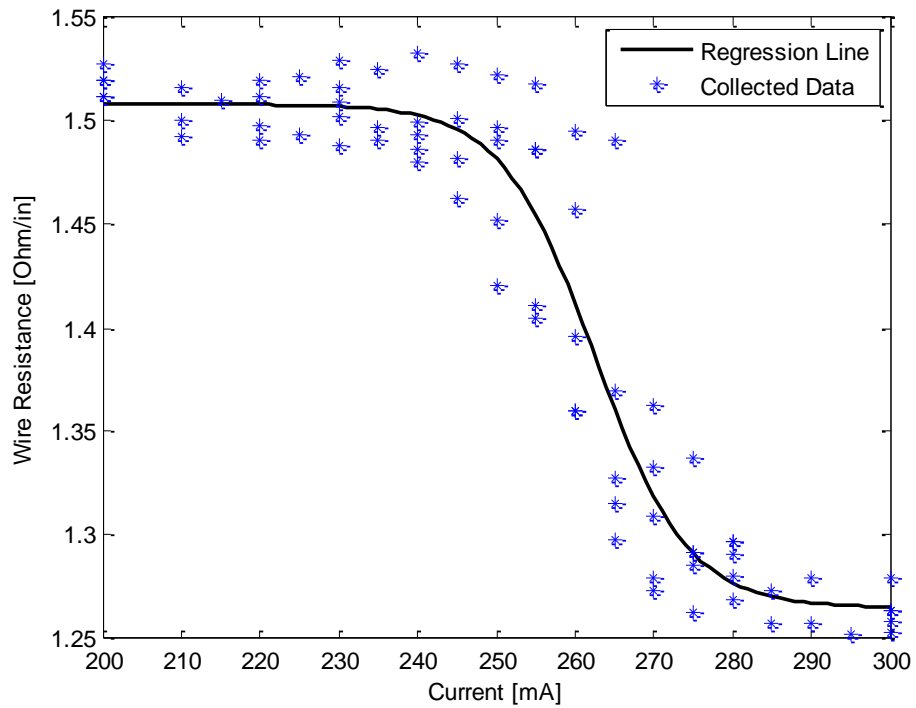


Figure B.38. Resistance curve for 6 mil diameter wire for increasing current values.



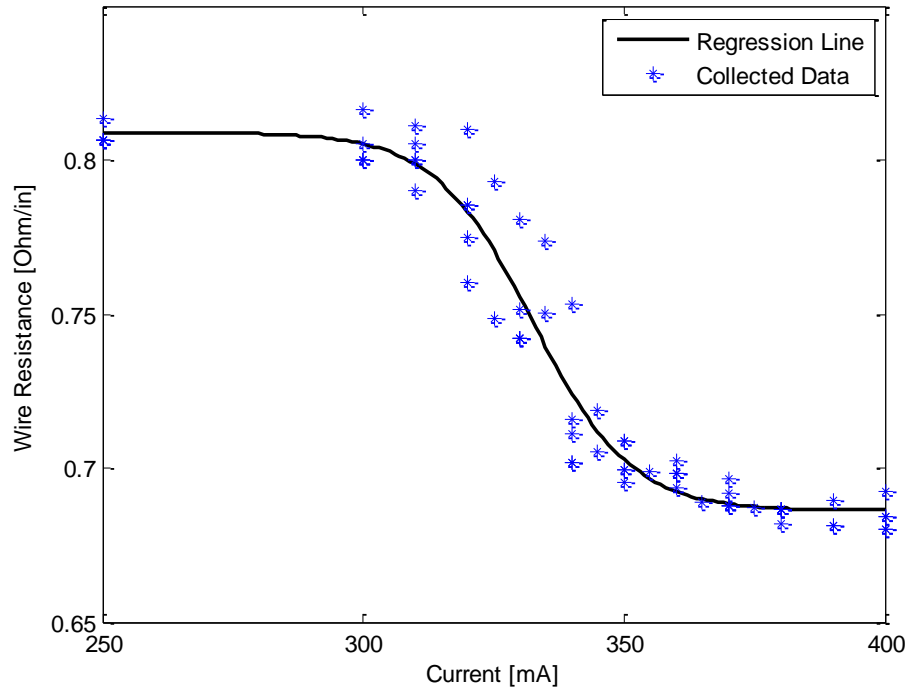


Figure B.39. Resistance curve for 8 mil diameter wire for increasing current values.

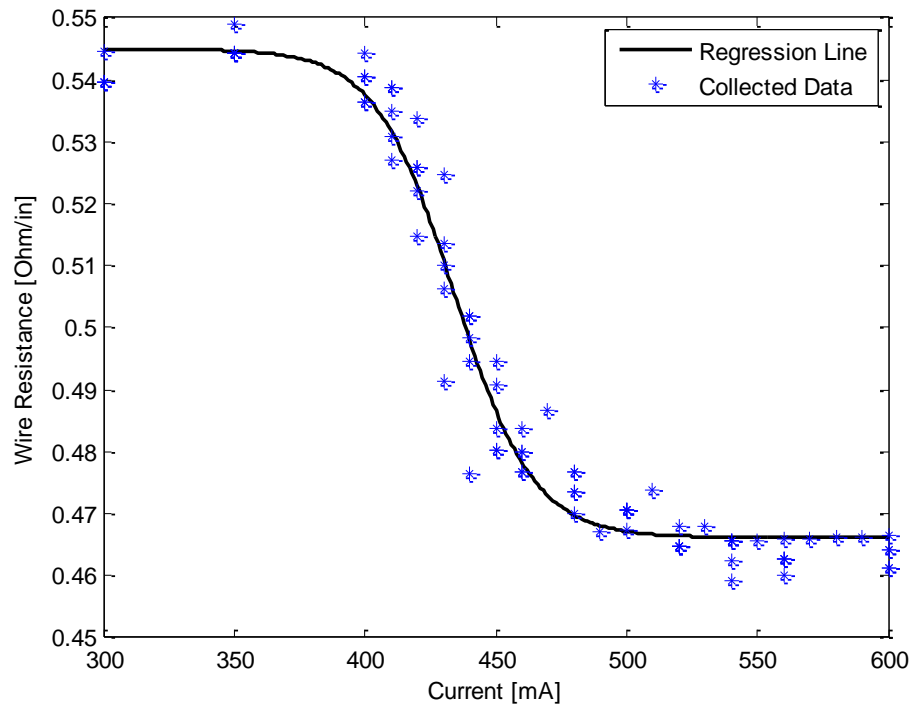


Figure B.40. Resistance curve for 10 mil diameter wire for increasing current values.

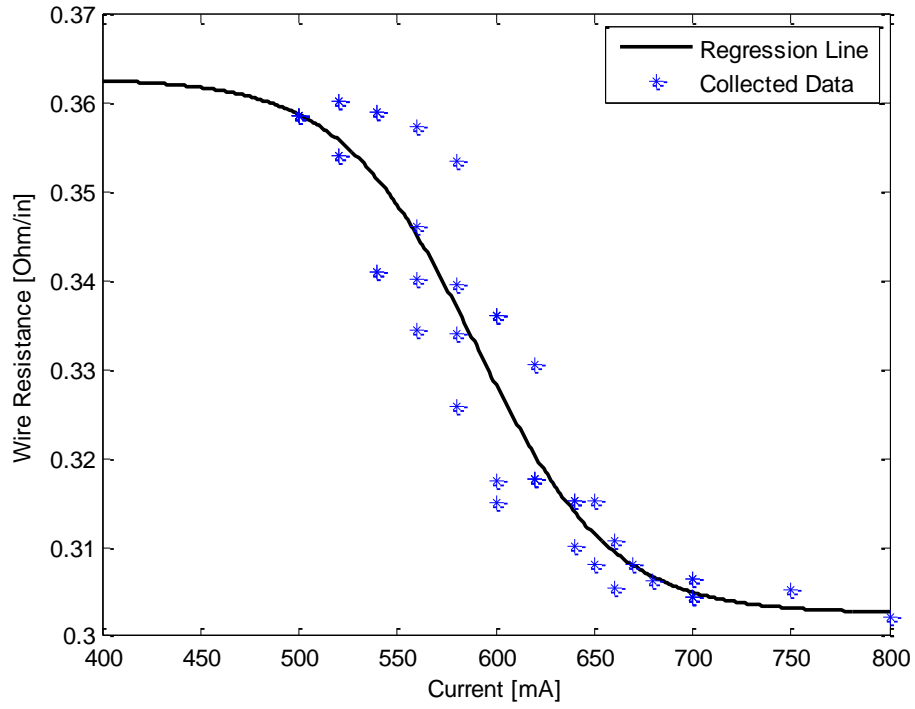


Figure B.41. Resistance curve for 12 mil diameter wire for increasing current values.

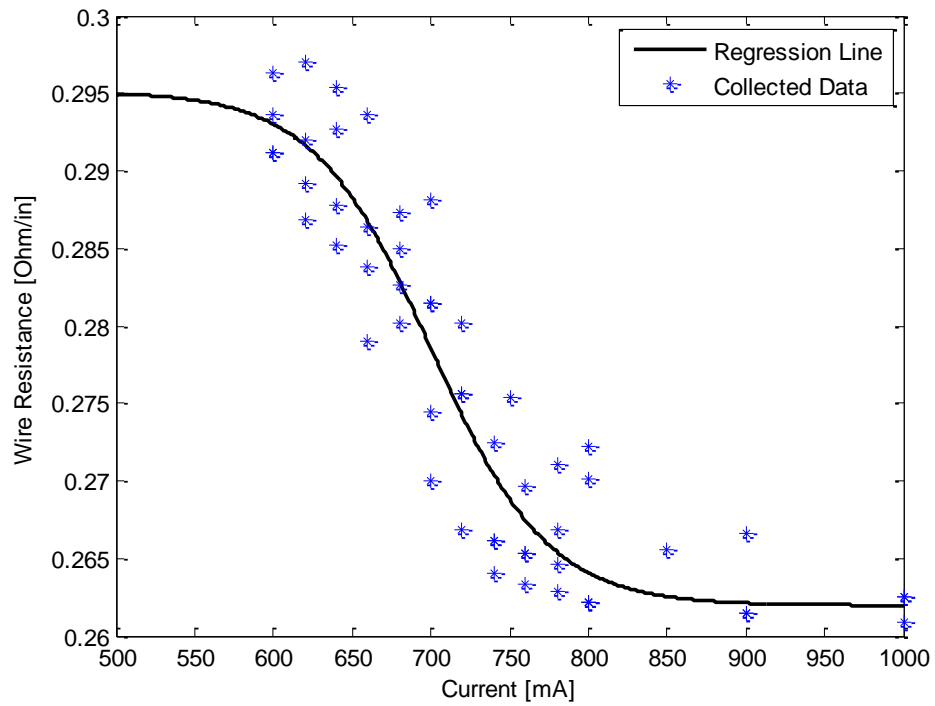


Figure B.42. Resistance curve for 15 mil diameter wire for increasing current values.

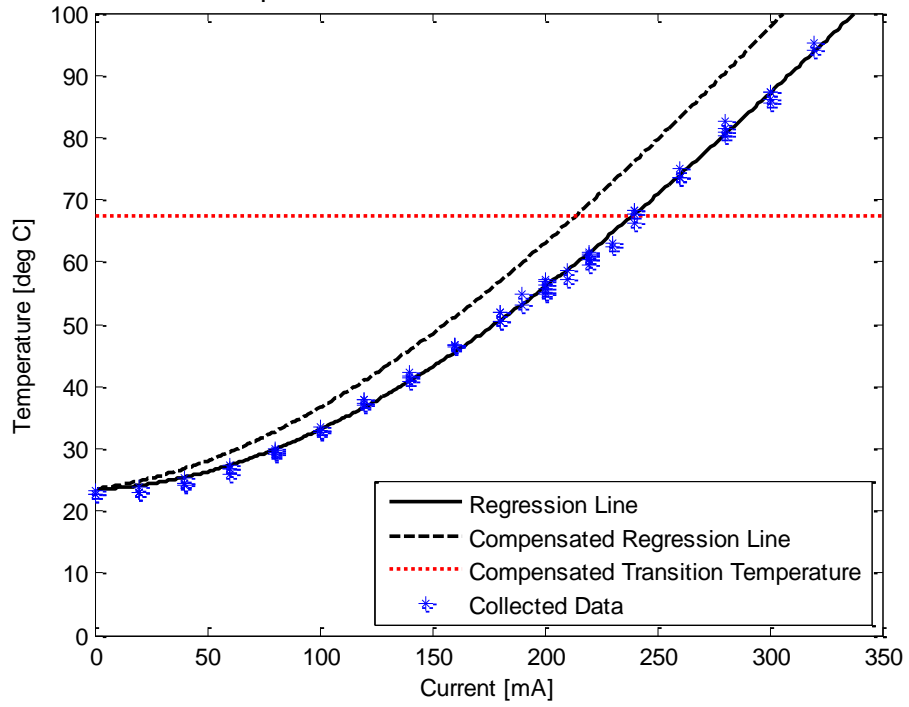


Figure B.43. Temperature curves with transition temperature for 5 mil diameter wire.

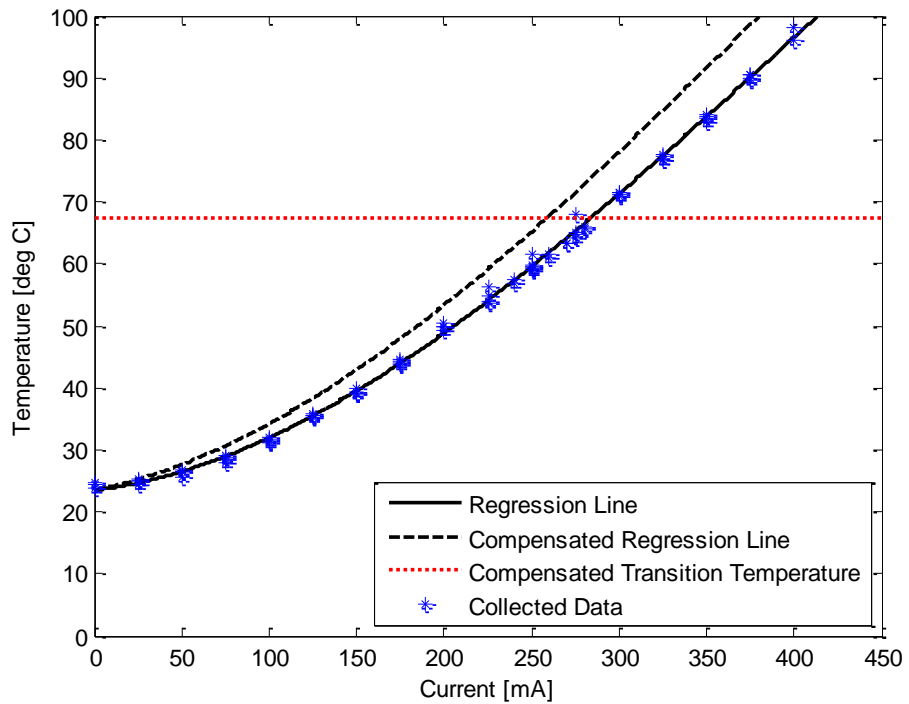


Figure B.44. Temperature curves with transition temperature for 6 mil diameter wire.

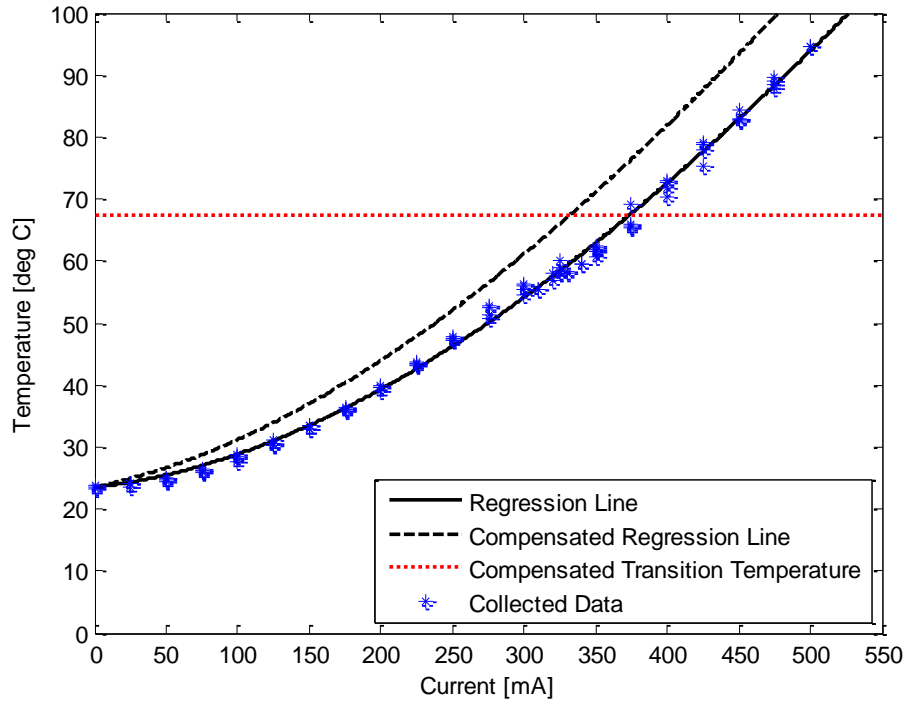


Figure B.45. Temperature curves with transition temperature for 8 mil diameter wire.

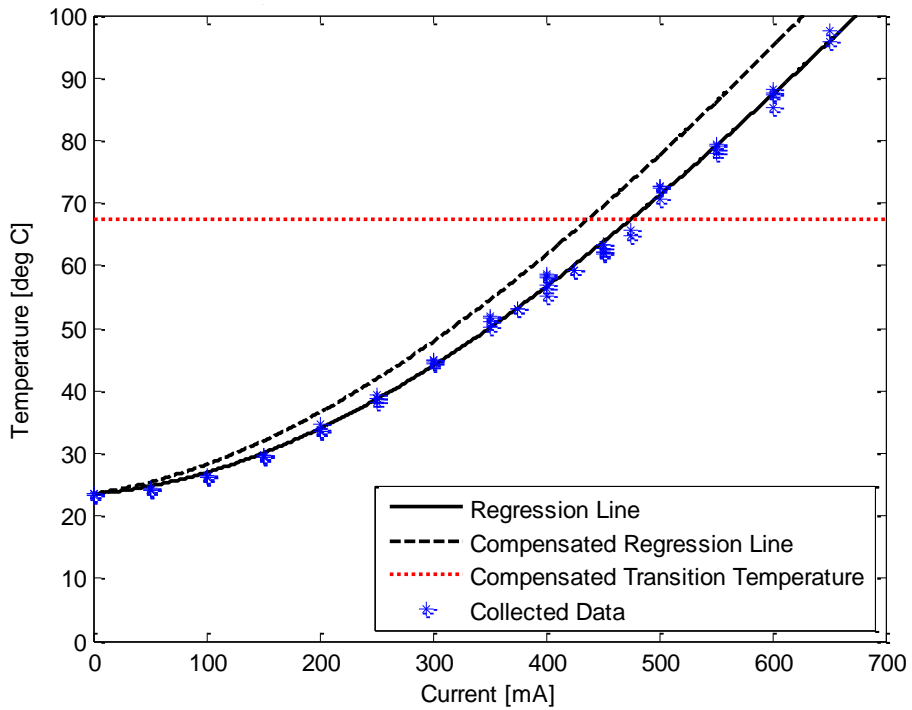


Figure B.46. Temperature curves with transition temperature for 10 mil diameter wire.

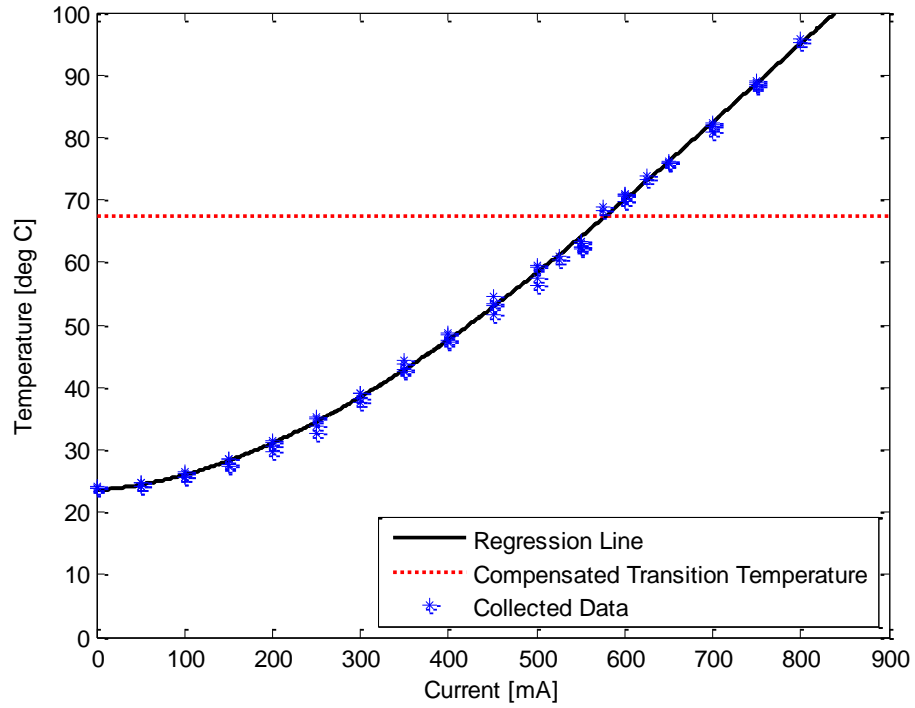


Figure B.47. Temperature curves with transition temperature for 12 mil diameter wire.

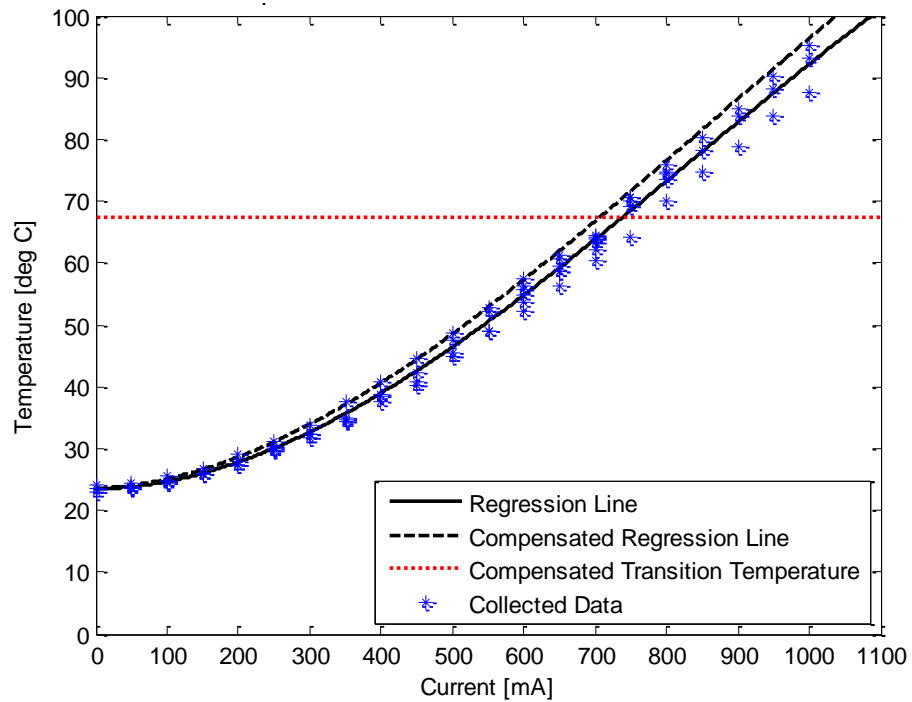


Figure B.48. Temperature curves with transition temperature for 15 mil diameter wire.

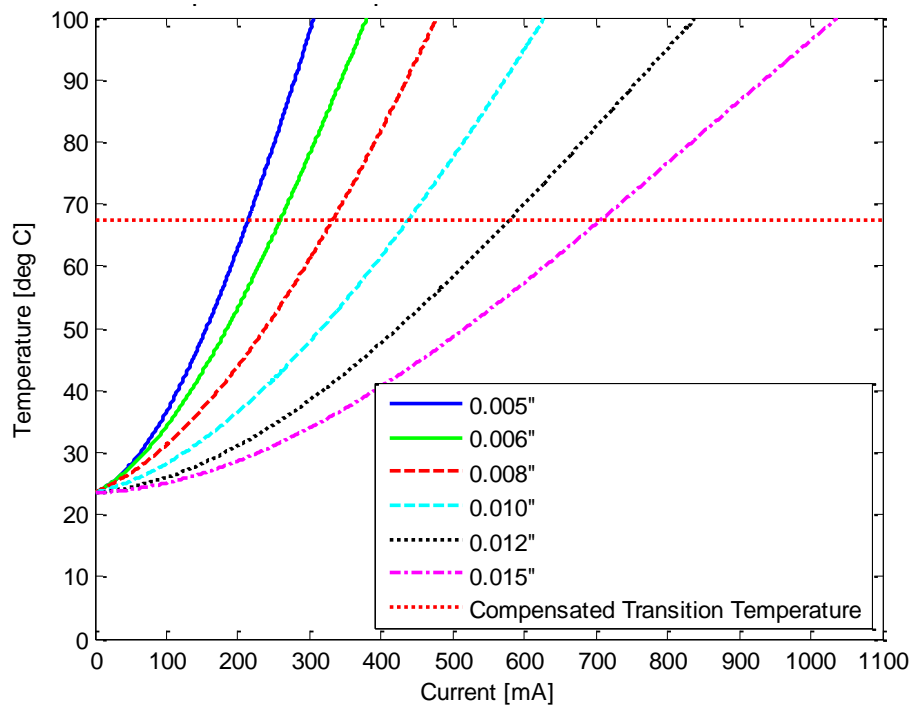


Figure B.49. Temperature curves with transition temperature for all wires.

## **APPENDIX C. SOLIDWORDS DRAWINGS AND PHOTOS OF ACTUATOR**

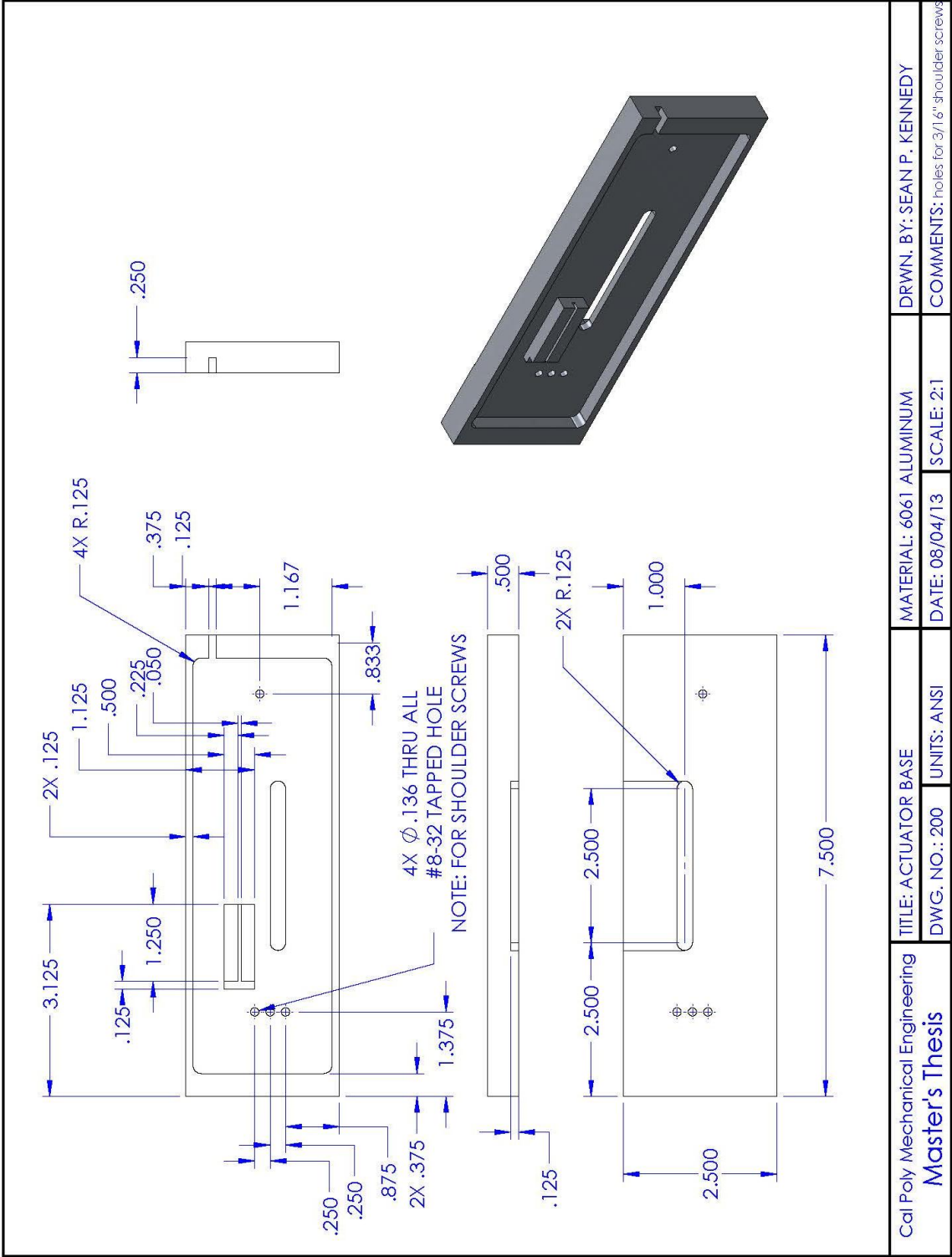


Figure C.1. Solidworks drawing of actuator base.



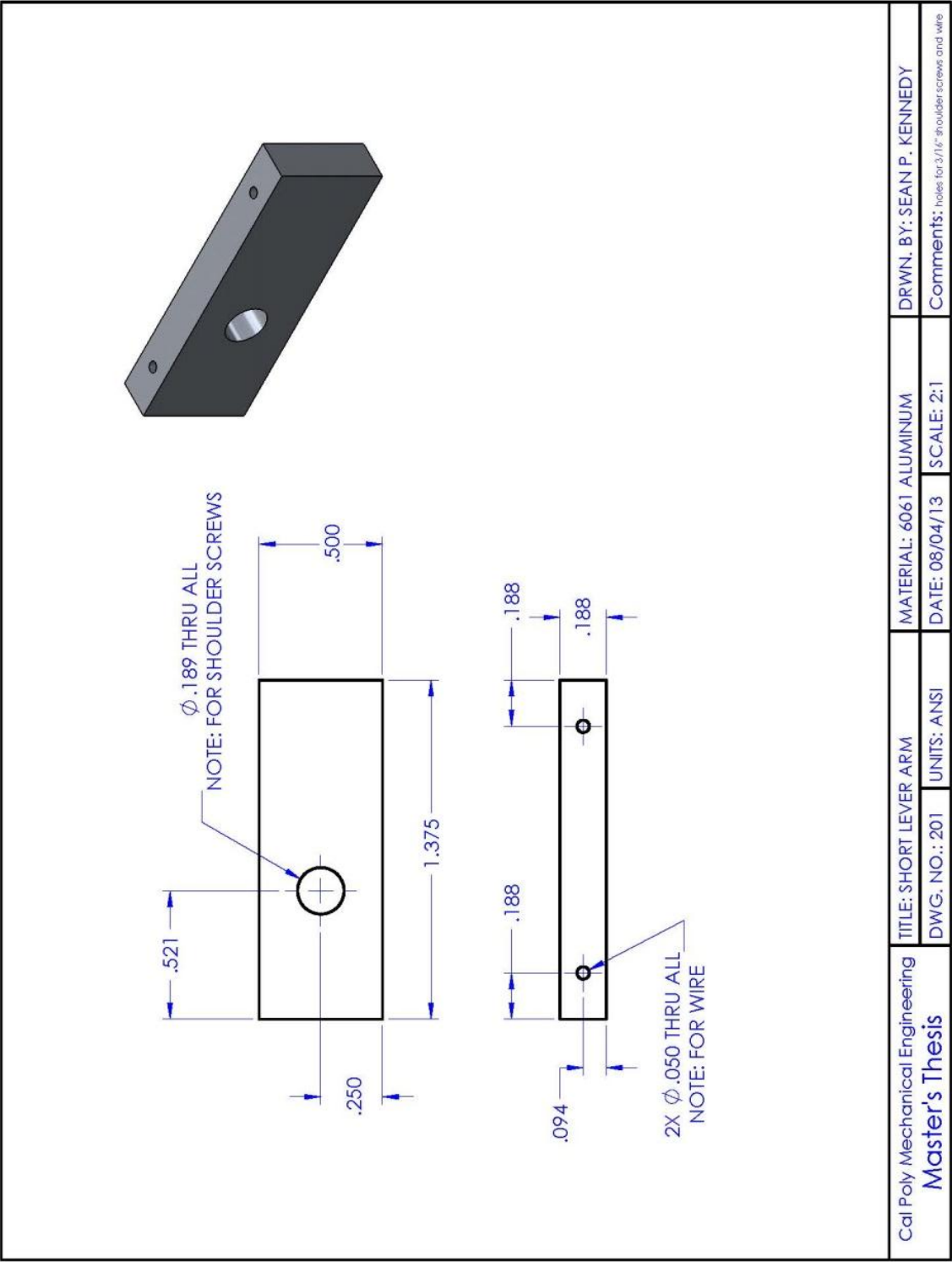


Figure C.2. Solidworks drawing of short lever arm.

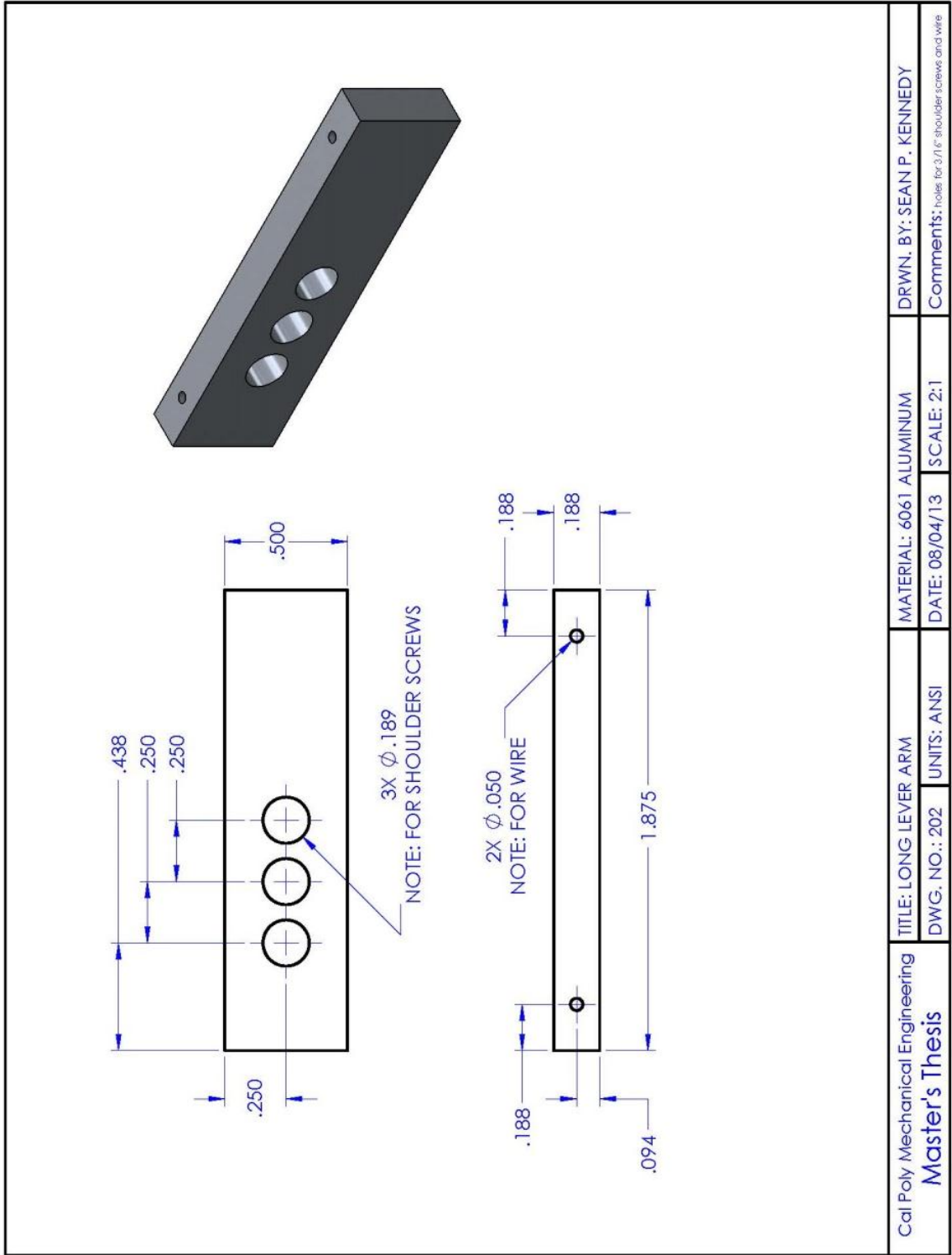


Figure C.3. Solidworks drawing of long lever arm.

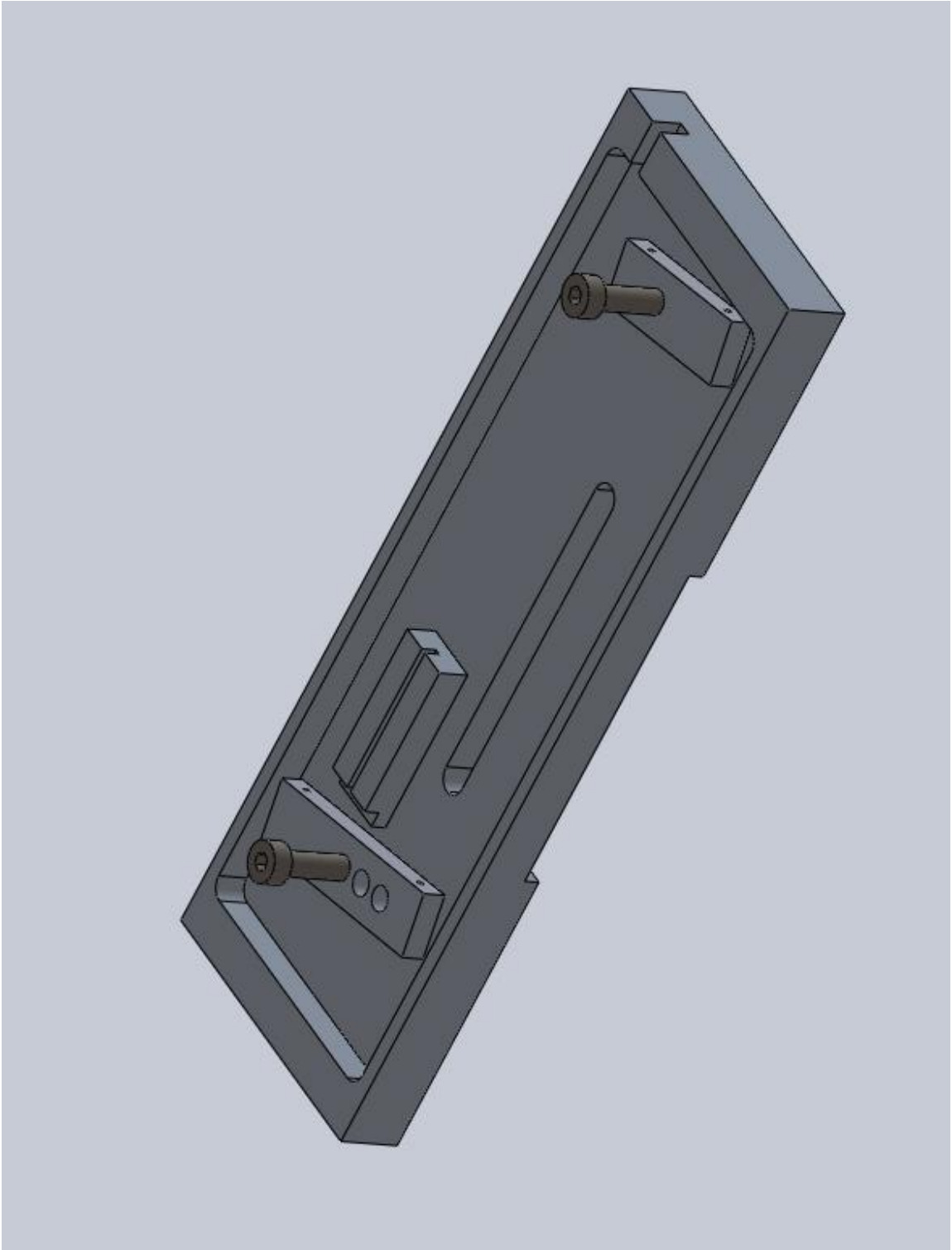


Figure C.4. Solidworks model of actuator design.

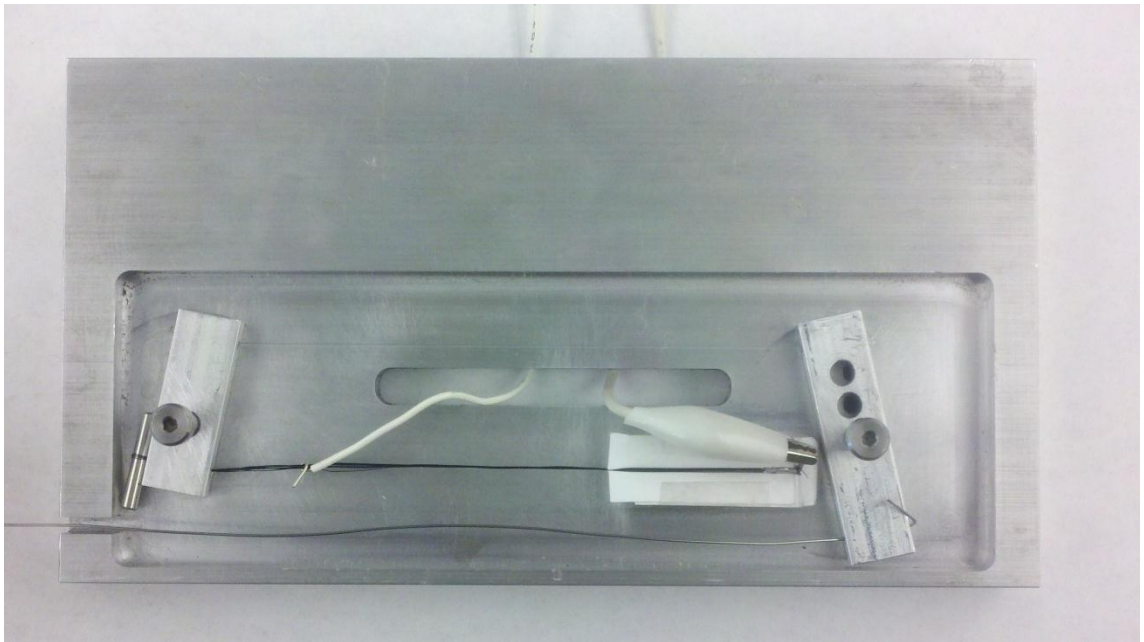


Figure C.5. Complete actuator assembly ready for testing.



Figure C.6. Nitinol wire attachment to actuator base.

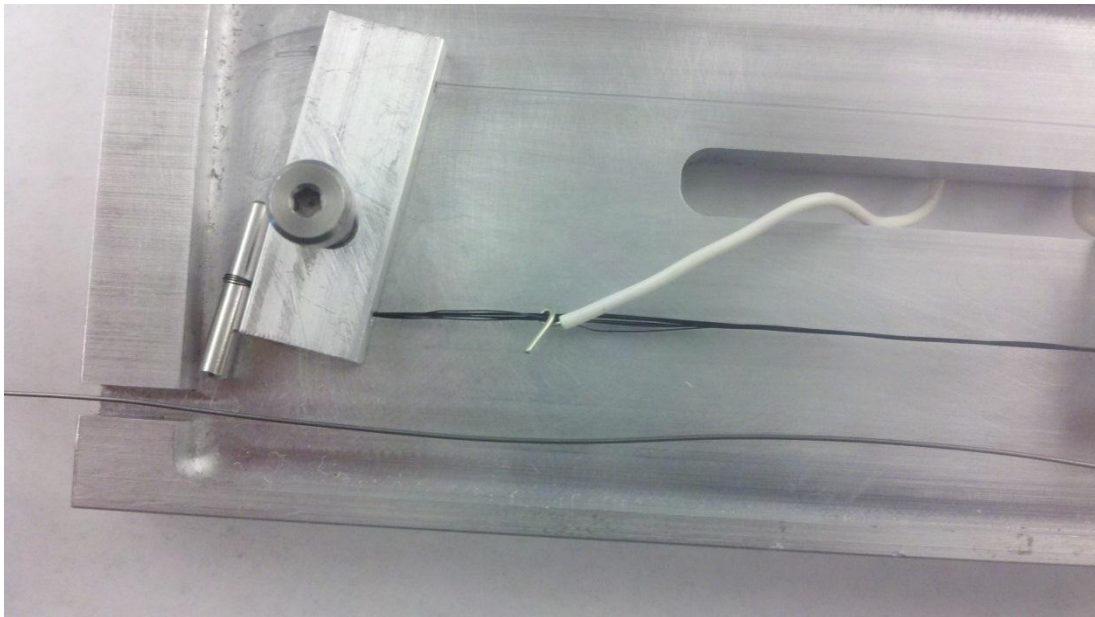


Figure C.7. Adjustable wire attachment to nitinol wire.



Figure C.8. Top view of actuator base.



Figure C.9. Bottom view of actuator base.

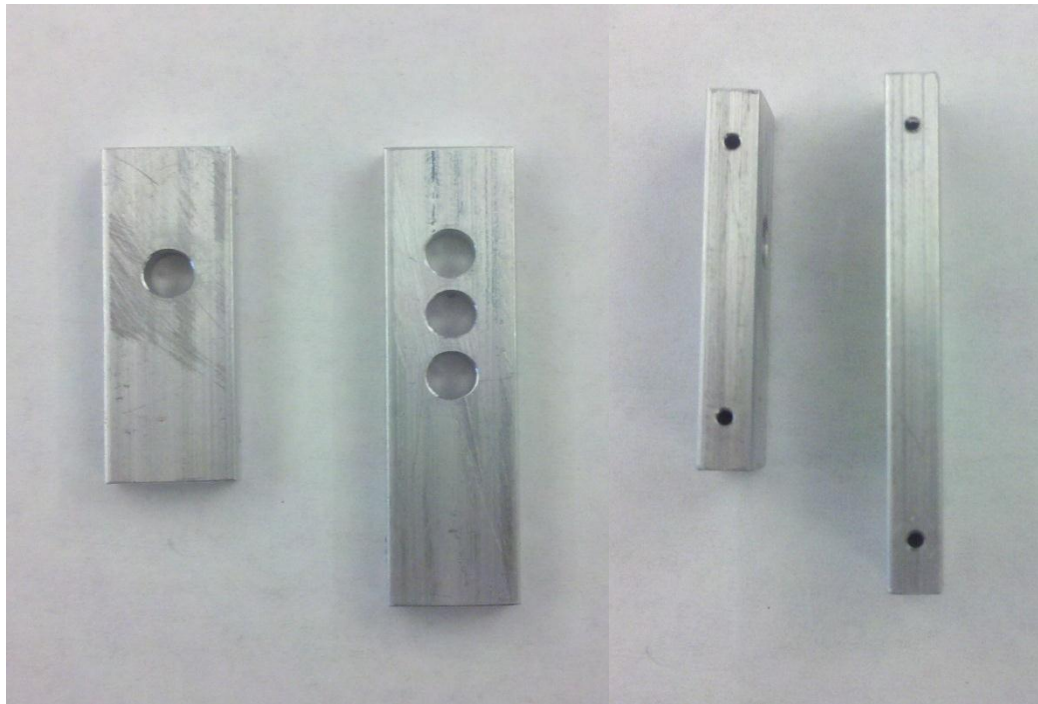


Figure C.10. Top and side views of short and long lever arms.